UNCLASSIFIED

AD 431886

DEFENSE DOCUMENTATION CENTER

FOR

SCIENTIFIC AND TECHNICAL INFORMATION

CAMERON STATION, ALEXANDRIA, VIRGINIA

UNCLASSIFIED

NOTICE: When government or other drawings, specifications or other data are used for any purpose other than in connection with a definitely related government procurement operation, the U. S. Government thereby incurs no responsibility, nor any obligation whatsoever; and the fact that the Government may have formulated, furnished, or in any way supplied the said drawings, specifications, or other data is not to be regarded by implication or otherwise as in any manner licensing the holder or any other person or corporation, or conveying any rights or permission to manufacture, use or sell any patented invention that may in any way be related thereto.

64-10

431886

AFCRL-64-40

CATALOGED BY DDC
AS AD No.

AN ADVANCED REDUCTION AND CALIBRATION FOR PHOTOGRAMMETRIC CAMERAS

Duane C. Brown

Instrument Corporation of Florida
P.O. Box 1226
Melbourne, Florida

Subcontractor - D. Brown Associates, Inc.
P.O. Box 1197
Eau Gallie, Florida

Contract No. AF19(604)-8493

Project No. 5930

Task No. 593003

FINAL REPORT

10 January 1964

DDC
MAR 13 1964
TISIA D

Prepared
for

AIR FORCE CAMBRIDGE RESEARCH LABORATORIES
OFFICE OF AEROSPACE RESEARCH
UNITED STATES AIR FORCE
BEDFORD, MASSACHUSETTS

431886

Requests for all additional copies by Agencies of the Department of Defense, their contractors, and other Government agencies should be directed to the:

DEFENSE DOCUMENTATION CENTER (DDC)
CAMERON STATION
ALEXANDERIA, VIRGINIA

All other persons and organizations should apply to the:

U.S. DEPARTMENT OF COMMERCE
OFFICE OF TECHNICAL SERVICES
WASHINGTON 25, D.C.

ABSTRACT

In order to fully exploit recent advances in photogrammetric technology it has been necessary to develop a comprehensive plate reduction appreciably more powerful than any hitherto employed. In addition to factors considered in previous plate reductions, an advanced reduction must treat with full physical and statistical rigour such factors as: random errors in catalogued stellar positions; atmospheric refraction (particularly at great zenith distances); higher-order symmetric radial distortion; tangential distortion and asymmetric radial distortion resulting from imperfectly centered optics; differential bias between measurements of different types of images; effective utilization of uncatalogued stars for photogrammetric control; introduction of a priori constraints on any ot the parameters of the reduction. Such a reduction is developed in this paper and illustrations of its practical application are provided. Special attention is given to decentering distortion, a topic inadequately treated in the photogrammetric literature. It is suggested that uncompensated decentering distortion has often in the past been the major obstacle to the full practical realization of theoretically attainable accuracies. The Advanced Plate Reduction is designed to be valid for any combination of focal length and angular field. By allowing for the possibility of correlated errors in the plate coordinates, it is also valid for cameras not having flat fields (e.g., the Baker Nunn Satellite Camera). Special note is taken of the application of the Advanced Plate Reduction for the definitive calibration of mapping cameras to be used for the analytical extension of photogrammetric control.

TABLE OF CONTENTS

		Page
1.0	Introduction	1
2.0	Star Catalog Errors	2
3.0	Atmospheric Refraction	5
4.0	Symmetric Radial Distortion	9
5.0	Parameterization of Differential Bias	11
6.0	The Observational Equations	15
7.0	The Linearized Observational Equations	22
8.0	The Minimum-Variance Adjustment	32
9.0	Error Propagation	42
10.0	Calibration of Distortion Caused by Lens Decentration	46
11.0	General Considerations	77
12.0	References	83
	APPENDIX	85
A.1	Introduction	86
A.2	Early Development of Stellar Oriented Fixed Camera Technique	87
A.3	Development of New Reductional Techniques at BRL	89
A.4	Developments at the Atlantic Missile Range	92
A.5	Recent Developments	97
A.6	Fixed Camera Vs. Sidereal Camera for Determination of Direction to Flashes	108
A.7	Relative Advantages of Fixed and Sidereal Cameras for Determination of Direction of Flashes	109
A.8	Conclusions	111
A.9	Selected Bibliography	112

AN ADVANCED PLATE REDUCTION AND CALIBRATION FOR PHOTOGRAMMETRIC CAMERAS

1.0 INTRODUCTION

In an earlier paper [1] the writer traced the evolution of plate reductions for ballistic cameras. It was pointed out that, during the formative years of ballistic camera photogrammetry in the early 1940's, techniques for plate reduction were largely borrowed from positional astronomy. Because of the relatively wide-angular fields of ballistic cameras, these techniques proved to be ill-suited to the ballistic camera application and were supplanted by the early 1950's by techniques developed by Schmid [2], [3] which were based on closed expressions rigorously defining the central projection of three-dimensional object space into two dimensional image space. Schmid's plate reduction was extended in 1956 by the writer [4] to include the calibration of radial distortion of the lens. As thus extended, Schmid's reduction proved adequate for data gathered from the types of ballistic cameras in general use through the 1950's. These cameras may be characterized as being of fairly short focal length (300mm and less) and of fairly wide angular field (33° square and greater). Changing and more stringent requirements led in 1960 to the development of the PC-1000 ballistic camera under the sponsorship of AFCRL. The 1000mm focal length of this camera is over three times greater than that of the 300mm ballistic camera. Experience with the PC-1000 demonstrated that many of the practices and procedures which were satisfactory with cameras of shorter length are unsatisfactory or marginal with cameras of long focal length. Indeed, long focus ballistic cameras have required development of significant refinements in photogrammetric theory and practice in order that their full potential for improved accuracy might be realized. In this report we shall develop an Advanced Plate Reduction designed to extract the practical ultimate from the informational content of a ballistic camera plate. Although the Advanced Plate Reduction was developed primarily to satisfy the special requirements of long focus ballistic cameras, we have taken pains to cast the solution in a form of universal applicability. Thus, the reduction, as presented, is equally valid for cameras of very short focal length and very wide angular field and for cameras of very long focal length and very narrow angular field. Special attention has been given to the following problems:

(a) rigorous consideration of random errors in star catalogue data,

(b) adequate compensation for atmospheric refraction, particularly at great zenith distances,

(c) calibration of radial distortion of the lens,

(d) calibration of tangential distortion and assymmetric radial distortion resulting from imperfect centering of the elements of the lens,

(e) utilization of uncatalogued stars as control points,

(f) utilization of "a priori" or independently measured elements of orientation,

(g) simultaneous utilization of measurements of stellar breaks and stellar punctiform images.

In [1] we discussed many of the properties of the Advanced Plate Reduction and some of the results of its application, as well as its relationship to earlier reductions. This reference is attached as an appendix to the present report because it is especially pertinent to the investigation at hand and because it was originally generated under the present contract. We suggest that the reader acquaint himself with the appendix before proceeding further, for it provides a heuristic and relatively nonmathematical introduction to the Advanced Plate Reduction.

2.0 STAR CATALOG ERRORS

Plate reductions currently in general use for ballistic camera reductions treat catalogued stellar positions as if they were perfectly known, random error being ascribed solely to the measured plate coordinates. As we shall see, the premise of perfect control is untenable for cameras of focal length appreciably in excess of 300 mm. The significance of a specific level of error in catalogued positions may best be gauged through a comparison with attainable plate measuring accuracies. Normal rms plate measuring accuracies for well-defined images are on the order of 2 to 3 microns and, for a fixed plate size, are largely independent of focal length. We have, however, observed a tendency for plate measuring accuracies to improve somewhat with increasing focal length, probably because of the superior and more uniform image quality generally characteristic of narrow angular fields (as long as diffraction is not a serious consideration). Therefore, we shall adopt the more stringent figure of 2 microns as a standard for plate measuring accuracies. It then becomes clear that errors in catalogued stellar positions assume significance with a

given camera if they exceed one micron when projected onto the plate.

In spite of its relative obsolescence, the General Catalog (GC) prepared by Benjamin Boss is still widely used in ballistic camera work because of its complete coverage of the celestial sphere (both northern and southern hemispheres are covered with good uniformity), because of its large number of stars (over 33,000 stars, an average of 0.8 stars per square degree), and because of its convenience in utilization (proper motions are provided for all stars; hence catalogues of different epochs need not be consulted in order to update stellar positions). The mean epoch of the GC is about 1900. Eichhorn [5] quotes the typical mean error of a stellar position at mean epoch as being 0".15 and the typical mean error of annual proper motion as being 0".010. It follows that the mean error of the typical star in the GC for year 1965 approaches 0".7. This is equivalent to errors of about 1 micron, 2 microns, and 3.5 microns on the plates of 300mm, 600mm, and 1000mm cameras respectively. Thus, errors in the GC are not of major significance for cameras of focal length of 300mm or less, are comparable in significance to plate measuring errors for cameras of focal length near 600mm, and are actually of greater significance than plate measuring errors for cameras of focal length of 1000mm or more. It is accordingly clear that, when the GC is used, a plate reduction which throws all of the adjustment on the plate coordinates may be unrealistic with cameras of moderately long focal length.

Because of its early mean epoch, the accuracies of the GC for a current epoch are appreciably lower than those of some of the more modern catalogues. We have summarized in Table 1 a number of pertinent characteristics of the major star catalogs of potential value for ballistic camera plate reductions. The accuracies quoted are adopted from papers of Eichhorn [5] and Scott [6],[7]. It should be appreciated that the compilation of many catalogues has consumed decades and that, therfore, the mean epoch may shift significantly from zone to zone. Thus, it is sometimes difficult and misleading to abstract a single figure to characterize the accuracy of a given catalogue. For this reason we suggest that the reader consult the papers cited above for more detailed and comprehensive treatments of the subject of star catalogues and their accuracies.

TABLE 1. SUMMARY OF DISTRIBUTION AND CURRENT ACCURACIES OF MAJOR STAR CATALOGUES

Catalog (1)	Mean Epoch (2)	No. of Stars (3)	Coverage in Declination (4)	Av. Dens. Stars/ Deg^2 (5)	Typical RMS Error for yr. 1965 (6)	Equivalent Plate coordinate RMS Error of Column (6) Expressed in Microns for Cameras of Focal Length:					
						300mm (7)	600mm (8)	1000mm (9)	1500mm (10)	2000mm (11)	3000mm (12)
1. GC (Boss)	1900	33,000	-90° to +90°	0.8	0".66	1.0	1.9	3.2	4.8	6.4	9.6
2. Cape	1932	80,000	-30° to -64°	9.5	0".55	0.8	1.6	2.7	4.0	5.3	8.0
3. Yale	1936	145,000	-30° to +30°	6.9	0".45	0.6	1.3	2.2	3.3	4.4	6.5
4. N30	1930	5,300	-90° to +90°	0.13	0".21	0.3	0.6	1.0	1.5	2.0	3.0
5. AGK3	1961	180,000	- 2° to +90°	8.3	0".15	0.2	0.4	0.7	1.1	1.4	2.2
6. FK4	1920	1,500	-90° to +90°	0.04	0".12	0.2	0.3	0.6	0.9	1.2	1.7

Remarks

(1) Yale Zones +50 to +60° and +85° to +90° have been completed but are not included in this summary.

(2) AGK3 is expected to be available in 1964. Extension of AGK3 to include entire southern hemisphere is goal of Southern Astrometric Program of the International Astronomical Union. Results are expected to be available by early 1970's.

(3) Extension of both Yale and Cape Catalogues to the Southern Pole is in progress.

In Table 1 we have also listed for cameras of various focal length the plate measuring error which is equivalent to catalogue error listed in column (6). Those entries of columns (7) - (12) which are one micron or greater (and, hence, are significant relative to attainable plate measuring accuracies) lie above the heavy, stepped line crossing the columns. We see that errors of even the best of the catalogues assume significance as focal lengths approach 2000mm. When the AGK-3 is published in 1964, the northern hemisphere of the celestial sphere will be covered with high density and high accuracy. Correspondingly dense coverage of the southern hemisphere, however, depends largely on the Yale and Cape Catalogues. Inasmuch as current accuracies of the Yale and Cape Catalogues are generally only one-half to one-third as great as those of the AGK-3, the problem of catalogue errors for the southern hemisphere will remain highly significant for long focus ballistic cameras until the completion of the Southern Astrometric Program towards the end of this decade.

From the foregoing it is clear that a truly rigorous plate reduction for long focus ballistic cameras must take into account not only random errors in plate coordinates, but also random errors in stellar control. The fact that each star carried as control can give rise to several successive images provides the means for the effective separation of plate measuring error from catalogue error, for the effects of catalogue error are essentially constant for all images of a given star, whereas those of plate measuring error are independent from image to image. We shall exploit this fact in our derivation of the Advanced Plate Reduction.

3.0 ATMOSPHERIC REFRACTION

Atmospheric refraction of the stellar control carried in ballistic camera reduction is rarely a significant problem for zenith distances less than 70°. This is true even though only very nominal corrections for refraction may have been applied. The reason stems from the fact that the relative refraction of points on a ballistic camera plate can be expressed to the first order as a linear combination of the elements of orientation. This means that the elements of orientation resulting from a stellar calibration can readily compensate for moderate errors in the refraction corrections

applied to the stellar directions. In particular, the calibrated principal distance and the calibrated zenith distance of the camera axis act in concert to compensate for residual refraction. However, as zenith distances increase beyond 70°, the elements of orientation rapidly lose their ability to compensate for uncorrected refraction. It is not unusual for ballistic camera observations to be made at zenith distances in excess of 70°. Indeed, observations of missile re-entries or of flashing lights for determination of the azimuth of Hiran lines are made to within a few degrees of the horizon. Thus, the problem of refraction for great zenith distances is of more than academic interest. We shall, therefore, accord it full consideration in the Advanced Plate Reduction.

In order to provide the mathematical model for the plate reduction with the necessary freedom to account fully for the relative refractive displacements of stars at great zenith distances, we must incorporate a sufficiently comprehensive refractive model. The conventional model for atmospheric refraction is of the form

$$(3.1) \qquad \delta\zeta = \sum_{i=0}^{\infty} p_i \tan^{2n+1}\zeta \quad ,$$

where $\delta\zeta$ denotes the astronomical refraction corresponding to the observed zenith distance ζ and the p_i are coefficients depending on the structure of the atmosphere. The model may also be expressed with the true, rather than the observed, zenith distance as the argument of the expansion. It then assumes the form

$$(3.2) \qquad \delta z = \sum_{i=0}^{\infty} q_i \tan^{2n+1} z \quad ,$$

where δz is the astronomical refraction corresponding to the true zenith distance z and the q_i are appropriate coefficients. If $\delta\zeta$ and δz are taken as positive quantities, we have by definition,

$$(3.3) \qquad \zeta = z + \delta z,$$

$$(3.4) \qquad z = \zeta - \delta\zeta \quad .$$

The above expansions for refraction become impractical for points near the horizon, inasmuch as $\tan\zeta$ and $\tan z$ increase without limit as ζ and z approach 90° (the series are nonetheless convergent since the coefficients p_i, q_i approach zero more rapidly than the powers of $\tan\zeta$ and $\tan z$ approach infinity). A more powerful and convenient expansion for astronomical refraction is that of Garfinkel [8]. With the observed zenith distance as the implicit argument, Garfinkel's expansion assumes the form

$$(3.5) \qquad \delta\zeta = \sum_{i=0}^{\infty} f_i \tan^{2n+1}\Phi \quad ,$$

where $\tan\Phi$ is an auxiliary function computed as follows from the observed zenith distance:

$$(3.6) \qquad \tan 2\Phi = \frac{1}{\gamma_0} \tan\zeta \quad ,$$

or, alternatively,

$$(3.7) \qquad \tan\Phi = (1 + \gamma_0^2 \cot^2\zeta)^{\frac{1}{2}} - \gamma_0 \cot\zeta \quad ,$$

in which γ_0 is an atmospheric constant equal to

$$(3.8) \qquad \gamma_0 = 8.16(273/T_0)^{\frac{1}{2}} \quad ,$$

where T_o is the temperature in degrees Kelvin at the observing station. Garfinkel's expansion may also be expressed with the true zenith distance as the implicit argument. In this case, one has

$$(3.9) \qquad dz = \sum_{i=\Phi}^{\infty} \eta_i \tan^{2n+1}\hat{\Phi} \quad ,$$

in which

$$(3.10) \qquad \tan 2\hat{\Phi} = \frac{1}{\gamma_0} \tan z \quad ,$$

or

$$(3.11) \qquad \tan \hat{\Phi} = (1 + \gamma_0^2 \cot^2 z)^{\frac{1}{2}} - \gamma_0 \cot z \quad ,$$

where γ_0 is as above.

The writer demonstrated in [9] that four terms of Garfinkel's expansion are functionally capable of representing astronomical refraction to accuracies on the order of a few tenths of a second of arc for all zenith distances from 0° to 90°. For instance, the writer found that, when four terms of the expansion were fitted by least squares to sets of actual refraction data for several different nights (Strand [10]), a mean error of fit of less than 0".2 resulted in every case, even though each sample included values of refraction at intervals of 2° for zenith distances down to and including 90°. The writer has consistently obtained similar results from least squares fits of Garfinkel's expansion to the results of extensive ray tracing through actual atmospheres sampled by balloonsondes. Even with refractive profiles affected by severe temperature inversions, four terms of Garfinkel's expansion have been found to yield rms accuracies of 0".2 or better for zenith distances to 90°. It follows that Garfinkel's expansion provides an exceptionally compact and flexible model for atmospheric refraction. Accordingly, we shall incorporate four terms of the expansion in the Advanced Plate

Reduction in order to accommodate zenith distances as great as 90°.

In [8] Garfinkel provides tables for the computation of astronomical refraction for any given observed zenith distance ζ and for any specified temperature (T), pressure (P) and height (h) at the observing station. By making several entries for different zenith distances, one can construct a refraction table appropriate to the observational situation. The coefficients of Garfinkel's expansion may then be estimated by fitting the expansion to the entries of the table. The absolute accuracy of such a refraction function is likely to be on the order of ±1 per cent. In view of the compensative capabilities of the elements of orientation, this is unquestionably adequate for zenith distances as great as 70°; only for zenith distances greater than 70° is there any merit in allowing adjustment of the coefficients of the expansion. For this reason, in the Advanced Plate Reduction, we shall constrain the values of the coefficients of Garfinkel's expansion resulting from the adjustment to be statistically consistent with the pre-computed values. As a practical matter, this means that the precomputed coefficients will undergo significant adjustment only for plates having stars at substantial zenith distances. At the higher zenith distances, refractive coefficients are essentially superfluous in a plate reduction, inasmuch as the elements of orientation alone are adequate to compensate for residual refraction. Here the inclusion of refractive coefficients as unknowns would ordinarily lead to an indeterminate or nearly indeterminate set of normal equations. By constraining the refractive coefficients resulting from the plate reduction to be statistically consistent with precomputed values, one obviates this tendency towards indeterminacy at small and moderate zenith distances and, at the same time, automatically allows the coefficients sufficient freedom for adjustment at great zenith distances.

4.0 SYMMETRIC RADIAL DISTORTION

The distortion of a perfectly centered lens whose axis is normal to the photographic plate is symmetrical about the principal point and is, consequently, a function of radial distance only. As the writer pointed out in [4], the distortion function δ is of the following form when the principal distance c is carried as an unknown in the plate reduction:

$$(4.1) \qquad \delta = k_1 r^3 + k_2 r^5 + k_3 r^7 + \ldots ,$$

where r is the radial distance (from the principal point) and the k's are the coefficients of distortion. The single coefficient k_1 is sufficient to account for the distortion of most simple lenses over their usable field. However, we have found that modern highly corrected lenses are likely to require the fifth and even the seventh order coefficients. Three coefficients of the expansion have proven adequate for all ballistic cameras encountered to date.

In the event that it is desired to enforce a specified principal distance in the plate reduction, the distortion function must assume the form

$$(4.2) \qquad \delta' = k'_0 r + k'_1 r^3 + k'_2 r^5 + k'_3 r^7 + \ldots .$$

If c denotes the principal distance associated with δ and $c' = c + \Delta c$ denotes the principal distance associated with δ', it follows from [4] that

$$(4.3) \qquad \delta' = \left(1 + \frac{\Delta c}{c}\right) \delta + \frac{\Delta c}{c} r ,$$

from which

$$(4.4) \qquad k'_0 = \frac{\Delta c}{c} , \quad k'_1 = \left(1 + \frac{\Delta c}{c}\right) k_1 , \quad k'_2 = \left(1 + \frac{\Delta c}{c}\right) k_2 , \quad \text{etc.}$$

This emphasizes that a distortion function is meaningful only when its associated principal distance is specified. The term $k'_0 r$ in (4.2) is equivalent to a constant scale factor. Therefore, one cannot arbitrarily carry both k'_0 and c' as unknowns in a plate reduction, for both parameters perform precisely the same function in the model; to do so would lead to an indeterminate set of normal equations. Accordingly, if the principal distance is carried as an unknown, the associated distortion function must be of the form (4.1); the form (4.2) may be used only if an arbitrary value of the principal distance is enforced. It is essentially immaterial which approach is taken, for the results of the one can be transformed to correspond to the other.

Because radial distortion is ideally invariant for a given lens, it is common practice to calibrate the coefficients of distortion in special massive reductions involving 150 to 200 or more stellar images. This generally yields a distortion function having a mean error of better than one micron at the extremities of the field. Such a function can be enforced in routine reductions without introducing significant error. From time to time the calibration of distortion may be repeated as a measure of quality control.

The rigorous determination of coefficients of distortion as an integral part of a ballistic camera reduction was first derived by the writer in [4]. We shall incorporate this solution into the Advanced Plate Reduction. In a later section, we shall take up the problem of the determination of the tangential and asymmetric radial distortion introduced by an imperfectly centered lens.

5.0 PARAMETERIZATION OF DIFFERENTIAL BIAS

Certain aspects of the rationale of the Advanced Plate Reduction are best understood through a consideration of the character of a typical stellar trace on a ballistic camera plate. In Figure 1 we have presented a sketch of a stellar trace optimized for a 1000mm camera for declinations between ±60°. The time scale associated with the trace indicates the relative durations of the shutter openings and closings. The sequence of exposures constituting the "precalibration" begins a few minutes before the tracking observations are to be made and consists, for the case depicted in Figure 1, of two repetitions of a basic cycle consisting of

(1) a ten second exposure leading to a short trail,
(2) a one second break,
(3) a ten second exposure leading to a second short trail,
(4) a ten second break,
(5) a one second exposure,
(6) a ten second break,
(7) a one-half second exposure,
(8) a ten second break,

(9) a one-quarter second exposure,

(10) a ten second break,

(11) a one-eighth second exposure,

(12) a ten second break.

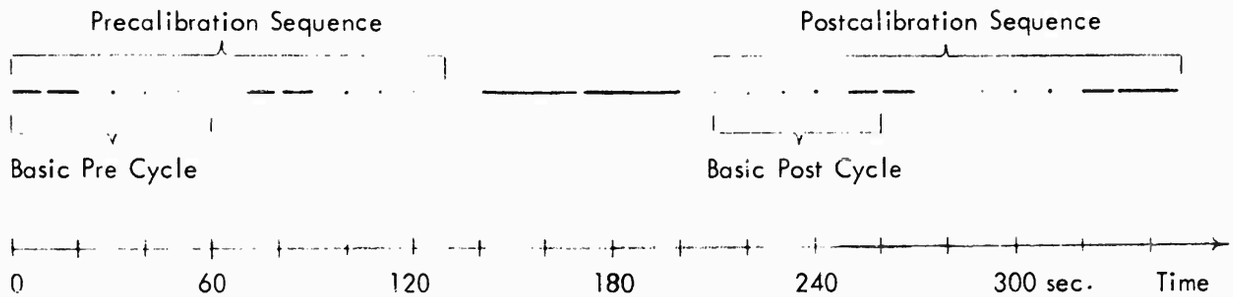

FIGURE 1. Sketch of typical stellar trace reflecting recommended exposure sequence for camera of 1000 mm focal length (7X enlargement).

Immediately after the completion of the precalibration, the camera shutter is opened to record the object being tracked (usually a flashing light beacon carried by a missile, a satellite or an aircraft). At approximately the center of the programmed tracking interval, the camera is closed for one second, thereby creating a short break which serves to provide a special check on the stability of the camera. Immediately after the completion of the tracking observations, the sequence of exposures constituting the "postcalibration" is performed. This sequence is usually the reverse of that employed in the precalibration, although reversal is by no means essential and is perhaps more aesthetic than functional. The final trail of the postcalibration is normally longer than the initial trail of the precalibration in order to indicate at a glance the direction of stellar motion.

We see that the stellar trace of Figure 1 contains a total of 21 potential control points, consisting of 5 breaks and 16 punctiform images. In most cases, the set of punctiform images of most nearly optimal quality (40 to 60 micron diameter) would be selected from each basic cycle of exposures for measurement. Thus, normally, four images would be measured on each trace, two from the precalibration and two from the

postcalibration. Stars of fainter magnitude are unlikely to yield punctiform images suitable for measurement. With the PC-1000, for instance, stars of 7th to 9th magnitude normally produce well-defined trails (and, hence, well-defined breaks as well), but only marginal punctiform images (if any). Therefore, the centers of breaks provide the only usable control points on the traces of fainter stars. While well-defined breaks can be measured with high precision, their inclusion in a reduction with punctiform images creates a potential problem stemming from the possibility of the existence of a significant personal bias in the measurements of breaks relative to points. Personal bias is of no consequence in a plate reduction provided that it is constant for all points, for then it has no effect on the relative positions of the measured points. For this reason, pains are taken in the selection of control to insure that the stellar images are of uniform quality closely matching the characteristics of the images of flashes (ideally, these would be so exposed as to be of optimal quality). When stellar breaks are also employed for control, one has no insurance that the personal bias in measurements of breaks will be the same as for points. Since the characteristics of stellar breaks are entirely different from those of punctiform images, personal bias for breaks and points may even be of opposite direction. Accordingly, appropriate provisions must be made for the problem of differential personal bias if different classes of control points are to be rigorously employed in a common reduction.

The classical way around the difficulty of differential personal bias involves the measurement of the plate in two positions, one rotated 180° with respect to the other. If the differential personal bias is persistent, it will then be removed when the two sets of measurements are averaged (after one set has been transformed into the coordinate system of the other). An equivalent, but more convenient, solution can be effected if the viewing system of the comparator incorporates a selectable reversing prism. Here, measurements would be made both with and without the reversing prism in position. Either approach doubles the measuring effort and may be self-defeating to the extent that personal bias may gradually be altered by measuring fatigue.

In our formulation of the Advanced Plate Reduction, we have adopted an alternative approach to the problem of differential bias in order to avoid the need for direct and reversed measurements. The approach consists of carrying the mean bias of breaks relative to points as additional unknowns in the plate reduction. The plate coordinates x_i, y_i for the ith point are expressed as

$$x_i = \bar{x}_i + \xi_i \Delta x \quad ,$$

$$y_i = \bar{y}_i + \xi_i \Delta y \quad ,$$

in which

$\bar{x}_i, \bar{y}_i$ are the measured plate coordinates,

Δx, Δy are the unknown mean biases of measured breaks relative to measured points,

$\xi_i = 0$ if the ith image is a point,

$\xi_i = 1$ if the ith image is a break.

In general, Δx and Δy will not exceed a few microns in absolute value. This knowledge may be exploited in the adjustment by treating Δx, Δy as if they were observations having values of zero and standard deviations $\sigma_{\Delta x}$, $\sigma_{\Delta y}$ of perhaps three microns. Thus constrained, the differential biases $\Delta x, \Delta y$ could easily adjust to any value within the range ± 3 microns, but would strongly be constrained from adjusting to a value as large as, say, 10 microns.

The parameterization of differential personal bias in the plate reduction can be convenient even when only one type of image is measured. For instance, in a reduction requiring an exceptionally large number of points (as in a definitive calibration of radial and tangential distortion), parameterization of personal bias would make it permissible for one individual to measure some of the points and another to measure the remainder (here the differential personal bias would be that of one individual relative to another). The parameterization of differential bias is also a powerful

diagnostic tool in fine-grained, statistical investigations of the internal consistency of one class of measured points relative to another. Although it is possible in principle to carry more than one set of differential biases in the reduction, we feel that inclusion of more than one set would unduly burden the Advanced Plate Reduction.

6.0 THE OBSERVATIONAL EQUATIONS

We are now in a position to consider the general observational equations for the plate reduction. Following the notation of reference [9], we begin with the fundamental projective equations

$$x = x_p + c\,\frac{A\lambda + B\mu + C\nu}{D\lambda + E\mu + F\nu}\,,$$

(6.1)

$$y = y_p + c\,\frac{A'\lambda + B'\mu + C'\nu}{D\lambda + E\mu + F\nu}\,,$$

in which

x, y	=	plate coordinates of image point,
λ, μ, ν	=	direction cosines of object point in arbitrary Cartesian frame,
x_p, y_p	=	plate coordinates of principal point,
c	=	principal distance,
$\begin{bmatrix} A & B & C \\ A' & B' & C' \\ D & E & F \end{bmatrix}$	=	orthogonal orientation matrix defining the rotational relationship between x,y,z axes of image space and the X,Y,Z axes of object space.

As in [9] we shall find it convenient to define our X,Y,Z system so that the origin is at the center of projection, the positive Z axis passes through the zenith and the positive X and Y axes pass through the East and North points of the horizon. Let ψ, ω, κ denote the angular elements of orientation of the camera corresponding to α, ω, κ defined in [9] (ψ = azimuth, ω = elevation, κ = roll). Then the orientation matrix may be expressed as the product of three rotations:

$$(6.2)\qquad \begin{bmatrix} A & B & C \\ A' & B' & C' \\ D & E & F \end{bmatrix} = \begin{bmatrix} -\cos\kappa & \sin\kappa & 0 \\ \sin\kappa & \cos\kappa & 0 \\ 0 & 0 & 1 \end{bmatrix} \begin{bmatrix} 1 & 0 & 0 \\ 0 & -\sin\omega & \cos\omega \\ 0 & \cos\omega & \sin\omega \end{bmatrix} \begin{bmatrix} \cos\psi & -\sin\psi & 0 \\ \sin\psi & \cos\psi & 0 \\ 0 & 0 & 1 \end{bmatrix} .$$

If we define

$$(6.3)\qquad \begin{aligned} s_1 &= \sin\psi, & s_2 &= \sin\omega, & s_3 &= \sin\kappa, \\ c_1 &= \cos\psi, & c_2 &= \cos\omega, & c_3 &= \cos\kappa, \end{aligned}$$

this reduces to

$$(6.4)\qquad \begin{bmatrix} A & B & C \\ A' & B' & C' \\ D & E & F \end{bmatrix} = \begin{bmatrix} -c_1c_3 - s_1s_2s_3 & s_1c_3 - c_1s_2s_3 & c_2s_3 \\ c_1s_3 - s_1s_2s_3 & -s_1s_3 + c_1s_2c_3 & c_2c_3 \\ s_1c_2 & c_1c_2 & s_2 \end{bmatrix} .$$

Let A, z denote the local azimuth and zenith distance of the unrefracted ray to a stellar control point of hour angle H and declination δ and let δz denote the refraction of the ray (δz is taken as a positive quantity). Then the local direction cosines of the observed ray may be written

$$(6.5)\qquad \begin{bmatrix} \lambda \\ \mu \\ \nu \end{bmatrix} = \begin{bmatrix} \sin A \sin(z-\delta z) \\ \cos A \sin(z-\delta z) \\ \cos(z-\delta z) \end{bmatrix}$$

If Φ denotes the latitude of the station and τ the sidereal time of the stellar observation, we may express the direction cosines λ', μ', ν' of the true (unrefracted) ray as

$$(6.6)\qquad \begin{bmatrix} \lambda' \\ \mu' \\ \nu' \end{bmatrix} = \begin{bmatrix} -1 & 0 & 0 \\ 0 & -\sin\Phi & \cos\Phi \\ 0 & \cos\Phi & \sin\Phi \end{bmatrix} \begin{bmatrix} \sin H \cos\delta \\ \cos H \cos\delta \\ \sin\delta \end{bmatrix}$$

or, since $H = \tau - \alpha$, where α is the right ascension of the star,

$$(6.7) \qquad \begin{bmatrix} \lambda' \\ \mu' \\ \nu' \end{bmatrix} = \begin{bmatrix} -1 & 0 & 0 \\ 0 & -\sin\Phi & \cos\Phi \\ 0 & \cos\Phi & \sin\Phi \end{bmatrix} \begin{bmatrix} -\cos\tau & \sin\tau & 0 \\ \sin\tau & \cos\tau & 0 \\ 0 & 0 & \end{bmatrix} \begin{bmatrix} \sin\alpha & \cos\delta \\ \cos\alpha & \cos\delta \\ & \sin\delta \end{bmatrix} .$$

Equation (6.5) may be put in the form

$$(6.8) \qquad \begin{bmatrix} \lambda \\ \mu \\ \nu \end{bmatrix} = \begin{bmatrix} \cos\delta z & 0 & -\sin A \sin\delta z \\ 0 & \cos\delta z & -\cos A \sin\delta z \\ \sin A \sin\delta z & \cos A \sin\delta z & \cos\delta z \end{bmatrix} \begin{bmatrix} \sin A \sin z \\ \cos A \sin z \\ \cos z \end{bmatrix} .$$

But the true direction cosines λ', μ', ν', are defined by the expression

$$(6.9) \qquad \begin{bmatrix} \lambda' \\ \mu' \\ \nu' \end{bmatrix} = \begin{bmatrix} \sin A \sin z \\ \cos A \sin z \\ \cos z \end{bmatrix} .$$

Hence, the direction cosines of the observed ray to a star are related to its right ascension and declination (α, δ) at the instant of exposure by the matrix equation

$$(6.10) \qquad \begin{bmatrix} \lambda \\ \mu \\ \nu \end{bmatrix} = \begin{bmatrix} \cos\delta z & 0 & -\sin A \sin\delta z \\ 0 & \cos\delta z & -\cos A \sin\delta z \\ \sin A \sin\delta z & \cos A \sin\delta z & \cos\delta z \end{bmatrix} \begin{bmatrix} 1 & 0 & 0 \\ 0 & -\sin\Phi & \cos\Phi \\ 0 & \cos\Phi & \sin\Phi \end{bmatrix}$$

$$\begin{bmatrix} -\cos\tau & \sin\tau & 0 \\ \sin\tau & \cos\tau & 0 \\ 0 & 0 & 1 \end{bmatrix} \begin{bmatrix} \sin\alpha \cos\delta \\ \cos\alpha \cos\delta \\ \sin\delta \end{bmatrix} .$$

It should not be overlooked that the azimuth A in the above expression is actually an implicit function of α, δ, Φ and τ and would normally be computed from

$$\sin A = \lambda'/\sin z \quad ,$$

(6.11)

$$\cos A = \mu'/\sin z \quad ,$$

where

(6.12) $$\sin z = (1 - (\nu')^2)^{\frac{1}{2}} \ ,$$

and where λ', μ', ν' are in turn computed from (6.7). The particular merit of the form of the relationship (6.10) is that the azimuth appears only in first order terms (since $\sin \delta z$ is of the first order). This greatly simplifies the linearization of the observational equations, for the implicit dependence of A on α, δ may be ignored in the differentiation of λ, μ, ν with respect to α, δ (such differentiation will ultimately be required inasmuch as we shall consider α, δ as subject to error)

As we have seen, the astronomical refraction corresponding to the true zenith distance z is given by the truncated expansion

(6.13) $$\delta z = \eta_1 \tan\theta + \eta_2 \tan^3\theta + \eta_3 \tan^5\theta + \eta_4 \tan^7\theta$$

in which

(6.14) $$\tan\theta = (1 + \gamma_0^2 \cot^2 z)^{\frac{1}{2}} - \gamma_0 \cot z \quad .$$

The substitution of the above expansion for δz into (6.10) introduces the refraction coefficients η_1, η_2, η_3, η_4 into the direction cosines λ, μ, ν and, thence, into the basic projective equations (6.1).

The x, y coordinates in the equations (6.1) were implicitly assumed to be free of distortion. If $\bar{x}, \bar{y}$ denote the distorted plate coordinates, we may write

$$
(6.15) \qquad
\begin{aligned}
x - x_p &= \left(1 + \frac{D}{r}\right)(\bar{x} - x_p) = (1 + k_1 r^2 + k_2 r^4 + k_3 r^6 + \ldots)(\bar{x} - x_p) , \\
y - y_p &= \left(1 + \frac{D}{r}\right)(\bar{y} - y_p) = (1 + k_1 r^2 + k_2 r^4 + k_3 r^6 + \ldots)(\bar{y} - y_p) ,
\end{aligned}
$$

in which

$$
(6.16) \qquad r = [(\bar{x} - x_p)^2 + (\bar{y} - y_p)^2]^{\frac{1}{2}} .
$$

The substitution of equations (6.15) into the projective equations (6.1) introduces the coefficients of distortion k_1, k_2, k_3 into the observational equations.

In order to handle the problem of differential bias of one class of points relative to another (usually of breaks relative to points), we replace $\bar{x}, \bar{y}$ in (6.15) and (6.16) by $\bar{x} + \xi \Delta x$, $\bar{y} + \xi \Delta y$, where, as indicated in Section 5, ξ is zero for one of the two classes of points and unity for the other.

Collecting foregoing results and introducing the convenient projective constant K, we may express the basic projective equations (6.1) for the ith measured image of the jth star as

$$
(6.17)\quad \begin{bmatrix} (1+\frac{D_{ij}}{r_{ij}})(\bar{x}_{ij}+\xi_{ij}\Delta x-x_p) \\ \\ (1+\frac{D_{ij}}{r_{ij}})(\bar{y}_{ij}+\xi_{ij}\Delta y-y_p) \\ \\ c \end{bmatrix} = K_{ij} \begin{bmatrix} -\cos\kappa & \sin\kappa & 0 \\ \sin\kappa & \cos\kappa & 0 \\ 0 & 0 & 1 \end{bmatrix} \begin{bmatrix} 1 & 0 & 0 \\ 0 & -\sin\omega & \cos\omega \\ 0 & \cos\omega & \sin\omega \end{bmatrix} \begin{bmatrix} \cos\psi & \sin\psi & 0 \\ \sin\psi & \cos\psi & 0 \\ 0 & 0 & 1 \end{bmatrix}
$$

$$
\begin{bmatrix} \cos\delta z_{ij} & 0 & -\sin A_{ij}\sin\delta z_{ij} \\ 0 & \cos\delta z_{ij} & -\cos A_{ij}\sin\delta z_{ij} \\ \sin A_{ij}\sin\delta z_{ij} & \cos A_{ij}\sin\delta z_{ij} & \cos\delta z_{ij} \end{bmatrix}
$$

$$
\begin{bmatrix} 1 & 0 & 0 \\ 0 & -\sin\Phi & \cos\Phi \\ 0 & \cos\Phi & \sin\Phi \end{bmatrix} \begin{bmatrix} -\cos\tau_{ij} & \sin\tau_{ij} & 0 \\ \sin\tau_{ij} & \cos\tau_{ij} & 0 \\ 0 & 0 & 1 \end{bmatrix} \begin{bmatrix} \sin\alpha_j\cos\delta_j \\ \cos\alpha_j\cos\delta_j \\ \sin\delta_j \end{bmatrix}.
$$

In these equations

$\bar{x}_{ij}, \bar{y}_{ij}$	are obtained by direct measurement,
α_{ij}, δ_{ij}	are computed from data taken from a star catalogue and current ephemeris,
τ_{ij}	is obtained from the reduction of recorded timing measurements of shutter openings and closings,
ξ_{ij}	is specified for each measured point (according to its classification),
Φ	is a station constant.

The following unknowns are explicit in (6.17):

ψ, ω, κ - the rotational elements of exterior orientation;

x_p, y_p, c - the elements of interior orientation (x_p, y_p are also implicit in D_{ij}/r_{ij});

$\Delta x, \Delta y$ - the differential biases in x, y measurements of different classes of points;

The following unknowns are implicit in the terms D_{ij} , δz_{ij} :

k_1, k_2, k_3 - the coefficients of distortion,

$\eta_1, \eta_2, \eta_3, \eta_4$ - the coefficients of refraction.

The projective constant K_{ij} may be eliminated by dividing the last of the three matrix equations implicit in (6.17) into the first two. Thus, we see that each pair of plate measurements gives rise to two independent equations involving as many as fifteen physically meaningful unknowns. In the absence of errors of any kind, the measurement of a sufficient number of well distributed images will lead to a sufficient number of equations to effect a solution for the unknowns, provided that the system is inherently determinate. The matter of determinacy is important, for it is by no means assured merely because the number of equations equals (or exceeds) the number of unknowns. For instance, one easily sees that, when the camera is in a zenith orientation, it becomes impossible to separate the coefficients of distortion from those of refraction (in this case, the atmosphere becomes, in effect, an additional, properly centered element of the lens).

Because all of the unknown parameters in the projective model have a physical interpretation, the attractive possibility arises of constraining the adjustment resulting from the use of the projective equations to be consistent (in a statistical sense) with specified a priori values of any of the parameters. The rotational elements of orientation ψ, ω, κ, for instance, would ordinarily be known in advance to an accuracy ranging from a few tenths of a degree from a camera mount of nominal precision (such as that of the PC-1000) to perhaps as good as ten seconds of arc from a mount of high precision (such as that of the BC-4). Similarly, the elements of interior orientation x_p, y_p, c may well be known in advance to a high degree of accuracy from previous calibrations. Differential biases $\Delta x, \Delta y$ should not depart from zero by more than a few microns. Coefficients of refraction $\eta_1, \eta_2, \eta_3, \eta_4$ computed according to Garfinkel's theory are probably accurate to about one per cent and most certainly are not off by more than two per cent. Coefficients of distortion k_1, k_2, k_3 may be known in advance to a certain degree from a previous calibration.

In order to be able to utilize a priori information in the plate reduction to whatever extent desired, we shall treat all parameters as if they were observed quantities. The reciprocals of the variances assigned to the a priori values of the parameters serve as weights in the adjustment. Therefore, zero weight may be assigned to any parameter which is to be unconstrained by a priori considerations.

7.0 THE LINEARIZED OBSERVATIONAL EQUATIONS

When K_{ij} is eliminated from (6.17), the resulting pair of equations may be considered to be of the functional form:

$$
(7.1) \qquad
\begin{aligned}
f_1(\bar{x}_{ij}, \bar{y}_{ij}, \alpha_j, \delta_j, u_1, u_2, \ldots, u_p) &= 0 , \qquad & i &= 1, 2, \ldots, n_j , \\
f_2(\bar{x}_{ij}, \bar{y}_{ij}, \alpha_j, \delta_j, u_1, u_2, \ldots, u_p) &= 0 , \qquad & j &= 1, 2, \ldots, n ,
\end{aligned}
$$

in which

$$
(7.2) \qquad
\begin{array}{lllll}
u_1 = \psi & u_4 = x_p & u_7 = \Delta x & u_9 = k_1 & u_{12} = \eta_1 \\
u_2 = \omega & u_5 = y_p & u_8 = \Delta y & u_{10} = k_2 & u_{13} = \eta_2 \\
u_3 = \kappa & u_6 = c & & u_{11} = k_3 & u_{14} = \eta_3 \\
 & & & & u_{15} = \eta_4 \quad .
\end{array}
$$

In (7.1) we have left ourselves uncommitted as to the number of unknown parameters. This is done for the sake of generality in order that the matrix representation of the adjustment will not be affected if parameters are added to or deleted from the model. In the event that certain parameters are deleted as unknowns, the numbering of the remaining parameters would be altered to preserve continuity of numbering.

In equations (7.1) the measured plate coordinates are subject to random errors; so are the right ascensions and declinations. The u's may on option be considered to be either measured quantities or completely unknown quantities. Because equations (7.1) are nonlinear, we shall employ a truncated Taylor's series to reduce them to linear form.

Accordingly, we write

$$
(7.3) \qquad \begin{aligned} \bar{x}_{ij} &= \bar{x}^0_{ij} + v_{1ij} \\ \bar{y}_{ij} &= \bar{y}^0_{ij} + v_{2ij} \end{aligned}
$$

where $\bar{x}^0_{ij}, \bar{y}^0_{ij}$ denote the measured plate coordinates for the ith measured image of the jth star, and v_{1ij}, v_{2ij} are the corresponding measuring residuals. For reasons to be made clear presently, in linearizing the projective equations we shall regard the right ascensions and declinations as unknown parameters rather than measured quantitites. Accordingly, we write

$$
(7.4) \qquad \begin{aligned} \alpha_j &= \alpha^{00}_j + \delta\alpha_j \\ \delta_j &= \delta^{00}_j + \delta\delta_j \quad , \qquad j = 1,2,\ldots,n \end{aligned}
$$

in which α^{00}_j, δ^{00}_j are arbitrary approximations to α_j, δ_j and $\delta\alpha_j$, $\delta\delta_j$ are the appropriate, but unknown corrections. In the linearization of the projective equations, we shall likewise treat all of the u_k as unknown parameters, even though some (or all) may be independently measured quantities. Thus, we write

$$
(7.5) \qquad u_k = u^{00}_k + \delta u_k \ , \qquad k = 1,2,\ldots,p
$$

where u^{00}_k are arbitrary approximations and the δu_k are appropriate, but unknown, corrections. The substitution of (7.3), (7.4), (7.5) into (7.1) puts the projective equations in the form

$$
(7.6)\qquad
\begin{aligned}
f_{1ij} &= f_1(\bar{x}^0_{ij} + v_{1ij},\ \bar{y}^0_{ij} + v_{2ij},\ \alpha^{00}_j + \delta\alpha_j,\ \delta^{00}_j + \delta\delta_j,\ u^{00}_1 + \delta u_1, \ldots, u^{00}_p + \delta u_p) = 0,\\
f_{2ij} &= f_2(\bar{x}^0_{ij} + v_{1ij},\ \bar{y}^0_{ij} + v_{2ij},\ \alpha^{00}_j + \delta\alpha_j,\ \delta^{00}_j + \delta\delta_j,\ u^{00}_1 + \delta u_1, \ldots, u^{00}_p + \delta u_p) = 0.
\end{aligned}
$$

Retaining the zero and first order terms of the Taylor's expansion of (7.6), we get

$$
(7.7)\qquad
\begin{aligned}
v_{1ij} + \dot{b}^1_{1ij}\,\delta u_1 + \dot{b}^2_{1ij}\,\delta u_2 + \ldots + \dot{b}^p_{1ij}\,\delta u_p + \ddot{b}^1_{1ij}\,\delta\alpha_j + \ddot{b}^2_{1ij}\,\delta\delta_j &= \epsilon_{1ij},\\
v_{2ij} + \dot{b}^1_{2ij}\,\delta u_1 + \dot{b}^2_{2ij}\,\delta u_2 + \ldots + \dot{b}^p_{2ij}\,\delta u_p + \ddot{b}^1_{2ij}\,\delta\alpha_j + \ddot{b}^2_{2ij}\,\delta\delta_j &= \epsilon_{2ij},
\end{aligned}
$$

in which

$$
(7.8)\qquad
\begin{aligned}
\epsilon_{1ij} &= -f_1(\bar{x}^0_{ij},\ \bar{y}^0_{ij},\ \alpha^{00}_j,\ \delta^{00}_j,\ u^{00}_1,\ u^{00}_2, \ldots, u^{00}_p)\\
\epsilon_{2ij} &= -f_2(\bar{x}^0_{ij},\ \bar{y}^0_{ij},\ \alpha^{00}_j,\ \delta^{00}_j,\ u^{00}_1,\ u^{00}_2, \ldots, u^{00}_p)
\end{aligned}
$$

and

$$
(7.9)\qquad \dot{b}^k_{1ij} = \left.\frac{\partial f_{1ij}}{\partial u_k}\right|_0, \qquad \dot{b}^k_{2ij} = \left.\frac{\partial f_{2ij}}{\partial u_k}\right|_0, \qquad k = 1,2,\ldots,p
$$

$$
(7.10)\qquad
\begin{aligned}
\ddot{b}^1_{1ij} &= \left.\frac{\partial f_{1ij}}{\partial \alpha_j}\right|_0, \qquad \ddot{b}^2_{1ij} = \left.\frac{\partial f_{1ij}}{\partial \delta_j}\right|_0,\\
\ddot{b}^1_{2ij} &= \left.\frac{\partial f_{2ij}}{\partial \alpha_j}\right|_0, \qquad \ddot{b}^2_{2ij} = \left.\frac{\partial f_{2ij}}{\partial \delta_j}\right|_0.
\end{aligned}
$$

In (7.9), (7.10) the symbol $\Big|_0$ is used to indicate that the partial derivatives are evaluated at the point $(\bar{x}^0_{ij}, \bar{y}^0_{ij}, \alpha^{00}_j, \delta^{00}_j, u^{00}_1, u^{00}_2, \ldots, u^{00}_p)$. We shall not concern ourselves here with the computational formulas for the partial derivatives, for their derivation is entirely straightforward.

The linearized projective equations for the ith measured image on the trace of the jth star may be put into the following matrix form

$$(7.11) \qquad v_{ij} + \dot{B}_{ij}\dot{\delta}_j + \ddot{B}_{ij}\ddot{\delta}_{ij} = \epsilon_{ij}$$

in which

$$(7.12) \qquad \underset{(2,1)}{v_{ij}} = \begin{bmatrix} v_{1ij} \\ v_{2ij} \end{bmatrix}, \quad \underset{(2,p)}{\dot{B}_{ij}} = \begin{bmatrix} \dot{b}^1_{1ij} & \dot{b}^2_{1ij} & \cdots & \dot{b}^p_{1ij} \\ \dot{b}^1_{2ij} & \dot{b}^2_{2ij} & \cdots & \dot{b}^p_{2ij} \end{bmatrix}, \quad \underset{(p,1)}{\dot{\delta}} = \begin{bmatrix} \delta u_1 \\ \delta u_2 \\ \cdot \\ \cdot \\ \cdot \\ \delta u_p \end{bmatrix},$$

$$\underset{(2,2)}{\ddot{B}_{ij}} = \begin{bmatrix} \ddot{b}^1_{1ij} & \ddot{b}^2_{1ij} \\ \ddot{b}^1_{2ij} & \ddot{b}^2_{2ij} \end{bmatrix}, \quad \ddot{\delta}_j = \begin{bmatrix} \delta\alpha_j \\ \delta\delta_j \end{bmatrix}, \quad \epsilon_{ij} = \begin{bmatrix} \epsilon_{1ij} \\ \epsilon_{2ij} \end{bmatrix}.$$

The set of $2n_j$ equations arising from the n_j images measured on the trace of the jth star may be written

$$(7.13) \qquad v_j + \dot{B}_j\dot{\delta}_j + \ddot{B}_j\ddot{\delta}_j = \epsilon_j \ .$$

wherein

$$(7.14)\quad \underset{(\bar{n}_j,1)}{v_j} = \begin{bmatrix} v_{1j} \\ v_{2j} \\ \vdots \\ v_{n_j j} \end{bmatrix}, \quad \underset{(\bar{n}_j,p)}{\dot{B}_j} = \begin{bmatrix} \dot{B}_{1j} \\ \dot{B}_{2j} \\ \vdots \\ \dot{B}_{n_j j} \end{bmatrix}, \quad \underset{(\bar{n}_j,2)}{\ddot{B}_j} = \begin{bmatrix} \ddot{B}_{1j} \\ \ddot{B}_{2j} \\ \vdots \\ \ddot{B}_{n_j j} \end{bmatrix}, \quad \underset{(\bar{n}_j,1)}{\epsilon_j} = \begin{bmatrix} \epsilon_{1j} \\ \epsilon_{2j} \\ \vdots \\ \epsilon_{n_j j} \end{bmatrix}$$

in which $\bar{n}_j = 2n_j$. Collecting the equations for all n stars, we have

$$(7.15)\quad v + \ddot{B}\delta + \ddddot{B}\delta = \epsilon$$

in which

$$(7.16)\quad \underset{(\bar{n},1)}{v} = \begin{bmatrix} v_1 \\ v_2 \\ \vdots \\ v_n \end{bmatrix}, \quad \underset{(\bar{n},p)}{\dot{B}} = \begin{bmatrix} \dot{B}_1 \\ \dot{B}_2 \\ \vdots \\ \dot{B}_n \end{bmatrix}, \quad \underset{(\bar{n},2n)}{\ddot{B}} = \begin{bmatrix} \ddot{B}_1 & 0 & \dots & 0 \\ 0 & \ddot{B}_2 & \dots & 0 \\ \vdots & \vdots & & \vdots \\ 0 & 0 & \dots & \ddot{B}_n \end{bmatrix}, \quad \underset{(2n,1)}{\ddot{\delta}} = \begin{bmatrix} \ddot{\delta}_1 \\ \ddot{\delta}_2 \\ \vdots \\ \ddot{\delta}_n \end{bmatrix}, \quad \underset{(\bar{n},1)}{\epsilon} = \begin{bmatrix} \epsilon_1 \\ \epsilon_2 \\ \vdots \\ \epsilon_n \end{bmatrix},$$

where $\bar{n}$ denotes the total number of equations

$$(7.17)\quad \bar{n} = \bar{n}_1 + \bar{n}_2 + \dots + \bar{n}_n = 2n_1 + 2n_2 + \dots + 2n_2.$$

We shall let Λ denote the covariance matrix of the observational vector associated with the full set of linearized projective equations. If we assume that the plate coordinates for different points are independent, Λ may be written

$$(7.18) \quad \underset{(\bar{n},\bar{n})}{\Lambda} = \begin{bmatrix} \Lambda_1 & 0 & \dots & 0 \\ 0 & \Lambda_2 & \dots & 0 \\ \vdots & \vdots & & \vdots \\ 0 & 0 & \dots & \Lambda_n \end{bmatrix}$$

in which Λ_j is the covariance matrix of the plate coordinates of the images on the jth stellar trace. Λ_j may, in turn, be written

$$(7.19) \quad \underset{(\bar{n}_j,\bar{n}_j)}{\Lambda_j} = \begin{bmatrix} \Lambda_{1j} & 0 & \dots & 0 \\ 0 & \Lambda_{2j} & \dots & 0 \\ \vdots & \vdots & & \vdots \\ 0 & 0 & \dots & \Lambda_{n_j j} \end{bmatrix}$$

in which Λ_{ij} denotes the covariance matrix of the plate coordinates $\bar{x}^0_{ij}, \bar{y}^0_{ij}$.
In order to allow the utmost flexibility in the choice of measuring method, we shall admit the possibility of correlation in the $\bar{x}$ and $\bar{y}$ coordinates of a given point. Thus, Λ_{ij} is considered to be of the form

$$(7.20) \quad \underset{(2,2)}{\Lambda_{ij}} = \begin{bmatrix} \sigma^2_{\bar{x}_{ij}} & \sigma_{\bar{x}_{ij}\bar{y}_{ij}} \\ \sigma_{\bar{x}_{ij}\bar{y}_{ij}} & \sigma^2_{\bar{y}_{ij}} \end{bmatrix}$$

The inverses of Λ, $\dot{\Lambda}_j$, and $\ddot{\Lambda}_{ij}$ will be denoted by W, $\dot{W}_j$, $\ddot{W}_{ij}$, respectively.

So far we have not used the fact that the right ascensions and declinations are actually measured quantities known to a high degree of accuracy. This information may be expressed by the following set of observational equations

$$
(7.21) \qquad \begin{aligned} \alpha_j &= \alpha_j^0 + v_{\alpha_j} , \\ \delta_j &= \delta_j^0 + v_{\delta_j} , \qquad j = 1,2,\ldots,n \end{aligned}
$$

in which α_j^0, δ_j^0 are the values computed from catalogue data and v_{α_j}, v_{δ_j} are the unknown random residuals associated with the "observed" right ascensions and declinations. Replacing α_j, δ_j in (7.21) by the values in (7.4), we get

$$
(7.22) \qquad \begin{aligned} v_{\alpha_j} - \delta\alpha_j &= \alpha_j^{00} - \alpha_j^0 , \\ v_{\delta_j} - \delta\delta_j &= \delta_j^{00} - \delta_j^0 . \end{aligned}
$$

These may be written

$$
(7.23) \qquad \ddot{v}_j - \ddot{\delta}_j = \ddot{\epsilon}_j
$$

in which $\ddot{\delta}_j$ is as in (7.12) and

$$
(7.24) \qquad \underset{(2,1)}{\ddot{v}_j} = \begin{bmatrix} v_{\alpha_j} \\ v_{\delta_j} \end{bmatrix} \qquad \underset{(2,1)}{\ddot{\epsilon}_j} = \begin{bmatrix} \alpha_j^{00} - \alpha_j^0 \\ \delta_j^{00} - \delta_j^0 \end{bmatrix} .
$$

It should be noted that since $\alpha_j^{00}, \delta_j^{00}$ are arbitrary initial approximations to α_j, δ_j, we may choose them to be equal to the observed values α_j^0, δ_j^0. This would reduce the elements of $\ddot{\epsilon}_j$ to zero. We have not done this because it may be necessary to iterate the adjustment in order to eliminate the effects of higher order terms neglected in the linearization of the projective equations. Although the initial approximations are wholly arbitrary, subsequent approximations are not arbitrary, but are determined by the preceding iterative cycles. It is to emphasize this fact that we do not regard $\ddot{\epsilon}_j$ as necessarily equal to zero, although at the outset this would ordinarily be the case.

Collecting all of the equations of the form(7.23), we have

$$(7.25) \qquad \ddot{v} - \ddot{\delta} = \ddot{\epsilon}$$

in which

$$(7.26) \qquad \underset{(2n,1)}{\ddot{v}} = \begin{bmatrix} \ddot{v}_1 \\ \ddot{v}_2 \\ \vdots \\ \ddot{v}_n \end{bmatrix}, \quad \underset{(2n,1)}{\ddot{\delta}} \begin{bmatrix} \ddot{\delta}_1 \\ \ddot{\delta}_2 \\ \vdots \\ \ddot{\delta}_n \end{bmatrix}, \quad \underset{(2n,1)}{\ddot{\epsilon}} = \begin{bmatrix} \ddot{\epsilon}_1 \\ \ddot{\epsilon}_2 \\ \vdots \\ \ddot{\epsilon}_n \end{bmatrix}.$$

The covariance matrix associated with the entire observational vector of right ascensions and declinations may be denoted by $\ddot{\Lambda}$. If errors in catalogued positions of different stars are regarded to be independent, we may write

$$(7.27) \qquad \underset{(2n,1)}{\ddot{\Lambda}} = \begin{bmatrix} \ddot{\Lambda}_1 & 0 & \dots & 0 \\ 0 & \ddot{\Lambda}_2 & \dots & 0 \\ \vdots & \vdots & & \vdots \\ 0 & 0 & \dots & \ddot{\Lambda}_n \end{bmatrix},$$

in which

$$(7.28) \qquad \underset{(2,2)}{\ddot{\Lambda}_j} = \begin{bmatrix} \sigma^2_{\alpha_j} & 0 \\ 0 & \sigma^2_{\delta_j} \end{bmatrix}$$

The variances $\sigma^2_{\alpha_j}$, $\sigma^2_{\delta_j}$ can be computed from information supplied in the star catalogue employed. In general

$$(7.29) \qquad \begin{aligned} \sigma^2_{\alpha_j} &= (\sigma^2_{\alpha_j})_{00} + (T - T_0)^2 \, \sigma^2_{\mu_{\alpha_j}} , \\ \sigma^2_{\delta} &= (\sigma^2_{\delta_j})_{00} + (T - T_0)^2 \, \sigma^2_{\mu_{\delta_j}} , \end{aligned}$$

in which

$(\sigma^2_{\alpha_j})_{00}, (\sigma^2_{\alpha_j})_{00}$ are the standard errors of the stellar position at the epoch T_0 of the catalogue,

$\sigma_{\mu_{\alpha_j}}$, $\sigma_{\mu_{\delta_j}}$ are the standard errors of the annual proper motion in α_j, δ_j,

T is the time in years of the observation.

We shall denote the inverses of $\ddot{\Lambda}$ and $\ddot{\Lambda}_j$ by $\ddot{W}$, $\ddot{W}_j$.

The additional information made available by a knowledge of a priori values of any of the parameters of the projective equations may be introduced through the incorporation of the appropriate set of observational equations. Let u^0_k denote the a priori value of the kth parameter. Then we may write

$$(7.30) \qquad u_k = u_k^0 + v_{u_k} \qquad (k = 1,2,\ldots,p).$$

in which v_{u_k} is the residual associated with the "observed" value of the kth parameter. Eliminating u_k, the adjusted value of the parameter, from equations (7.5) and (7.30), we get

$$(7.31) \qquad v_{u_k} - \delta_{u_k} = u_k^{00} - u_k^0 \qquad (k = 1,2,\ldots,p).$$

This entire system of observational equations may also be written

$$(7.32) \qquad \dot{v} - \dot{\delta} = \dot{\epsilon}$$

in which

$$(7.33) \qquad \underset{(p,1)}{\dot{v}} = \begin{bmatrix} v_{u_1} \\ v_{u_2} \\ \vdots \\ v_{u_p} \end{bmatrix}, \quad \underset{(p,1)}{\dot{\delta}} = \begin{bmatrix} \delta_{u_1} \\ \delta_{u_2} \\ \vdots \\ \delta_{u_p} \end{bmatrix}, \quad \underset{(p,1)}{\dot{\epsilon}} = \begin{bmatrix} u_1^{00} - u_1^0 \\ u_2^{00} - u_2^0 \\ \vdots \\ u_p^{00} - u_p^0 \end{bmatrix}.$$

As with the discrepancy vector $\ddot{\epsilon}$ for right ascensions and declinations, the initial discrepancy vector $\dot{\epsilon}$ for the projective parameters may be made equal to zero by the simple expedient of choosing each arbitrary initial approximation u_k^{00} to be equal to its specified a priori value u_k^0. Again, for presentational purposes we shall not require that this be done because in doing so one can easily lose sight of the fact that $\dot{\epsilon}$ will no longer be zero after the initial solution of the iterative process required to account for the higher order terms of the Taylor's expansion.

We shall let $\dot{\Lambda}$ denote the pxp covariance matrix of the vector of a priori values of the p parameters and shall let $\dot{W}$ denote its inverse. If the kth parameter is to be totally unconstrained, it is merely necessary to employ zeroes for all elements in the kth row and column of $\dot{W}$. On the other hand, the a priori value u_k^0 of an arbitrary parameter may be enforced by choosing u_k^{00} equal to u_k^0 and by setting $\dot{w}_{kk}$, the kth diagonal element of $\dot{W}$, equal to infinity (or to a practical computational equivalent).

8.0 THE MINIMUM-VARIANCE ADJUSTMENT

Now that all of the information available has been expressed in the form of observational equations, we are ready to consider the problem of adjustment. First, however, we shall consolidate our three basic sets of observational equations, namely,

$$
(8.1) \qquad \begin{aligned}
v + \dot{B}\dot{\delta} + \ddot{B}\ddot{\delta} &= \epsilon , \\
\dot{v} - \dot{\delta} &= \dot{\epsilon} , \\
\ddot{v} - \ddot{\delta} &= \epsilon ,
\end{aligned}
$$

into the single matrix equation

$$
(8.2) \qquad \bar{v} + \bar{B}\delta = \bar{\epsilon}
$$

in which

$$
(8.3) \qquad \underset{(N,1)}{\bar{v}} = \begin{bmatrix} v \\ \dot{v} \\ \ddot{v} \end{bmatrix} , \quad \underset{(N,P)}{\bar{B}} = \begin{bmatrix} \dot{B} & \ddot{B} \\ -I & 0 \\ 0 & -I \end{bmatrix} , \quad \underset{(P,1)}{\delta} = \begin{bmatrix} \dot{\delta} \\ \ddot{\delta} \end{bmatrix} , \quad \underset{(N,1)}{\bar{\epsilon}} = \begin{bmatrix} \epsilon \\ \dot{\epsilon} \\ \ddot{\epsilon} \end{bmatrix} .
$$

where

$$(8.4) \qquad N = \bar{n} + P, \qquad P = 2n + p .$$

Similarly we shall consolidate the three covariance matrices Λ, $\dot{\Lambda}$, $\ddot{\Lambda}$ and their associated inverses (or weight matrices), W, $\dot{W}$, $\ddot{W}$ into the composite matrices $\bar{\Lambda}$ and $\bar{W}$ where

$$(8.5) \qquad \underset{(N,N)}{\bar{\Lambda}} = \begin{bmatrix} \Lambda & 0 & 0 \\ 0 & \dot{\Lambda} & 0 \\ 0 & 0 & \ddot{\Lambda} \end{bmatrix} , \qquad \underset{(N,N)}{\bar{W}} = \begin{bmatrix} W & 0 & 0 \\ 0 & \dot{W} & 0 \\ 0 & 0 & \ddot{W} \end{bmatrix} .$$

Inasmuch as the consolidated system of observational equations (8.2) involves a total of N equations in $N+2n+p$ unknowns (N residuals in the vector $\bar{v}$ and $2n+p$ parameters in the vector δ), there are more unknowns than equations. Therefore, an infinite number of possible solutions exist. The writer has shown in [11] that if the observational errors have the multivariate normal distribution, the solution of maximum likelihood is that which satisfies the observational equations (8.2) while minimizing the quadratic form

$$(8.6) \qquad s = \underset{(1,N)}{\bar{v}^T} \; \underset{(N,N)}{\bar{W}} \; \underset{(N,1)}{\bar{v}} .$$

Even if the observational distribution is not multivariate normal, this solution will lead to unbiased estimates of the parameters having the smallest possible variances. Because the criterion of minimum variance does not require a knowledge of the observational distribution, we shall consider our subsequent results to constitute the minimum variance solution tothe problem at hand, understanding, of course, that they also constitute the maximum likelihood solution when the observational distribution is multivariate normal or the least squares solution when the covariance matrix of the multivariate normal distribution is diagonal.

The particular vector δ which leads to the residual vector minimizing the quadratic form s is shown in [11] to be defined by the system of normal equations

$$(8.7) \qquad \underset{(P,P)}{N} \; \underset{(P,1)}{\delta} = \underset{(P,1)}{c}$$

in which

$$(8.8) \qquad \underset{(P,P)}{N} = \underset{(P,N)}{\bar{B}^T} \; \underset{(N,N)}{\bar{W}} \; \underset{(N,P)}{\bar{B}} \; ,$$

$$(8.9) \qquad \underset{(P,1)}{c} = \underset{(P,N)}{\bar{B}^T} \; \underset{(N,N)}{\overline{W}} \; \underset{(N,1)}{\bar{\epsilon}} \; .$$

Once δ has been determined from the solution of (8.7), the residual vector v can be obtained from (8.2).

While the foregoing constitutes the formal solution to the problem at hand, it is not in a practical form because of the excessive order of the normal equations for a moderate number of stellar control points. For instance, if n were to equal 50 and p were to equal 15, the order of the normal equations would be $N = 2(50) + 15 = 115$. In view of this, our approach is clearly impractical unless vast simplifications can be effected. As we shall see, the structure of the normal equations is such that an altogether practical solution can be derived no matter how large N may be. The general nature of the solution is similar to that derived by the writer in [12] for the general problem of multistation analytical stereotriangulation.

By virtue of the partitioning of (8.3) and (8.5), the normal equations (8.7) can be put into the form

$$(8.10) \qquad \begin{bmatrix} \dot{N} & \bar{N} \\ \bar{N}^T & \ddot{N} \end{bmatrix} \begin{bmatrix} \dot{\delta} \\ \ddot{\delta} \end{bmatrix} = \begin{bmatrix} \dot{c} \\ \ddot{c} \end{bmatrix} ,$$

in which

$$\underset{(p,p)}{\dot{N}} = \underset{(p,\bar{n})}{\dot{B}^T} \underset{(\bar{n},\bar{n})}{W} \underset{(\bar{n},1)}{\dot{B}} + \underset{(p,p)}{\dot{W}} , \qquad \underset{(p,2n)}{\bar{N}} = \underset{(1,\bar{n})}{\dot{B}^T} \underset{(\bar{n},\bar{n})}{W} \underset{(\bar{n},2n)}{\ddot{B}} ,$$

$$(8.11) \qquad \underset{(2n,p)}{\bar{N}^T} = \underset{(2n,\bar{n})}{\ddot{B}^T} \underset{(\bar{n},\bar{n})}{W} \underset{(\bar{n},p)}{\dot{B}} , \qquad \underset{(2n,2n)}{\ddot{N}} = \underset{(2n,\bar{n})}{\ddot{B}^T} \underset{(\bar{n},\bar{n})}{W} \underset{(\bar{n},2n)}{\ddot{B}} + \underset{(2n,2n)}{\ddot{W}} ,$$

$$\underset{(p,1)}{\dot{c}} = \underset{(p,\bar{n})}{\dot{B}^T} \underset{(\bar{n},\bar{n})}{W} \underset{(\bar{n},1)}{\epsilon} - \underset{(p,p)}{\dot{W}} \underset{(p,1)}{\dot{\epsilon}} , \qquad \underset{(2n,1)}{\ddot{c}} = \underset{(2n,\bar{n})}{\ddot{B}^T} \underset{(\bar{n},\bar{n})}{W} \underset{(\bar{n},1)}{\epsilon} - \underset{(2n,2n)}{\ddot{W}} \underset{(2n,1)}{\ddot{\epsilon}} .$$

Employing the partitioning of (7.16), (7.18) and (7.27) in equations (8.11), we can express the normal equations (8.10) as

$$(8.12) \qquad \left[\begin{array}{c|cccc} \sum_{j=1}^{n} \dot{N}_j + \dot{W} & \bar{N}_1 & \bar{N}_2 & \cdots & \bar{N}_n \\ \hline \bar{N}_1^T & \ddot{N}_1 + \ddot{W}_1 & 0 & \cdots & 0 \\ \bar{N}_2^T & 0 & \ddot{N}_2 + \ddot{W}_2 & \cdots & 0 \\ \vdots & \vdots & \vdots & & \vdots \\ \bar{N}_n^T & 0 & 0 & \cdots & \ddot{N}_n + \ddot{W}_n \end{array}\right] \left[\begin{array}{c} \dot{\delta} \\ \hline \ddot{\delta}_1 \\ \ddot{\delta}_2 \\ \vdots \\ \ddot{\delta}_n \end{array}\right] = \left[\begin{array}{c} \sum_{j=1}^{n} \dot{c}_j - \dot{W}\dot{\epsilon} \\ \hline \ddot{c}_1 - \ddot{W}_1 \ddot{\epsilon}_1 \\ \ddot{c}_2 - \ddot{W}_2 \ddot{\epsilon}_2 \\ \vdots \\ \ddot{c}_n - \ddot{W}_n \ddot{\epsilon}_n \end{array}\right]$$

in which the broken lines partition the system in accordance with the partitioning of (8.10).

In (8.12)

$$\underset{(p,1)}{\dot{N}_j} = \underset{(p,\bar{n}_j)}{\dot{B}_j^T} \; \underset{(\bar{n}_j,\bar{n}_j)}{W_j} \; \underset{(\bar{n}_j,1)}{\hat{B}_j} \;, \qquad \underset{(p,2)}{\bar{N}_j} = \underset{(p,\bar{n}_j)}{\dot{B}_j^T} \; \underset{(\bar{n}_j,\bar{n}_j)}{W_j} \; \underset{(\bar{n}_j,2)}{\ddot{B}_j} \;,$$

$$(8.13) \qquad \underset{(2,p)}{\bar{N}_j^T} = \underset{(2,\bar{n}_j)}{\ddot{B}_j^T} \; \underset{(\bar{n}_j,\bar{n}_j)}{W_j} \; \underset{(\bar{n}_j,p)}{\dot{B}_j} \;, \qquad \underset{(2,2)}{\ddot{N}_j} = \underset{(2,\bar{n}_j)}{\ddot{B}_j^T} \; \underset{(\bar{n}_j,\bar{n}_j)}{W_j} \; \underset{(\bar{n}_j,2)}{\ddot{B}_j} \;,$$

$$\underset{(p,1)}{\hat{c}_j} = \underset{(p,\bar{n}_j)}{\hat{B}_j^T} \; \underset{(\bar{n}_j,\bar{n}_j)}{W_j} \; \underset{(\bar{n}_j,1)}{\epsilon_j} \;, \qquad \underset{(2,1)}{\ddot{c}_j} = \underset{(2,\bar{n}_j)}{\ddot{B}^T} \; \underset{(\bar{n}_j,\bar{n}_j)}{W_j} \; \underset{(\bar{n}_j,1)}{\epsilon_j} \;.$$

Equation (8.12) shows that the lower right hand portion of the coefficient matrix corresponding to $\ddot{N} + \ddot{W}$ consists of a diagonal matrix of n two by two matrices (the $\ddot{N}_j + \ddot{W}_j$). We may exploit this fact to invert N by the method of partitioning. First let us set

$$(8.14) \qquad M = \begin{bmatrix} \dot{M} & \bar{M} \\ \bar{M}^T & \ddot{M} \end{bmatrix} = N^{-1} = \begin{bmatrix} \dot{N} & \bar{N} \\ \bar{N}^T & N \end{bmatrix}^{-1}$$

where the matrices $\dot{M}$, $\bar{M}$, $\ddot{M}$ are of the same order, respectively, as their counterparts $\dot{N}$, $\bar{N}$ and $\ddot{N}$. Because M is the inverse of N we may write

$$(8.15) \qquad \begin{bmatrix} \dot{N} & \bar{N} \\ \bar{N}^T & \ddot{N} \end{bmatrix} \begin{bmatrix} \dot{M} & \bar{M} \\ \bar{M}^T & \ddot{M} \end{bmatrix} = \begin{bmatrix} I & 0 \\ 0 & I \end{bmatrix} .$$

This leads to the four simultaneous matrix equations

$$
(8.16)\quad
\begin{aligned}
&(a) \quad \dot{N}\dot{M} + \bar{N}\bar{M}^T = I \ , \\
&(b) \quad \dot{N}\bar{M} + \bar{N}\ddot{M}^T = 0 \ , \\
&(c) \quad \bar{N}^T\dot{M} + \ddot{N}\bar{M}^T = 0 \ , \\
&(d) \quad \bar{N}^T\bar{M} + \ddot{N}\ddot{M} = I \ .
\end{aligned}
$$

The solution of (8.16(c)) for $\bar{M}^T$ is

$$(8.17) \qquad M^T = -\ddot{N}^{-1}\bar{N}^T\dot{M} \ ,$$

which, substituted in (8.16(a)) and (8.16(d)), gives

$$(8.18) \qquad \dot{N}\dot{M} - \bar{N}\ddot{N}^{-1}\bar{N}^T\dot{M} = I \ ,$$

$$(8.19) \qquad -\bar{N}^T\dot{M}\bar{N}\ddot{N}^{-1} + \ddot{N}\ddot{M} = I \ .$$

These may be solved for $\dot{M}$ and $\ddot{M}$, yielding

$$(8.20) \qquad \underset{(p,p)}{\dot{M}} = (\underset{(p,p)}{\dot{N}} - \underset{(p,2n)}{\bar{N}} \ \underset{(2n,2n)}{\ddot{N}^{-1}} \ \underset{(2n,p)}{\bar{N}^T}) \ ,$$

$$(8.21) \qquad \underset{(2n,2n)}{\ddot{M}} = \underset{(2n,2n)}{\ddot{N}^{-1}} + \underset{(2n,2n)}{\ddot{N}^{-1}} \ \underset{(2n,p)}{\bar{N}^T} \ \underset{(p,p)}{\dot{M}} \ \underset{(p,2n)}{\bar{N}} \ \underset{(2n,2n)}{\ddot{N}^{-1}} \ .$$

Because $\ddot{N}$ is a diagonal matrix of 2x2 matrices, the computation of $\ddot{N}^{-1}$ in (8.20) is the equivalent of the inversion of n two by two matrices and, thus, presents no practical difficulties; this is the key to the derivation of an efficient computational procedure. Once $\dot{M}$ has been computed from (8.20), $\ddot{M}$ can be computed from (8.21) and $\bar{N}$ can be computed from (8.17). However, $\ddot{M}$ is a completely filled 2n by 2n matrix and, thus, would require inordinate storage for large n. At this point we are, therefore, still short of our goal of achieving a computationally feasible reduction, even though the largest individual matrix requiring inversion has been reduced to the order of $\dot{N}$. Proceeding further, we note that the solution of the normal equations (8.10) is formally

$$(8.22) \qquad \begin{bmatrix} \delta \\ \ddot{\delta} \end{bmatrix} = \begin{bmatrix} \dot{N} & \bar{N} \\ N^T & \ddot{N} \end{bmatrix} \begin{bmatrix} \dot{c} \\ \ddot{c} \end{bmatrix} = \begin{bmatrix} \dot{M} & \bar{M} \\ M^T & \ddot{M} \end{bmatrix} \begin{bmatrix} \dot{c} \\ \ddot{c} \end{bmatrix} ,$$

from which

$$(8.23) \qquad \dot{\delta} = \dot{M}\dot{c} + \bar{M}\ddot{c} ,$$

$$(8.24) \qquad \ddot{\delta} = \bar{M}^T\dot{c} + \ddot{M}\ddot{c} .$$

If we define

$$(8.25) \qquad \underset{(2n,p)}{Q} = \underset{(2n,2n)}{\ddot{N}^{-1}} \; \underset{(2n,p)}{\bar{N}^T}$$

and note from (8.17) that

$$(8.26) \qquad \bar{M} = -\dot{M}Q^T ,$$

we can express (8.23) as

$$(8.27) \qquad \dot{\delta} = \dot{M}(\dot{c} - Q^T \ddot{c}) \quad .$$

Once $\dot{\delta}$ has been computed, an alternative formula for $\ddot{\delta}$ may be derived from the second of the pair of matrix equations implicit in (8.10), namely,

$$(8.28) \qquad \bar{N}^T \dot{\delta} + \ddot{N}\ddot{\delta} = \ddot{c} \quad .$$

The solution of this for $\ddot{\delta}$ in terms of $\dot{\delta}$ is

$$(8.29) \qquad \ddot{\delta} = \ddot{N}^{-1} \ddot{c} - Q\dot{\delta} \quad .$$

This formula for $\ddot{\delta}$ is preferable to that of (8.24) because it does not require the evaluation of $\ddot{M}$.

To avoid operating with large matrices in the solution for $\dot{\delta}$ and $\ddot{\delta}$, we may exploit the partitioning implicit in (8.12). We see that

$$(8.30) \qquad \dot{N} = \sum_{j=1}^{n} \dot{N}_j + \dot{W} \quad ,$$

$$(8.31) \qquad \underset{(p,2n)}{\bar{N}} = (\bar{N}_1 \; \bar{N}_2 \ldots \bar{N}_n) \quad ,$$

$$(8.32) \qquad \underset{(2n,2n)}{\ddot{N}} = \operatorname{diag}(\underset{(2,2)}{\ddot{N}_j} + \underset{(2,2)}{\ddot{W}_j}) \quad ,$$

$$(8.33) \qquad \underset{(p,1)}{\dot{c}} = \sum_{j=1}^{n} c_j - \dot{W}\dot{\epsilon} \quad ,$$

$$(8.34) \qquad \underset{(2n,1)}{\ddot{c}} = \begin{bmatrix} \ddot{c}_1 - \ddot{W}_1 \ddot{\epsilon}_1 \\ \ddot{c}_2 - \ddot{W}_2 \ddot{\epsilon}_2 \\ \vdots \\ \ddot{c}_n - \ddot{W}_n \ddot{\epsilon}_n \end{bmatrix}$$

$$(8.35) \qquad \underset{(2n,1)}{\ddot{\delta}} = \begin{bmatrix} \ddot{\delta}_1 \\ \ddot{\delta}_2 \\ \vdots \\ \ddot{\delta}_n \end{bmatrix} .$$

Therefore, if we define the auxiliary matrices

$$(8.36) \qquad \underset{(2,p)}{Q_j} = (\underset{(2,2)}{\ddot{N}_j} + \underset{(2,2)}{\ddot{W}_j})^{-1} \underset{(2,p)}{\bar{N}_j^T} ,$$

$$(8.37) \qquad \underset{(p,p)}{R_j} = \underset{(p,2)}{\bar{N}_j} \underset{(2,p)}{Q_j} ,$$

$$(8.38) \qquad \underset{(p,p)}{S_j} = \underset{(p,p)}{N_j} - \underset{(p,p)}{R_j} ,$$

$$(8.39) \qquad \underset{(p,1)}{\bar{c}_j} = \underset{(p,1)}{\dot{c}_j} - \underset{(p,2)}{Q_j^T} \underset{(2,1)}{\ddot{c}_j} \quad ,$$

$$(8.40) \qquad \underset{(p,p)}{S} = \sum_{j=1}^{n} S_j \quad ,$$

$$(8.41) \qquad \underset{(p,1)}{\bar{c}} = \sum_{j=1}^{n} \bar{c}_j \quad ,$$

we can readily verify that $\dot{M}$ in (8.20) is given by

$$(8.42) \qquad \underset{(p,p)}{\dot{M}} = (S + \dot{W})^{-1}$$

and that the expression (8.27) for $\dot{\delta}$ becomes

$$(8.43) \qquad \dot{\delta} = \underset{(p,p)}{(S + \dot{W})^{-1}} \underset{(p,1)}{(\bar{c}} - \underset{(p,p)}{\dot{W}} \underset{(p,1)}{\dot{\epsilon})} \quad .$$

Similarly, we find that the elements of $\ddot{\delta}$ in (8.29) become

$$(8.44) \qquad \underset{(2,1)}{\ddot{\delta}_j} = \underset{(2,2)}{\ddot{N}_j^{-1}} \underset{(2,1)}{(\ddot{c}_j} - \underset{(2,2)}{\ddot{W}_j} \underset{(2,1)}{\ddot{\epsilon}_j)} - \underset{(2,p)}{Q_j} \underset{(p,1)}{\dot{\delta}}$$

From the foregoing we see that the computations can be so arranged that the largest individual matrix to be operated on is of order pxp. Even though the order of the original normal equations is $(2n+p) \times (2n+p)$, the total number of computations for $n >> p$ is proportional to $p^2 n$ rather than n^3 as would have been the case had the diagonal character of $\ddot{N}$ not been exploited. It follows that the overall computational effort tends to increase linearly with the number of stars carried despite the fact that each additional star introduces two additional unknowns. Because of these characteristics, the Advanced Plate Reduction is well suited to programmed computation on a digital computer.

9.0 ERROR PROPAGATION

Because of the possible influence of neglected higher order terms of the Taylor's expansion of the projective equations, it may be necessary to iterate the adjustment by treating the results of the initial solution as improved approximations. In this case the values of $\dot{\delta}$ and $\ddot{\delta}$, resulting from the ith iteration of equations (8.43) and (8.44), may be expressed as

$$(9.1) \qquad \dot{\delta}^{(i)} = (S^{(i)} + \dot{W})^{-1} (\bar{c}^{(i)} - \dot{W}\dot{\epsilon}^{(i)}) \quad ,$$

$$(9.2) \qquad \ddot{\delta}_j^{(i)} = (\ddot{N}_j^{(i)})^{-1} (\ddot{c}_j^{(i)} - \ddot{W}\ddot{\epsilon}^{(i)}) \quad .$$

The initial solution corresponds to the case $i = 0$, and subsequent solutions result from the relinearization of the observational equations using the results of the preceeding solution as improved approximations. The process of iteration is best continued until the mean error of the adjustment (to be discussed below) stabilizes sufficiently according to a sound criterion.

If the initial approximations to the parameters are chosen to be equal to their a priori or measured values (as may be legitimately done), the initial discrepancy vectors $\dot{\epsilon}^{(0)}$, $\ddot{\epsilon}^{(0)}$ will both reduce to zero. In this case the discrepancy vectors for the first iteration will be

$$\dot{\epsilon}^{(1)} = \dot{\epsilon}^{(0)} + \dot{\delta}^{(0)} = \dot{\delta}^{(0)} , \tag{9.3}$$

$$\ddot{\epsilon}^{(1)} = \ddot{\epsilon}^{(0)} + \ddot{\delta}^{(0)} = \ddot{\delta}^{(0)} . \tag{9.4}$$

and in general

$$\dot{\epsilon}^{(i)} = \dot{\epsilon}^{(i-1)} + \dot{\delta}^{(i-1)} = \dot{\delta}^{(0)} + \dot{\delta}^{(1)} + \ldots + \dot{\delta}^{(i-1)} , \tag{9.5}$$

$$\ddot{\epsilon}^{(i)} = \ddot{\epsilon}^{(i-1)} + \ddot{\delta}^{(i-1)} = \ddot{\delta}^{(0)} + \ddot{\delta}^{(1)} + \ldots + \ddot{\delta}^{(i-1)} . \tag{9.6}$$

Hence, discrepancy vectors subsequent to zero initial vectors are not necessarily zero, but rather are equal to sum of all preceeding adjustments of the parameters.

After the solution has converged to the point where further adjustments of the parameters are insignificant, the vectors of measuring residuals may be obtained from

$$\begin{aligned} v &= \epsilon \\ \dot{v} &= \dot{\epsilon} \\ \ddot{v} &= \ddot{\epsilon} \end{aligned} \tag{9.7}$$

in which ϵ, $\dot{\epsilon}$, $\ddot{\epsilon}$ denote the final discrepancy vectors of the iterative process. The quadratic form of the residuals is

$$s = v^T W v + \dot{v}^T \dot{W} \dot{v} + \ddot{v}^T \ddot{W} \ddot{v} . \tag{9.8}$$

The degrees of freedom associated with the adjustment is equal to the number of observations in excess of the minimum number required for a unique solution. From (8.1) we see that the total number of observational equations is

(9.9) $N = \bar{n} + 2n + p.$

In (9.9) the number of measured plate coordinates is

(9.10) $\bar{n} = 2n_1 + 2n_2 + .. + 2n_n$

where n_j denotes the number of different images measured on the trace of the jth star; the number of "observed" right ascensions and declinations is 2n and the number of "observed" projective parameters is p. Precisely offsetting the 2n "observed" stellar coordinates and the p "observed" projective parameters are the 2n unknown stellar coordinates, and the p unknown projective parameters. Thus the degrees of freedom are

$f = \bar{n}$ = number of measured plate coordinates.

In the event that $\hat{p}$ of the p projective parameters and $2\hat{n}$ of the 2n stellar coordinates are regarded as completely unknown quantities, rather than observed quantities of known variance, the degrees of freedom become reduced to

(9.11) $f = \bar{n} - \hat{p} - 2\hat{n}.$

The mean error of the adjustment is

(9.12) $m = \sqrt{s/f}\ .$

Inasmuch as unit variance was implicitly taken equal to unity, the quadratic form s has the χ^2 distribution with f degrees of freedom (provided that the distribution of the original observational vector is multivariate normal). The probability of obtaining a value of χ^2 as large as s with f degrees of freedom can be determined from a table of the chi square distribution. If this probability should be excessively small (say less than 5 percent), one may conclude that the residuals from the adjustment are not statistically consistent with the covariance matrix of the observational vector. This would indicate the presence of significant systematic error.

The inverse of the coefficient matrix of the normal equations provides the covariance matrix of the unknowns. In particular, the covariance matrix of the p projective parameters resulting from the adjustment is

$$(9.13) \qquad \underset{(p,p)}{\dot{\Sigma}} = \dot{M}$$

and that of the vector of adjusted stellar positions is

$$(9.14) \qquad \underset{(2n,2n)}{\ddot{\Sigma}} = \ddot{M} .$$

By virtue of the equations (8.21) and (8.25), we may write

$$(9.15) \qquad \underset{(2n,2n)}{\ddot{\Sigma}} = \underset{(2n,2n)}{\ddot{N}^{-1}} + \underset{(2n,p)}{Q} \; \underset{(p,p)}{\dot{M}} \; \underset{(p,2n)}{Q^T} .$$

The submatrix of $\ddot{\Sigma}$ corresponding to the coordinates of the jth star are

$$(9.17) \qquad \underset{(2,2)}{\ddot{\Sigma}} = \underset{(2,2)}{(\ddot{N}_j} + \underset{(2,2)}{\ddot{W}_j)^{-1}} + \underset{(2,p)}{Q_j} \; \underset{(p,p)}{\dot{M}} \; \underset{(p,2)}{Q_j^T} .$$

in this equation the first term, $(\ddot{N}_j + \ddot{W}_j)^{-1}$, represents the covariance matrix of the adjusted stellar position under the assumption that perfect projective parameters are known and the second term, $Q_j \dot{M} Q_j^T$, represents the contribution of errors in the projective parameters resulting from the adjustment. By carrying a sufficiently large number of stellar control points, one can suppress the magnitude of the second term to insignificance relative to the first. This is a basic objective of the plate reduction, for the errors in the computed directions to the various unknown points (stars or flashes) will be significantly correlated with each other if the projective parameters are not established to sufficient accuracy; by adequately suppressing $Q \dot{M} Q^T$ through effective exploiting of redundancy, one can maximize the informational content of the computed directions of unknown points measured on a given plate.

As we have seen, uncatalogued stars can be carried through the Advanced Plate Reduction by treating their unknown stellar coordinates as observations of zero weight and noting that observations of zero weight do not contribute to the degrees of freedom of the adjustment. For an uncatalogued star to be of metric value in the adjustment it is necessary that at least two images be carried. If only a single image is carried, an uncatalogued star becomes totally extraneous and contributes nothing to the observational redundancy. An extraneous observation, nonetheless, can be carried

through the adjustment, even though it has absolutely no effect on the adjustment and, in turn, is totally unaffected by the adjustment. The only merit in doing so arises from the fact that the computed direction of the star and its covariance matrix then becomes convenient by-products of the adjustment via equations (8.44) and (9.17). For the same reason, the plate coordinates of flashes may be carried through the adjustment even though they can make no contribution to the adjustment (here a flash would be treated as if it were an unknown star).

10. CALIBRATION OF DISTORTION CAUSED BY LENS DECENTRATION

The theory presented thus far presupposes that the lens is perfectly centered (i.e., that the centers of curvature of all optical surfaces are collinear). A significant degree of decentering will introduce tangential distortion and asymmetric radial distortion. The suppression of such distortion to a value not exceeding five microns over the plate format requires appreciable skill and patience on the part of the optical technician in aligning the lens. Its suppression to a value not exceeding two microns calls perhaps for an element of luck in addition to skill and patience. In view of our decision to regard as significant any factor contributing the equivalent of one micron or more of error in plate coordinates, it is clear that we cannot ignore the effects of errors of lens centration. Neither can we circumvent the problem by asserting that cameras which display significant tangential distortion should not be employed in metric applications, for to do so would be tantamount to rejecting virtually every camera in existence (as long as we set one micron as the level of significance). It is fortunate, therefore, that we have found that distortion caused by errors of centering is fully as amenable to calibration as symmetric radial distortion. This being so, it becomes admissable in analytical photogrammetry to employ cameras which are affected by appreciable tangential and asymmetric radial distortion; in fact, decentering can be tolerated to the extent that it does not sensibly affect the quality of images.

Only a few reference books on optics touch on the subject of decentered optical systems (e.g., Hardy and Perrin [13], Strong [14]). These state that the optical properties of a slightly decentered lens can be very nearly duplicated by placing an appropriately

oriented thin prism of appropriate deviation in front of the perfectly centered lens. The thin prism model is also adopted in the few papers we have been able to find in the literature concerning tangential distortion or lens decentering (Bennett [15], Washer [16], Carman [17], Pennington [18], Sewell [19], Sharp [20], Livingston [21]). We should note that, in the thin prism model, a single prism is adequate to account for the composite effect of any number of decentered elements, for a group of individual thin prisms in object space (one associated with each decentered element) can be replaced by an equivalent, single prism.

Bennett [15] was one of the first to test the thin prism model against actual observational data. Washer [16] considers the effect of decentering (or of a bent optical axis) on the determination of the principal point. Carman [17] presents the results of numerical ray tracing through a thin prism of points on a grid and demonstrates that a suitable choice of principal point can minimize (though not eliminate) the effects of decentering. Pennington [18] takes note of the systematic effects of tangential distortion on photogrammetric extension of control and discusses the practical determination of tangential distortion, pointing out that its observed characteristics agree with the thin prism model. In [19] Sewell gives an example of the determination of tangential distortion by photographing a straight-line array of targets across both diagonals of the format. Using Pennington's technique, Livingston [21] reports the measured tangential distortion across both diagonals of the photographic format of 33 Metrogon lenses and one Topogon lens. As we shall see presently, Livingston's results are actually not generally in strict accordance with the thin prism model for angles in excess of 25° from the axis of the camera. However, the "cosine variation" of tangential distortion seems to be well substantiated by his results.

It is well to consider at this point the behavior of tangential distortion according to the thin prism model. As described by Pennington [19], there exists on the plate an axis passing through the principal point along which the tangential distortion is maximum. At right angles to the axis of maximum tangential distortion is an axis of zero tangential distortion. The tangential distortion along any other axis passing through the principal

point is proportional to that along the axis of maximum tangential distortion, the constant proportionality being the cosine of the angle between the axis in question and the axis of maximum tangential distortion. Couched in analytical terms, the model may be described as follows:

$$(10.1)\quad \Delta_t(\bar{x},\bar{y}) = P(r)\cos(\Phi-\Phi_0) = \left(\frac{\bar{x}}{r}\cos\Phi_0 + \frac{\bar{y}}{r}\sin\Phi_0\right)P(r)$$

in which

$\Delta_t(\bar{x},\bar{y})$ = tangential distortion at $\bar{x}$, $\bar{y}$ ($\bar{x}$, $\bar{y}$ are referred to principal point);

r = $(\bar{x}^2+\bar{y}^2)^{\frac{1}{2}}$ = radial distance;

$P(r)$ = profile of tangential distortion along axis of maximum tangential distortion;

Φ_0 = clockwise (in the strict mathematical sense) angle between positive $\bar{x}$ axis of maximum tangential distortion;

Φ = clockwise angle between positive $\bar{x}$ axis and radius vector from principal point and $\bar{x}$, $\bar{y}$.

The profile function $P(r)$ is zero at the principal point and is tangent to the $\bar{x}$ axis at the principal point. This suggests that $P(r)$ is an even powered expansion in r:

$$(10.2)\quad P(r) = J_1 r^2 + J_2 r^4 + \ldots \quad .$$

During the course of the past decade we have had the opportunity to study the residual vectors from scores of stellar plates, each taken explicitly for the calibration of radial distortion and each containing typically from 100 to 200 fairly uniformly distributed images. On the occasions when discernible tangential distortion was encountered, the pattern did correspond approximately with that described by Pennington, particularly with regard to the cosine variation. However, the tangential distortion was definitely nonzero at the principal point. Moreover, a peculiar form of asymmetric radial distortion was found to accompany the tangential distortion.

In order to resolve the partial discrepancies between theory and observation, we undertook a special investigation. The first step was to gain greater insight into the physical properties of the thin prism mechanism by performing a rigorous analytical ray tracing through such a prism. We should point out here that Carman's [17] results and all others we have encountered are either consequences of numerical ray tracing or else are restricted to first order approximations of tangential distortion and thus do not clearly define the full and precise relationship between the parameters of the prism and analytical characteristics of the resulting distortion. We shall present only the essential results of our ray tracing rather than the detailed derivation, inasmuch as it is fairly involved, though entirely straightforward. First we define the following:

ϵ = angle of prism,

μ = index of refraction of prism,

Φ_0 = angle between image of edge of prism and positive $\bar{x}$ axis of plate coordinate system (when $\Phi_0 = 0°$, a line normal to the image of the edge of the prism and directed through the principal point coincides with the positive $\bar{y}$ axis; when $\Phi_0 = 180°$, such a line coincides with the negative $\bar{y}$ axis.),

Φ = angle between radius vector to image $(\bar{x},\bar{y})$ and positive $\bar{x}$ axis,

θ_0 = angle between undeviated principal axis and ray to image point $(\bar{x},\bar{y})$; undeviated principal axis is arbitrarily taken to be normal to the front surface of the prism,

θ_1 = angle between principal ray and image ray after refraction by first surface of prism,

θ_2 = angle between normal to second surface to prism and refracted image ray within prism,

θ_3 = angle between emergent ray and normal to rear surface of prism,

c = principal distance of camera.

For points of infinity, the distance of the prism from the lens is of no consequence. Similarly, without essential loss of generality, the prism can be oriented with one of its faces normal to the principal axis. This leaves only the three parameters ϵ, μ, Φ_0 as essential to the complete specification of the prism.

From analytical ray tracing, we ultimately arrive at the following formulas for the radial and tangential components of distortion:

$$(10.3)\quad \Delta_r(\bar{x},\bar{y}) = P\sin(\Phi-\Phi_0)\ ,$$

$$(10.4)\quad \Delta_t(\bar{x},\bar{y}) = P\cos(\Phi-\Phi_0)\ ,$$

in which

$$(10.5)\quad P = c\,[(\cos\theta_1\cos\mu\epsilon - \cos\theta_3)\sin\mu\epsilon + (1-\cos\epsilon\cos\mu\epsilon)\sin\theta_0\sin(\Phi-\Phi_0)]\,.$$

Starting with the coordinates $\bar{x}$, $\bar{y}$ of the image point, we can, for specified ϵ, μ and Φ_0, compute the quantities in the expression for P by means of the following sequence of equations:

$$(10.6)\quad r = (\bar{x}^2+\bar{y}^2)^{\frac{1}{2}}\ ,$$

$$(10.7)\quad \sin\theta_0 = r/(r^2+c^2)^{\frac{1}{2}}\ ,$$

$$(10.8)\quad \sin\Phi = \bar{y}/r \quad \cos\Phi = \bar{x}/r\ ,$$

$$(10.9)\quad \sin\theta_1 = \frac{1}{\mu}\sin\theta_0,\ \cos\theta_1 = (1-\sin^2\theta_1)^{\frac{1}{2}}\ ,$$

$$(10.10)\quad \cos\theta_2 = \sin(\Phi-\Phi_0)\sin\theta_1\sin\epsilon + \cos\theta_1\cos\epsilon\ ,$$

$$(10.11)\quad \sin\theta_2 = (1-\cos^2\theta_2)^{\frac{1}{2}}\ ,$$

$$(10.12)\quad \sin\theta_3 = \mu\sin\theta_2,\ \cos\theta_3 = (1-\sin^2\theta_3)^{\frac{1}{2}}\ .$$

The expression given for P is closed; no approximations were invoked in its derivation. If ϵ is regarded as a small angle and only first order terms are retained, P reduces to the form

$$(10.13)\quad P \cong c(\cos\theta_1 - \cos\theta_3)(\mu\epsilon)$$

and this in turn can be replaced by the expansion

$$(10.14)\quad P \cong \frac{c\mu\epsilon}{2}\left(1-\frac{1}{\mu^2}\right)\sin^2\theta_0 + c\,\mathcal{O}(\Phi,\sin^4\theta_0)\,.$$

This indicates neither μ nor ϵ is individually of primary consequence, but rather that both combine to form the essential parameter of the prism given by the coefficient of $\sin^2\theta_0$, namely,

$$(10.15) \quad P_1 \cong \frac{c\mu\epsilon}{2}\left(1-\frac{1}{\mu^2}\right).$$

Thus, for all practical purposes one may specify an arbitrary value such that $\mu > 1$ and $\epsilon > 0$ for either μ or ϵ, but not for both simultaneously. It is convenient to specify a value for μ which is typical of a glass and to let ϵ assume the role of the free parameter. We shall adopt the value $\mu = \sqrt{2}$, since it lends an aesthetically satisfying character to some of the ray tracing formulae.

The explicit formulation provided by equations (10.3), (10.4) and (10.5) shows clearly that the radial component of distortion of the thin prism model is fully as important as the tangential component. Yet, the radial component has been almost universally ignored, virtually all consideration of the effects of decentering being restricted to tangential distortion. From (10.3) we see that the behavior of radial distortion is precisely the same as that for tangential distortion except for a 90° shift of phase. Thus, the axis of maximum radial distortion corresponds to the axis of zero tangential distortion and vice versa. At phase angles of $\Phi - \Phi_0 = n\frac{\pi}{4}$, the radial and tangential components are of equal magnitude for a specified radial distance.

From (10.10) we see that θ_2, and hence θ_3, are weakly dependent upon the "phase" angle Φ. This means that the profile function P is not strictly a function of radial distance alone, as indicated in (10.1), but varies weakly with Φ as well. However, for small (though significant) decenterings, the dependence of the profile function on Φ may be considered to be negligible.

Operating on the relations (10.3) and (10.4), we can readily derive the result

$$(10.16) \quad P\cos\Phi_0 = \Delta_r \sin\Phi + \Delta_t \cos\Phi$$

$$(10.17) \quad P\sin\Phi_0 = \Delta_r \cos\Phi + \Delta_t \sin\Phi$$

in which Δ_r, Δ_t are short for $\Delta_r(\bar{x},\bar{y})$, $\Delta_t(\bar{x},\bar{y})$. If we let Δ_x, Δ_y denote the $\bar{x}$, $\bar{y}$ components of the distortion, we can show that

$$(10.18) \quad \Delta_x = \Delta_r \cos \Phi - \Delta_t \sin \Phi,$$

$$(10.19) \quad \Delta_y = \Delta_r \sin \Phi + \Delta_t \cos \Phi.$$

It follows from these and (10.16), (10.17) that

$$(10.20) \quad \Delta_x = -P \sin \Phi_0,$$

$$(10.21) \quad \Delta_y = P \cos \Phi_0 .$$

Hence,

$$(10.22) \quad P = (\Delta_x^2 + \Delta_y^2)^{\frac{1}{2}}$$

and

$$(10.23) \quad \sin \Phi_0 = -\Delta_x / P,$$

$$(10.24) \quad \cos \Phi_0 = \Delta_y / P.$$

If we adhere strictly to the thin prism model, P can assume only positive values and the above formulae for P and Φ_0 are entirely unambiguous. At a later point in our discussions, however, we shall partially relax the thin prism model to the extent of letting the profile function P assume both positive and negative values. To avoid ambiguities of sign under such circumstances, we shall invoke symmetry to restrict Φ_0 to the range $0 \leqq \Phi_0 \leqq 180°$. This means that $\sin \Phi_0$ can assume only positive values and, hence, that the sign of P must always be taken opposite that of Δ_x.

Before we take up the extension of the Advanced Plate Reduction to calibrate distortion resulting from centering error, we shall study how distortion arising from the thin prism model propagates through a least squares plate reduction. This will provide us with the insight we require for the correct interpretation of least squares residuals within the framework of the thin prism hypothesis. Figure 2 shows the residual vectors when a 16 cm x 16 cm grid is projected through a thin prism onto the plate of a camera of 600 mm focal length and 17° x 17° field of view(all but one of the figures of this section have been placed at the end of the section). The residual vectors are exaggerated in scale by a factor of 1000. The parameters of the prism are

ϵ = 10 minutes of arc,

$\mu = \sqrt{2}$,

$\Phi_0 = 0°$.

In the projection of Figure 2, the true elements of orientation were taken as $\psi = 0$, $\omega = 0$, $\kappa = 0$, $x_p = 0$, $y_p = 0$, $c = 600$ mm and were rigidly enforced. Therefore, the elements of orientation in this case can afford no compensation whatever for thin prism distortion and the residuals strictly follow equations (10.20), (10.21). We note that the residuals in x are all zero by virtue of our choice of $\Phi_0 = 0$.

In Figure 3a the plate coordinates of the distorted grid were subjected to a least squares adjustment. The resulting adjusted elements of orientation are $\psi = 0$, $\omega = 0\overset{\circ}{.}0255$ $\kappa = 0$, $x_p = 0$, $y_p = 0.260$ mm, $c = 600.000$ mm. This demonstrates that basic mechanism afforded by elements of orientation for compensation of thin prism distortion consists of

(1) a shift of the principal point away from the edge of the prism,

(2) a tilt of the camera axis away from the edge of the prism.

It is noteworthy that the principal distance does not enter into the compensative process. Indeed, only the equivalent of two of the six essential projective parameters afford partial compensation for thin prism distortion. We note that the profile function in Figure 3a is no longer zero at the principal point and that it now assumes both positive and negative values. In comparing Figures 2 and 3a one should observe that the scale of the residual vectors in Figure 3a is twice that of the residual vectors in Figure 2.

With narrow projective bundles a small shift of the principal point is very nearly the photogrammetric equivalent of a small tilt of the camera axis. The approximate equivalence of translation and rotation no longer holds for wide projective bundles. In order to determine the nature of the compensative process for wide projective bundles, we repeated the computations leading to Figures 2 and 3a for a lens of 115 mm focal length and 76° x 76° field of view. In order to maintain the same general magnitude of thin prism distortion, we changed the prism angle from 10 minutes of arc to 2 minutes of arc (the absolute effects on plate coordinates of thin prism distortion for a fixed plate format vary inversely with the focal length). The two sets of residual patterns for the 115mm camera turned out to be practically identical with Figures 2 and 3a respectively. The only essential difference in

the overall results was that the principal point underwent no adjustment with the wide projective bundle; all compensation resulted from a tilt of the camera axis away from the edge of the prism. Only when the adjustment was repeated with the tilt angle enforced to its true value, did the principal point shift. The resulting compensation was significantly less than that of the tilt. This demonstrates that, in the case of wide projective bundles, the essential compensative process afforded by the unconstrained elements of orientation consists solely of a tilt of the principal axis; a shift of the principal point is actually effective only in the absence of the tilt mechanism.

If b and γ denote the magnitude of the compensative translation and tilt (in radians), the residuals Δ_x, Δ_y in Figure 3a can be shown to satisfy the equations

$$(10.25) \qquad \Delta_x = -(P+b-c\gamma)\sin\Phi_0 - \frac{\gamma}{c} r^2 \cos\Phi \sin(\Phi-\Phi_0) \quad ,$$

$$(10.26) \qquad \Delta_y = (P+b-c\gamma)\cos\Phi_0 - \frac{\gamma}{c} r^2 \sin\Phi \sin(\Phi-\Phi_0) \quad .$$

The corresponding equations in terms of radial and tangential components are

$$(10.27) \qquad \Delta_r = \left(P+b-c\gamma - \frac{\gamma}{c} r^2\right) \sin(\Phi-\Phi_0) \quad ,$$

$$(10.28) \qquad \Delta_t = (P+b-c\gamma) \cos(\Phi-\Phi_0) \quad .$$

By largely (though not completely) offsetting the effect of tilt, the translation b permits the application of a tilt which would otherwise be excessively large; it is this which makes the expression $\frac{\gamma}{c} r^2$ sufficiently large to be effective in the compensative process for narrow angle cameras. When the b and γ are taken equal to zero, equations (10.25), (10.26) reduce to (10.20) and (10.21) and equations (10.27), (10.28) reduce to (10.3) and (10.4). In Figures 4 and 5 we have plotted the radial and tangential components of the residual vectors of Figure 3.

At the origin $\bar{x} = \bar{y} = 0$, the profile function P is equal to zero. Therefore, when $\bar{x} = \bar{y} = 0$ and $\Phi = \Phi_0$, the tangential distortion Δ_t given by (10.27) becomes equal to $b - c\gamma$. This demonstrates that tangential distortion is not zero at the principal point in the case where partial compensation is afforded by the tilt and translation resulting from a least squares plate reduction. Moreover, since $P + b - c\gamma$ passes through zero at a sufficiently large radial distance, tangential distortion can assume both positive and negative values across the format.

The compensation for tangential distortion is limited to a translation of the profile function P by the amount $b - c\gamma$. This "balances" the profile across the format but does not alter its shape. On the other hand, the compensative process for the radial component involves not only the translation $b - c\gamma$, but also the second order term $-\frac{\gamma}{c}r^2$, which partially counteracts the initial term of the expansion of P given by (10.14). Accordingly, the compensative process is more effective in reducing the radial component of thin prism distortion than in reducing the tangential component. In comparing Figures 3b and 3c, for example, we see that the mean error of the radial component is 2.5 microns, which is about 60% of the 4.2 micron mean error of the tangential component. This is perhaps one reason why the radial effects of decentering have received virtually no attention in the literature. Another possible reason is that the nature of the radial component is such that it has no effect on the angle subtended by pairs of radially symmetric points. This renders impossible the direct measurement of the radial component of decentering distortion by those conventional procedures of camera calibration which depend intrinsically on the determination of the relative radial displacements of opposing pairs of targets symmetrically arrayed across various diagonals passing through the center of the format. Indeed, when we contemplate the character of the residuals of thin prism distortion as resulting from compensative tilt and translation (Figure 3a), we can appreciate that techniques of camera calibration which measure only angles subtended across central diagonals are incapable of truly definitive calibration of cameras. The power of the stellar technique of calibration lies in the fact that it exploits a knowledge of the direction of each stellar control point relative to <u>all</u> other stellar control points.

In view of our fuller knowledge of thin prism distortion and particularly of our newly gained appreciation of the precise nature of compensative tilt and translation, we reviewed the residual plots from all stellar calibrations of radial distortion performed by our Photogrammetric Laboratory. We found that all occurrences of reasonably well-defined tangential distortion and asymmetric radial distortion conformed to the thin prism model as modified by the compensative process. Our sample consisted of a total of 32 cameras, all having angular fields not exceeding 33°x33°. In a great majority of cases, possible thin prism distortion was sufficiently small relative to the random measuring error to make its detection by visual inspection virtually impossible.

For this reason we resorted to a physical experiment in order to shed further light on the matter. In cooperation with Space Systems Laboratory (SSL) we obtained stellar plates from a pair of Pth 60 Phototheodolites manufactured by SSL. The cameras have focal lengths of nominally 600 mm, effective apertures of about 200 mm, and angular fields of 17° x 17°. One of the two cameras (Camera 001) was known by inspection on an optical lathe to be out of alignment to the extent that small further physical adjustments would have clearly been worthwhile. The second camera (Camera 002) was considered to be aligned to the limit of the optical art and hence was considered not to be subject to further meaningful physical improvement.

The stellar plates from the two cameras were exposed simultaneously and were of a common zenithal star field. The plates were photographically processed together and were measured by the same operator on different days. A total of 155 well-distributed stellar images were measured on each plate. The plate measurements were subjected to the Advanced Plate Reduction considered earlier. However, no allowance was made for star catalog error, even though the GC was employed (the typical GC error is equivalent to about 2 microns on the plate of a 600 mm camera). This was deliberate and was done to prevent any possibility that the adjustment of stellar positions might partially compensate for locally significant systematic effects. The x, y residuals therefore reflect not only random error in the plate coordinates, but also random error in stellar coordinates as well as any systematic error unaccounted for by the mathematical model of the reduction. The residual vectors for Camera 001 are plotted in Figure 4a. The radial and tangential components of the residual vectors are plotted in Figures 4b and 4c. The corresponding results for Camera 002 are plotted in Figures 5a, 5b, and 5c respectively.

Very definite systematic tendencies of the residual vectors are obvious from a visual inspection of Figure 4a. These are more clearly defined in Figures 4b and 4c (especially in Figure 4c). When due allowance is made for the random component of the residual vectors, we see that the patterns of radial and tangential components in Figures 4b and 4c are in excellent correspondence with the patterns of Figures 3b and 3c provided that Φ_0 is taken as approximately 70°. Even though strong systematic effects are evident, it is noteworthy that

the mean error of the residual vectors in Figure 4a is only 3.9 microns. This demonstrates the effectiveness of tilt compensation.

The systematic effects so pronounced for Camera 001 are absent from Camera 002 (Figures 5a, 5b, 5c). This does not necessarily mean that thin prism distortion is insignificant for Camera 002, but rather that it is sufficiently small relative to the random error to elude visual detection. It is altogether conceivable that even after tilt compensation such distortion might amount to as much as 3 to 4 microns in some areas of the plate and might have a mean error of perhaps as much as 2 microns. It is therefore clear that we require a method of evaluating possible thin prism distortion which is more powerful and less subjective than mere visual inspection of least squares residuals. Clearly such a method would result if the mathematical model we derived for thin prism distortion were incorporated directly into the Advanced Plate Reduction. Before we take up the details of the appropriate modification of the least squares plate reduction, we shall investigate further the applicability of the thin prism model.

As we have already noted, Livingston's results from wide angle lenses (Metrogons subtending 74° x 74° fields) are not generally in strict accord with the thin prism model. The discrepancy stems from the fact that the typical profile function P found by Livingston (Figure 6) is not monotonic as required by the thin prism model but rather reverses its direction towards the edge of the field. The broken curve in Figure 6 shows the nature of the profile function to be expected from the thin prism model. We see that the thin prism model holds well out to about 25° from the camera axis and thereafter becomes increasingly inadequate. It follows that the thin prism model is more correctly viewed as a first approximation to the true model. For narrow angle cameras (less than 30° x 30°) the model appears to be sufficiently valid as it stands; for medium to wide angle cameras it clearly requires modification.

In the light of our analytical results coupled with the empirical results of Livingston, it would appear that a generally suitable choice for the profile function is

$$(10.29)\ P = J_1 r^2 + J_2 r^4 + \ldots ,$$

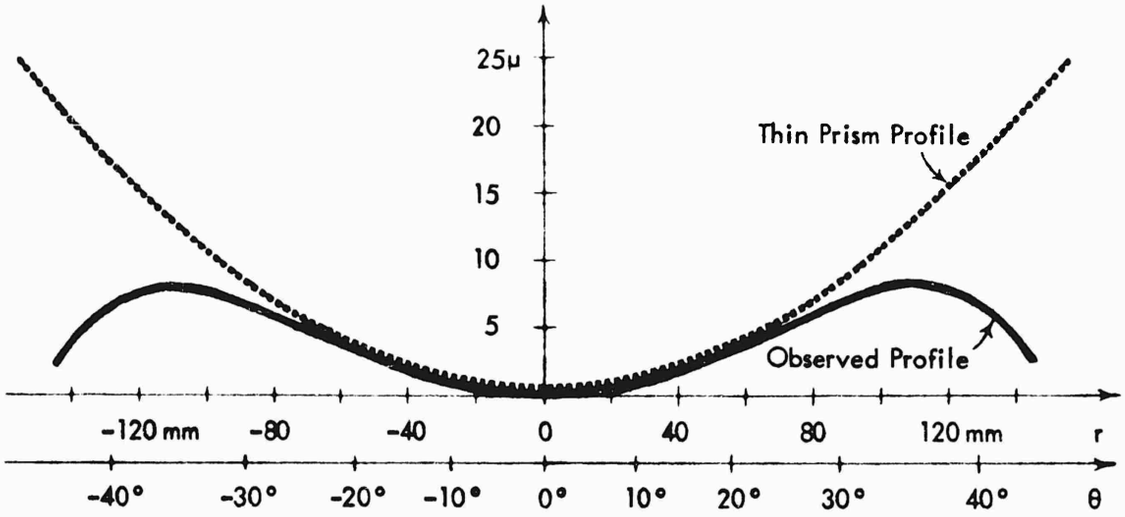

FIGURE 6. Average Profile function of tangential distortion obtained by Livingston from measurements of 33 Metrogon lenses as compared with most nearly equivalent thin prism profile.

where no constraints are placed on the coefficients (in the corresponding expansion of the profile function of the thin prism model the coefficients are all of the same sign; moreover, all are direct functions of μ and ε and are weakly dependent on Φ). The mathematical model which we shall adopt for centering error combines the above profile function with equations (10.20) and (10.21). Thus we have

$$(10.30) \qquad \Delta_x = -P \sin \Phi_0 = -(J_1 r^2 + J_2 r^4 + \ldots) \sin \Phi_0 ,$$

$$(10.31) \qquad \Delta_y = P \cos \Phi_0 = (J_1 r^2 + J_2 r^4 + \ldots) \cos \Phi_0 .$$

The $\bar{x}$, $\bar{y}$ plate coordinates corrected for symmetric radial distortion, differential bias and decentering distortion are then

$$(10.32) \qquad x = (1 + \frac{D}{r})(\bar{x} - x_p) + \xi \Delta x - P \sin \Phi_0 ,$$

$$(10.33) \qquad y = (1 + \frac{D}{r})(\bar{y} - y_p) + \xi \Delta y + P \cos \Phi_0 .$$

When decentering distortion is to be calibrated, these expressions therefore must replace their counterparts in the general projective equations (6.17).

The modification of the least squares plate reduction to account also for decentering distortion is entirely straightforward. Inasmuch as experience to date indicates that the first two terms of the expansion of P are sufficient for wide angle cameras, we shall truncate the expansion at this level. The incorporation of the model for decentering distortion therefore involves three additional parameters: J_1, J_2, Φ_0. We shall let $J_1^{\circ\circ}$, $J_2^{\circ\circ}$, $\Phi^{\circ\circ}$ denote initial approximations to these parameters and shall set

$$(10.34)\quad J_1 = J_1^{\circ\circ} + \delta J_1, \quad J_2 = J_2^{\circ\circ} + \delta J_2, \quad \Phi_0 = \Phi_0^{\circ\circ} + \delta\Phi_0 \ .$$

Then if we reinterpret the model to embrace the three additional parameters of decentering distortion, the matrix $\dot{B}_{ij}$ in (7.11) must be augmented by

$$(10.35)\quad [\dot{B}_{ij}] = \begin{bmatrix} \dot{b}^{16}_{1ij} & \dot{b}^{17}_{1ij} & \dot{b}^{18}_{1ij} \\ \dot{b}^{16}_{2ij} & \dot{b}^{17}_{2ij} & \dot{b}^{18}_{2ij} \end{bmatrix}$$

in which

$$(10.36)\quad \begin{aligned} \dot{b}^{16}_{1ij} &= \left.\frac{\partial f_{1ij}}{\partial u_{16}}\right|_0, & \dot{b}^{17}_{1ij} &= \left.\frac{\partial f_{1ij}}{\partial u_{17}}\right|_0, & \dot{b}^{18}_{1ij} &= \left.\frac{\partial f_{1ij}}{\partial u_{18}}\right|_0, \\ \dot{b}^{16}_{2ij} &= \left.\frac{\partial f_{2ij}}{\partial u_{16}}\right|_0, & \dot{b}^{17}_{2ij} &= \left.\frac{\partial f_{2ij}}{\partial u_{17}}\right|_0, & \dot{b}^{18}_{2ij} &= \left.\frac{\partial f_{2ij}}{\partial u_{18}}\right|_0, \end{aligned}$$

where

$$(10.37)\quad u_{16} = J_1, \quad u_{17} = J_2, \quad u_{18} = \Phi_0 \ .$$

With $\dot{B}_{ij}$ thus augmented and with the vectors $\dot{\delta}$, $\dot{\epsilon}$ and the matrix $\dot{W}$ correspondingly augmented, the matrix representation of the adjustment proceeds exactly as outlined in Section 8.

The determination of initial approximations for $J_1^{\circ\circ}$, $J_2^{\circ\circ}$, $\Phi^{\circ\circ}$ poses something of a problem. Unlike the initial approximations for the coefficients k_1, k_2, ... of symmetric radial distortion, the initial approximations for J_1, J_2 cannot arbitrarily be taken equal to zero, for this would make the coefficients of $\delta\Phi_0$ in the linearized projective equations

equal to zero for all points which, in turn, would lead to an indeterminate system of normal equations. Thus $J_1{}^{oo}$, at least, has to be sensibly finite.

One approach to the problem of determining suitable initial approximations consists of performing an initial least squares plate reduction without J_1, J_2, Φ_0 and of then estimating $\Phi_0{}^{oo}$ and the approximate profile function from a visual examination of the resulting residuals. This approach works quite well when decentering distortion is sufficiently large to be readily discernable as in Figures 4a, b, c. On the other hand, it is of little value when decentering distortion is less than or comparable to random measuring error as in Figures 5a, b, c.

An alternative approach requiring one or two extra iterations of the adjustment but having the merit of being entirely automatic is the following. The phase angle Φ_0 is regarded as having the 'a priori' value of

$$(10.38) \quad \Phi_0{}^{o} = 90^{o} = \pi/2,$$

the standard deviation of which is taken as

$$(10.39) \quad \sigma_{\Phi_0{}^{o}} = 180^{o} = \pi \ .$$

The value $\Phi_0{}^{o} = 90^{o}$ is midway between the extremities of the admissable range of Φ_0, namely: $0 \leqq \Phi_0 \leqq 180^{o}$. The initial approximation to Φ_0 is taken as $\Phi_0{}^{oo} = \Phi_0{}^{o}$. In order to produce an initial approximation to J_1 we resort to gross physical considerations suggested by the expansion (10.14) and write

$$(10.40) \quad J_1{}^{oo} = \frac{\mu \epsilon^{oo}}{2c^{oo}} \left(1 - \frac{1}{\mu^2}\right)$$

in which

c^{oo} = approximate focal length of camera in same units as plate measurements,

$\mu = \sqrt{2}$,

$\epsilon^{oo} = g c^{oo}$.

If the plate measurements are expressed in meters, a suitable value for g in the formula for ϵ^{00} is $g = 0.5 \times 10^{-9}$. This leads to a moderately significant prism angle for the focal length under consideration. Since $J_1{}^{oo}$ is finite, $J_2{}^{oo}$ may arbitrarily be taken equal to zero. Although our initial approximation to J_1 has been taken to be positive, the fact that Φ_0 is considered to be restricted to the range $0 \leqq \Phi_0 \leqq 180°$ makes it equally possible for J_1 to be negative. The possibility that the approximation $J_1{}^{oo}$ may be of the wrong sign causes no difficulties, for this will automatically be rectified in the initial adjustment. The important thing is for the adjustment to have a finite starting value on which to operate. An initial choice of the wrong sign will merely entail an extra iteration of the adjustment.

By means of the artifice of treating Φ_0 as a very weakly constrained a priori observation we prevent the solution from becoming indeterminate in the event that the profile function actually were zero (in this case, of course, Φ_0 would be undefined since there could be no axis of maximum tangential distortion). On the other hand, the constraint on Φ_0 is so weak as to be of no practical consequence in the event that the profile function were strongly defined. The fact that the initial approximation $\Phi_0{}^{oo} = 90°$ may be off by as much as ±90° is not of serious consequence, for the second adjustment of $\Phi_0{}^{oo}$ will ordinarily be within a few degrees of the final value. As with our approximation for $J_1{}^{oo}$, the only drawback to this approach is that it entails one or two extra iterative cycles over what would have been required with sharp initial approximations. With electronic computation this is not a serious consideration.

The covariance matrix of the parameters defining decentering distortion may be abstracted from $\dot{M}$, the covariance matrix of the entire vector of projective parameters. If we denote this matrix by $[\dot{M}]_{J_1, J_2, \Phi_0}$, the covariance matrix of the x and y components of decentering distortion is given by

$$(10.41) \quad \begin{bmatrix} \sigma^2_{\Delta_x} & \sigma_{\Delta_x \Delta_y} \\ \sigma_{\Delta_{xy}} & \sigma^2_{\Delta_y} \end{bmatrix} = \underset{(2,3)}{\Delta_{x,y}} \; \underset{(2,3)}{[M]_{J_1, J_2, \Phi_0}} \; \underset{(3,2)}{\Delta^T_{x,y}}$$

in which

$$(10.42)\quad \underset{(2,3)}{\Delta_{x,y}} = \frac{\partial(\Delta_x, \Delta_y)}{\partial(J_1, J_2, \Phi_0)} = r^2 \begin{bmatrix} -\sin\Phi_0 & -r^2\sin\Phi_0 & -(J_1 + J_2 r^2) & \cos\Phi_0 \\ \cos\Phi_0 & r^2\cos\Phi_0 & -(J_1 + J_2 r^2) & \sin\Phi_0 \end{bmatrix} .$$

Thus not only does the extended version of the Advanced Plate Reduction lead to optimal (minimum variance) estimates of the distortion functions Δ_x, Δ_y, it also provides estimates of their accuracies for any specified radial distances.

Using the data giving rise to Figures 4 and 5, we applied the Advanced Plate Reduction in its extended form (considering decentering distortion) to SSL Cameras 001 and 002. Results of three different reductions at varying levels of refinement are summarized for each camera in Table 2.

TABLE 2. MEAN ERRORS RESULTING FROM VARIOUS ADJUSTMENTS WITHIN FRAMEWORK OF ADVANCED PLATE REDUCTION.

Camera	Number of Control Points	Case I	Case II	Case III	
		Mean Error of Plate Coord. Residuals	Mean Error of Plate Coord. Residuals	Mean Error of Plate Coord. Residuals	Mean Error of Stellar Coord. Residuals
SSL 001	155	3.9μ	2.5μ	2.1μ	0".27
SSL 002	155	3.4μ	3.1μ	2.8μ	0".34

Case I. Star catalogue error and decentering distortion are not explicitly considered in the adjustment (residuals plotted in Figures 4 and 5).

Case II. Decentering distortion, but not star catalogue error, is rigorously treated in the adjustment.

Case III. Star catalogue error and decentering distortion are both rigorously treated in the adjustment (plate coordinate residuals for Camera 001 are plotted in Figure 7).

The calibrated profile functions P(r) for Cameras 001 and 002 are plotted together with their one sigma confidence limits in Figure 8. We see that the decentering distortion for Camera 001 is nearly three times as great as that for Camera 002 and amounts to about 15 microns at a radial distance of 100 mm. Although the calibrated profile function for Camera 002 grows to 5 microns at 100 mm, it should be kept in mind that this is representative of the profile

function without the benefit of compensative tilt and translation. When such compensation is operative (as it is in Figures 5a, b, c), the maximum value of the profile function for Camera 002 is reduced to about 3 microns and its rms value is on the order of 1.5 microns. This provides a good illustration of how decentering distortion can be significant and yet not be apparent from visual inspection of the residuals.

In comparing the residual vectors of Figures 4a, and 7, we see that the Advanced Plate Reduction has been most effective in removing the systematic components of the residuals of Figure 4a. The mean error of 2.1 microns in Figure 7 is only slightly greater than half the 3.9 micron mean error of Figure 4a and is fully consistent with basic plate measuring accuracies. Moreover, the randomness of the residual vectors of Figure 7 leaves nothing to be desired.

Inasmuch as random errors in catalogued stellar positions were rigorously taken into account in the adjustment, residuals are also obtained for stellar positions. It will be noted in Table 2 that the mean error of the stellar residuals for Camera 001 is only 0".27 which corresponds to 0.9μ on the plate. This relatively low value reflects the fact that the stellar field employed (Cygnus) is especially well determined in the GC (two thirds of the 42 different stars carried had updated mean errors of less than 0".40 and only 4 had updated mean errors in excess of 0".60).

In our experience over the past decade the full scale stellar calibration of over 50 different ballistic cameras, at least three quarters of the calibrations have yielded mean errors in the range of 3.5 to 5.0 microns, a range incompatibly large relative to the 2 to 3 microns normally attributable to the combined effect of plate measuring errors and random instability of the photographic emulsion. Because of this it was often necessary in routine reductions to resort to tedious piecewise procedures wherein two or three overlapping groups of stars encircling different portions of long flashing light traces were individually reduced, the purpose being to give the elements of orientation greater freedom for local compensation of unmodeled systematic

errors. In the light of our present findings we have become convinced that the excessively large mean errors frequently encountered in past full scale stellar calibrations are primarily attributable to uncompensated decentering distortion. As the confidence limits of the profile functions of Figure 9 indicate, this difficulty has now been overcome, for the Advanced Plate Reduction provides a practical and effective means for calibrating decentering distortion to rms accuracies of better than one micron out to the very corners of the plate format. It follows that absence of significant decentering distortion need no longer be considered (or be fancied) to be a requirement for metric cameras, particularly for cameras employed in analytical photogrammetry. Indeed, in many instances decentering can be tolerated almost to the point where it begins to have a sensible effect on image quality, for 30 microns of decentering distortion can be calibrated and removed just as effectively as 3. Insofar as ballistic cameras are concerned, stability of the optical system should be of particular concern. An adverse thermal environment is especially to be avoided, for it can induce unstable decentering distortion of a form unamenable to practical calibration.

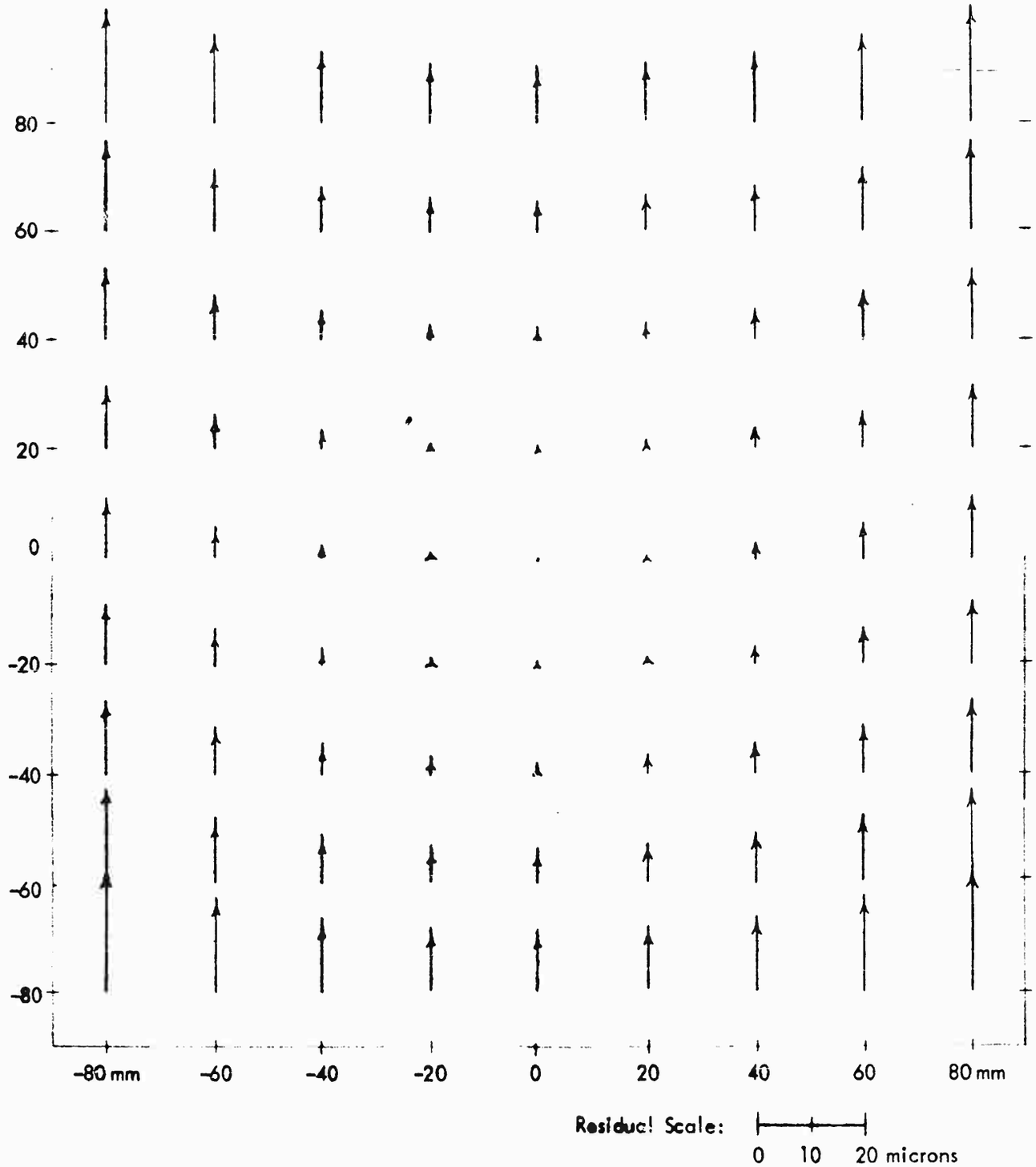

FIGURE 2. Residual vectors of thin prism distortion when true elements of orientation are enforced ($\mu = \sqrt{2}$, $\epsilon = 10'$, $\Phi = 0$, $c = 600$ mm); mean error = 7.7μ.

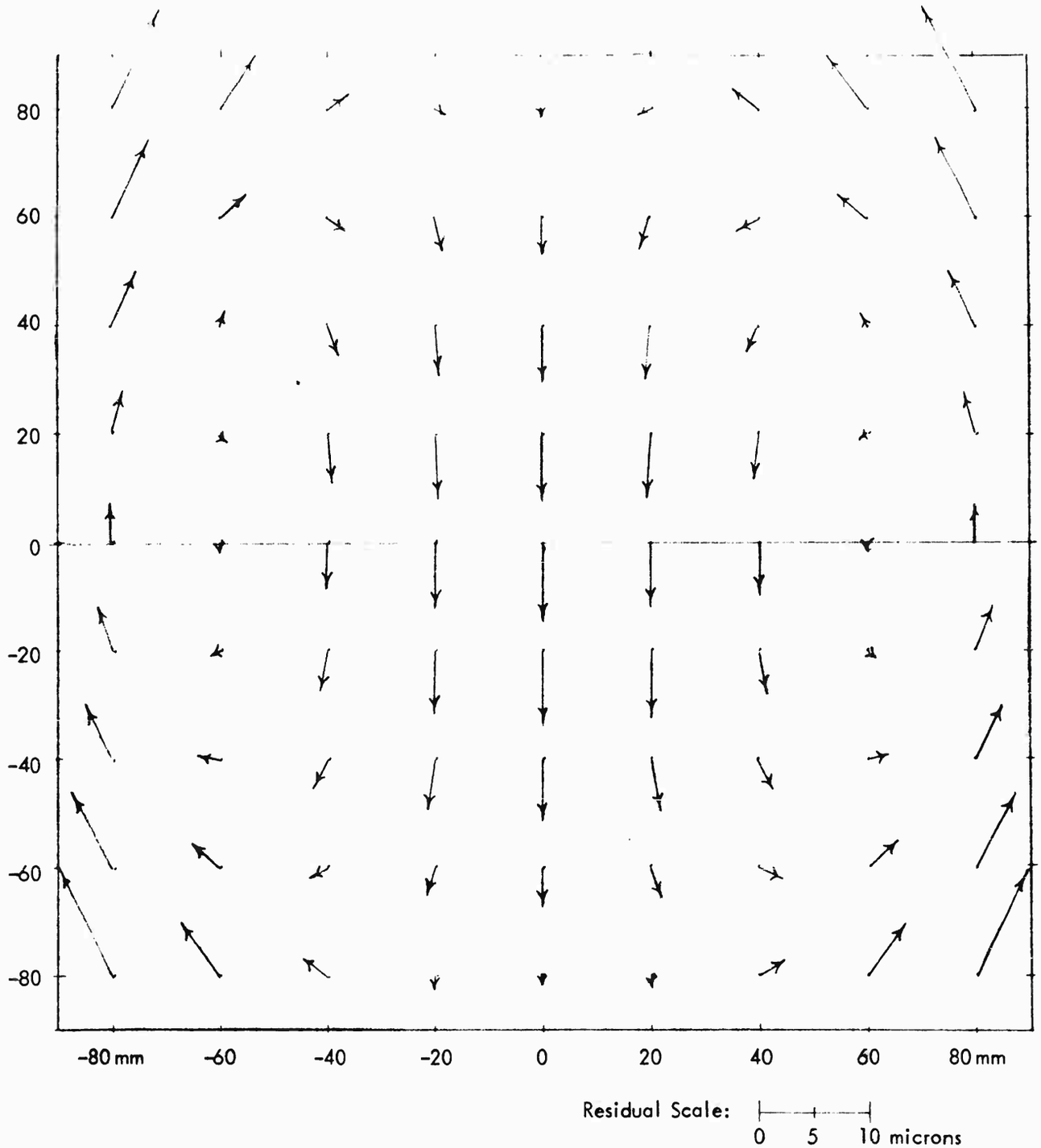

FIGURE 3a. Residual vectors of thin prism distortion when elements of orientation are obtained from least squares adjustment (same thin prism parameters as in Figure 2); mean error = 3.6u.

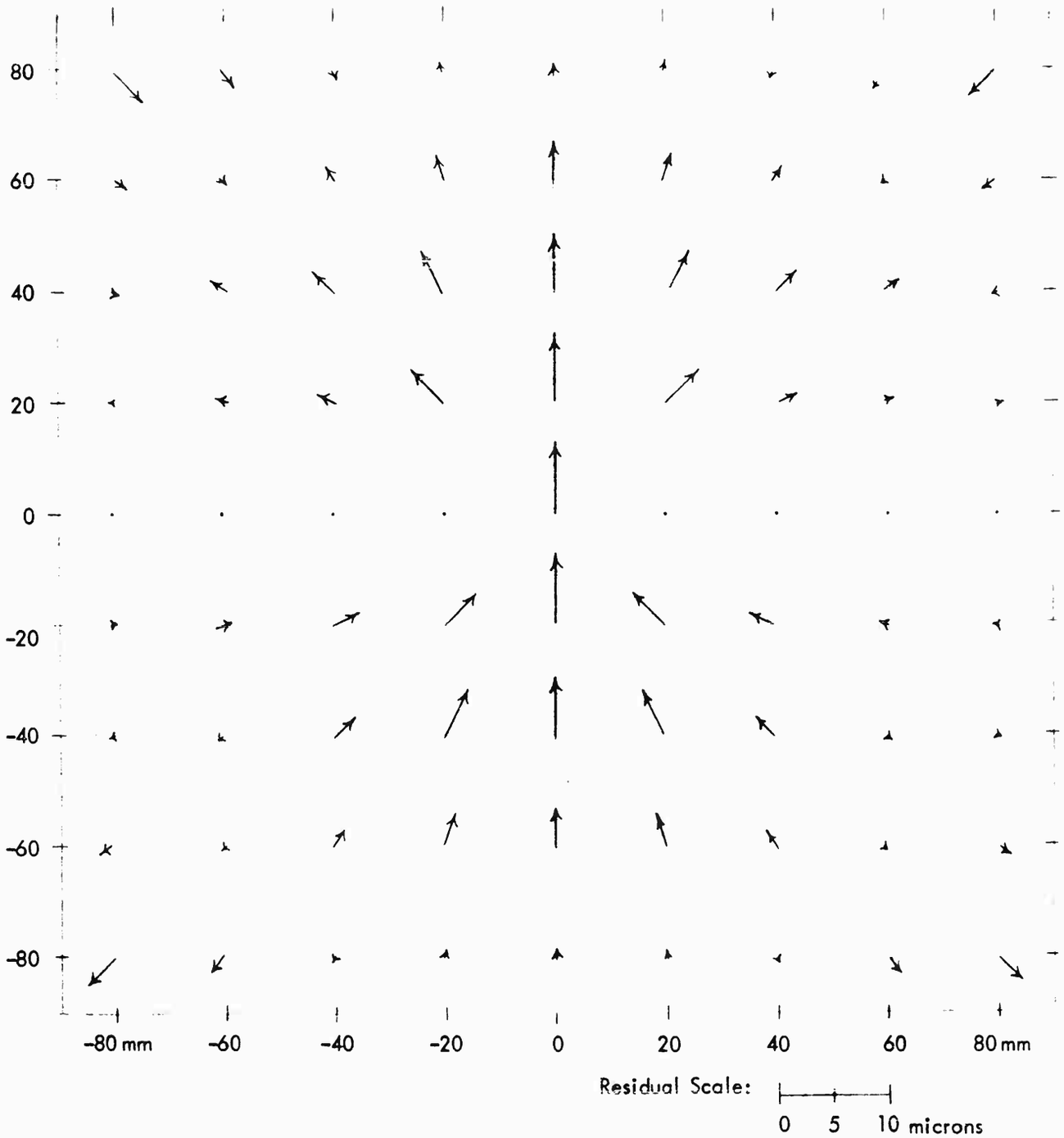

FIGURE 3b. Radial components of residual vectors of Figure 3a; mean error = 2.5u.

note: Fig 3b is upside down.

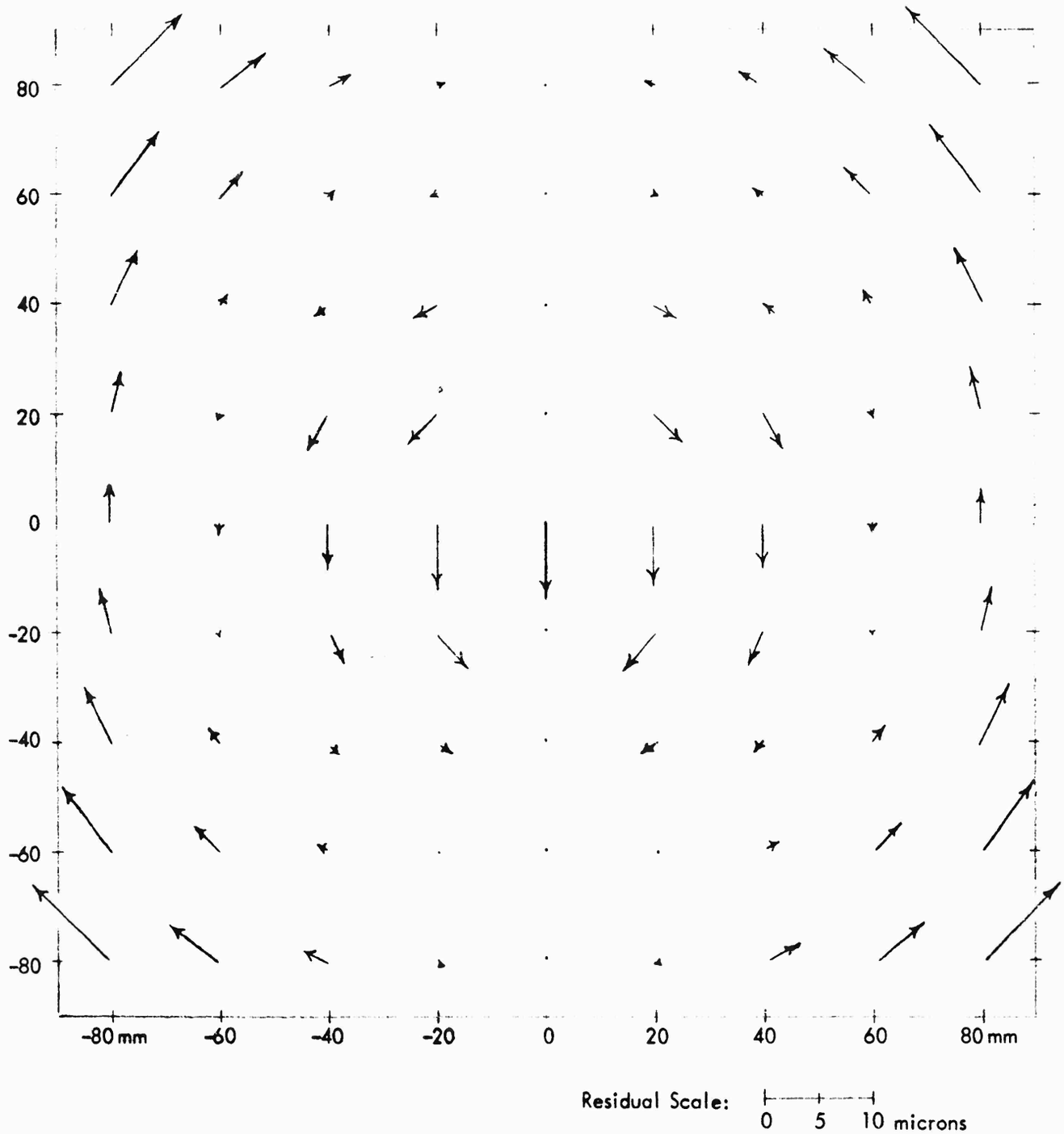

FIGURE 3c. Tangential components of residual vectors of Figure 3a; mean error = 4.2μ.

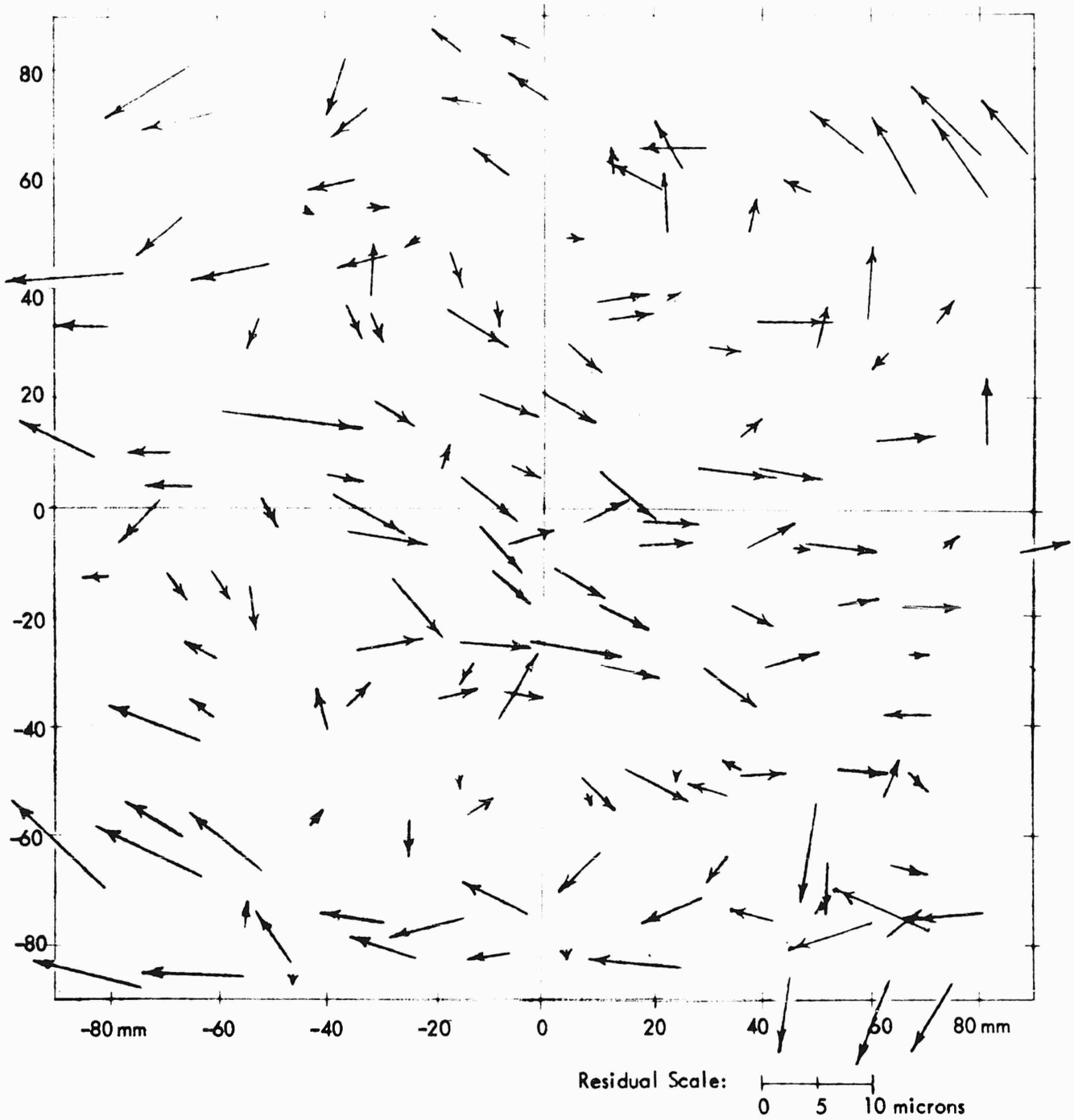

FIGURE 4a. Residual vectors from stellar calibration of SSL Camera 001 as obtained from least squares solution for elements of orientation (no parameters carried for decentering distortion); mean error = 3.9μ.

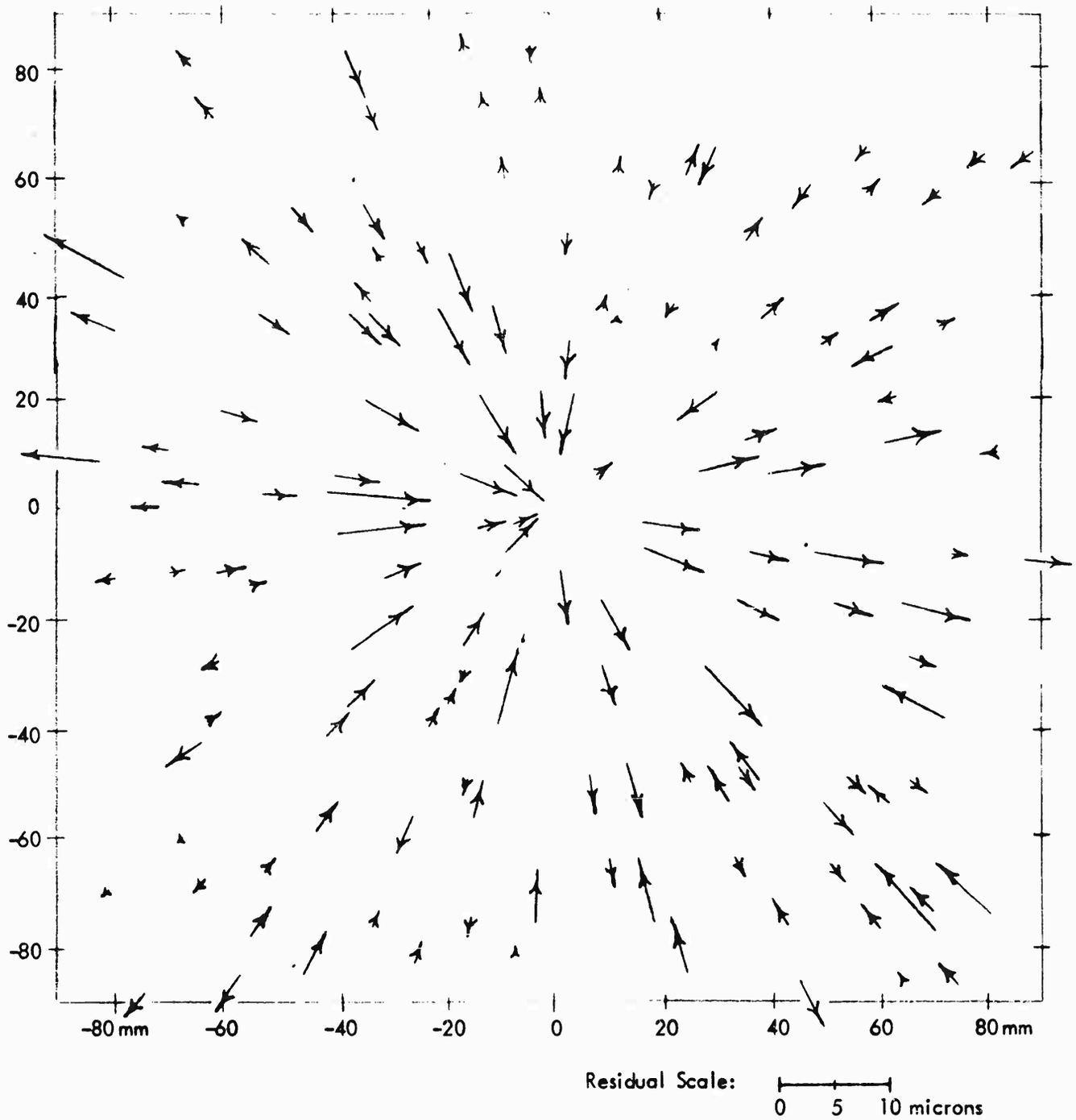

FIGURE 4b. Radial components of residual vectors of Figure 4a; mean error = 3.2μ

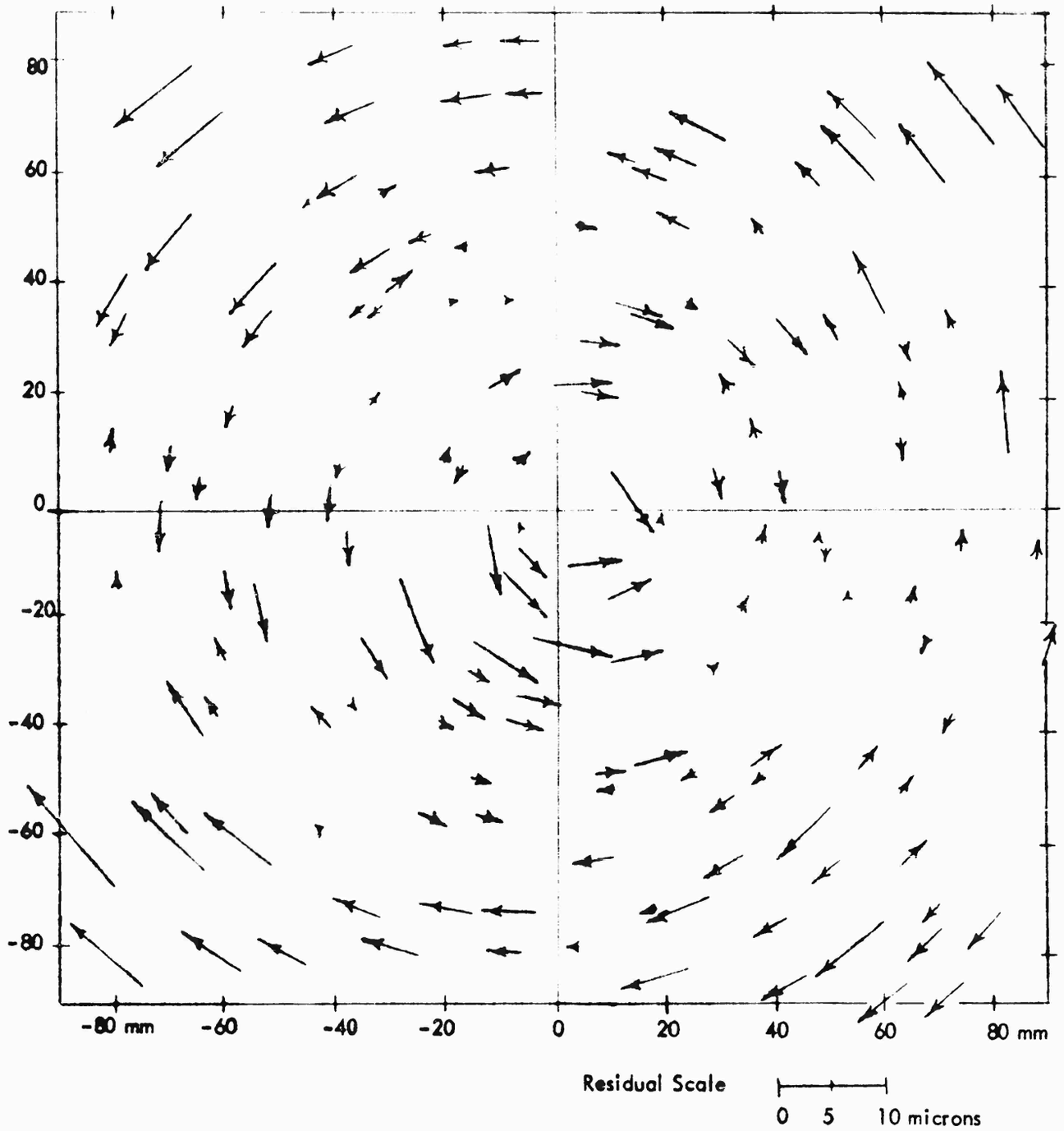

FIGURE 4c. Tangential components of residual vectors of Figure 4a; mean error = 4.5 μ.

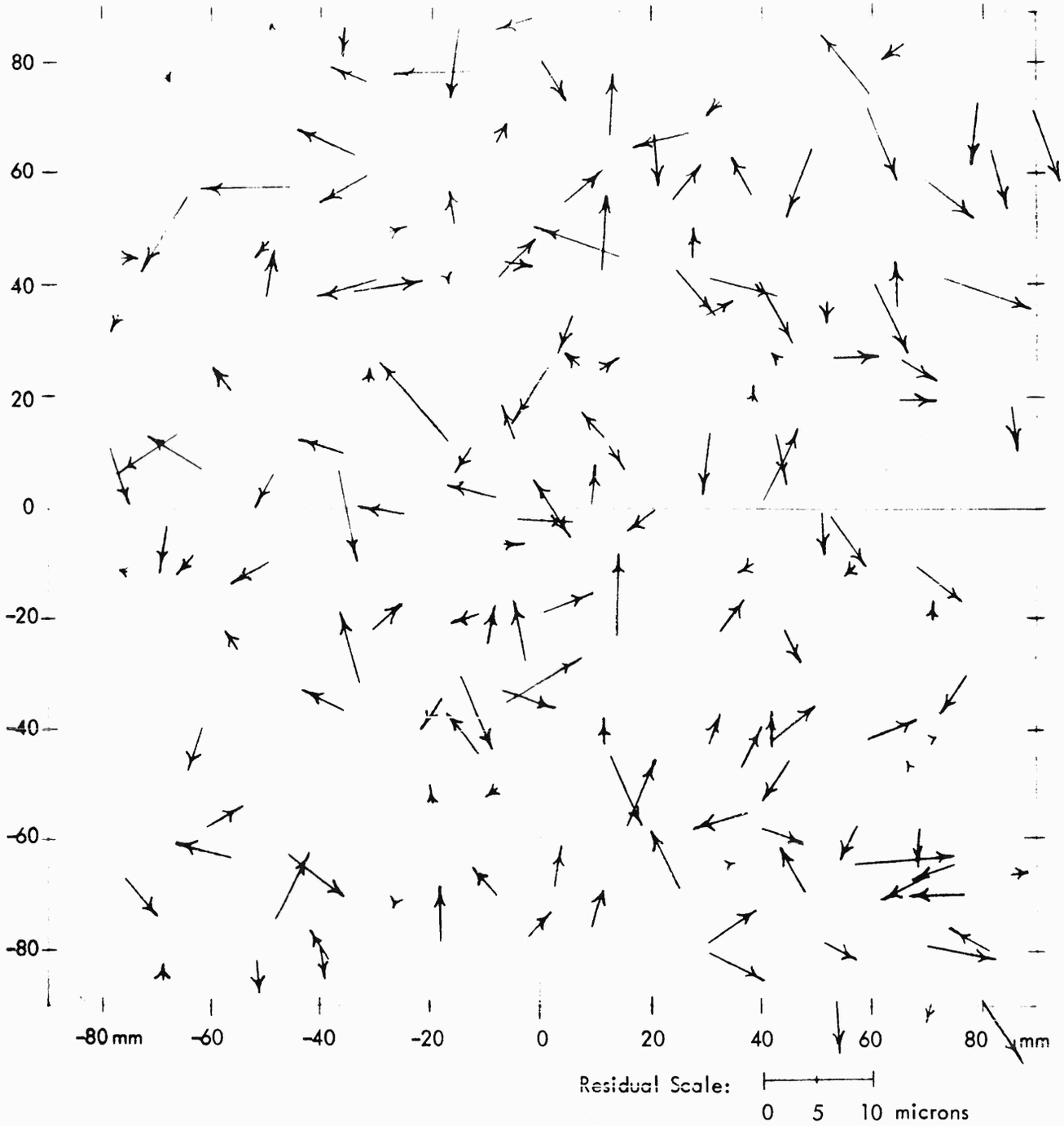

FIGURE 5a. Residual vectors from stellar calibration of SSL Camera 002 as obtained from least squares solution for elements of orientation (no parameters carried for decentering distortion); mean error = 3.4μ.

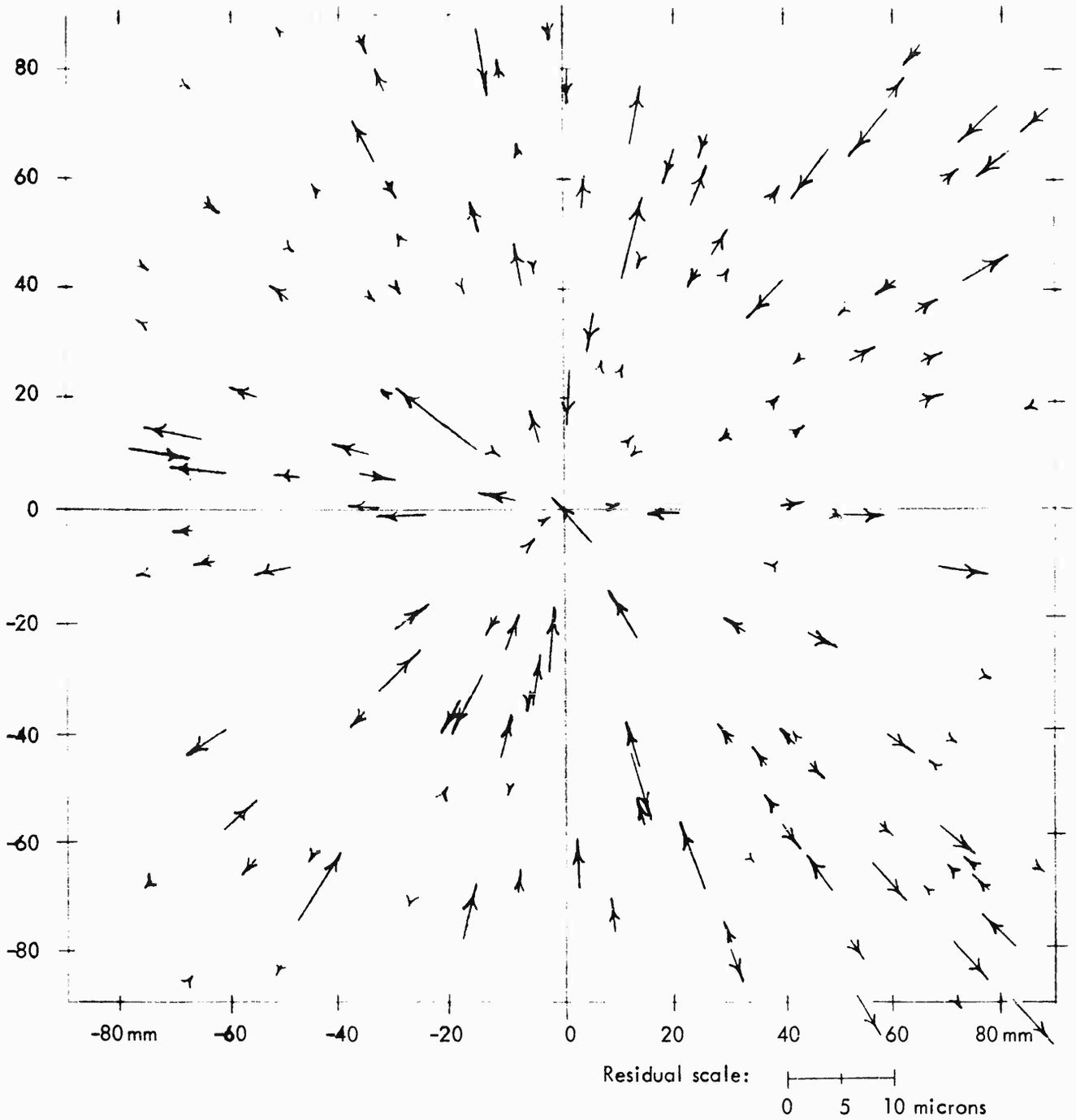

FIGURE 5b. Radial components of residual vectors of Figure 5a; mean error = 3.2μ.

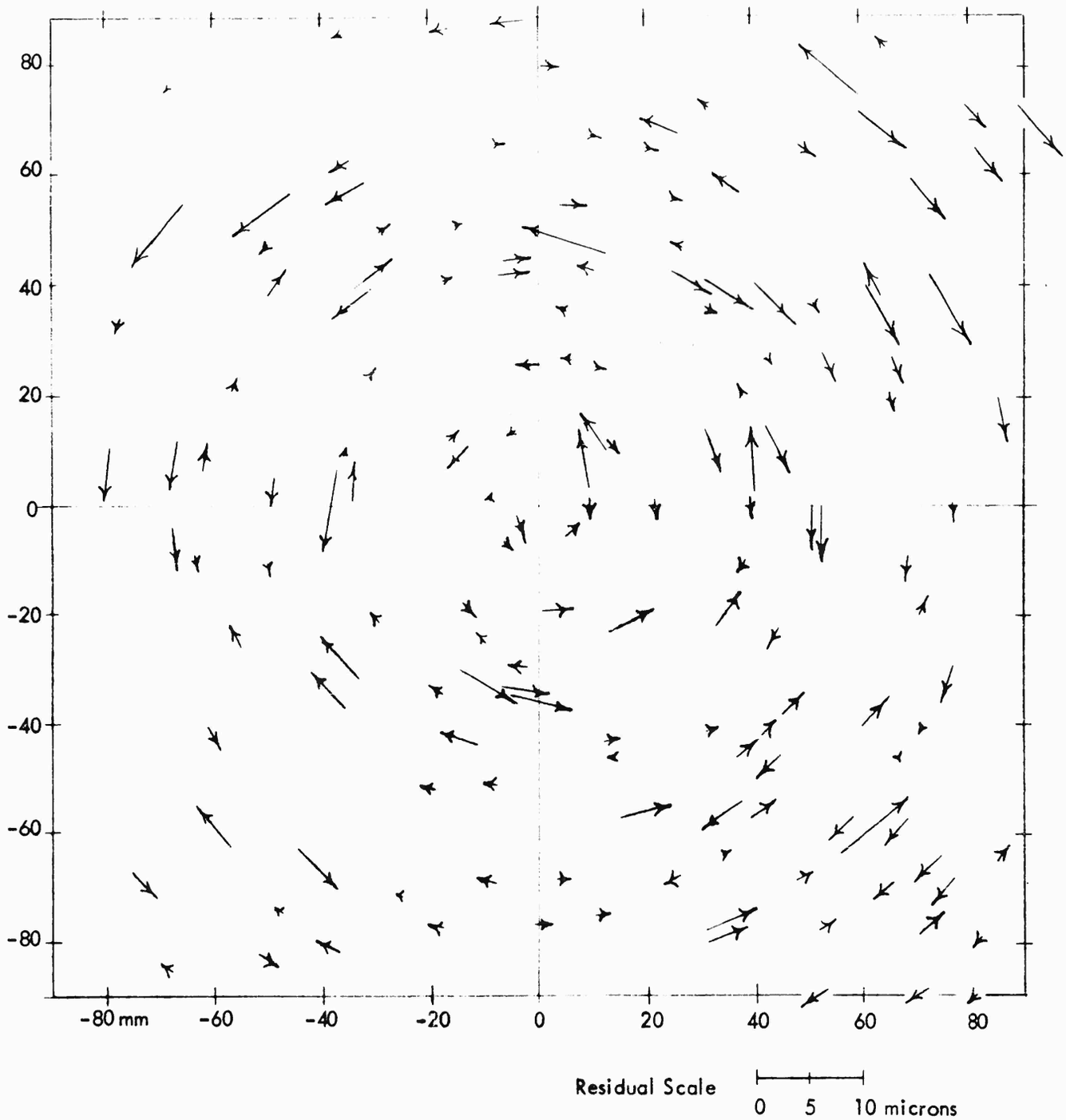

FIGURE 5c. Tangential components of residual vectors of Figure 5a; mean error = 3.4μ

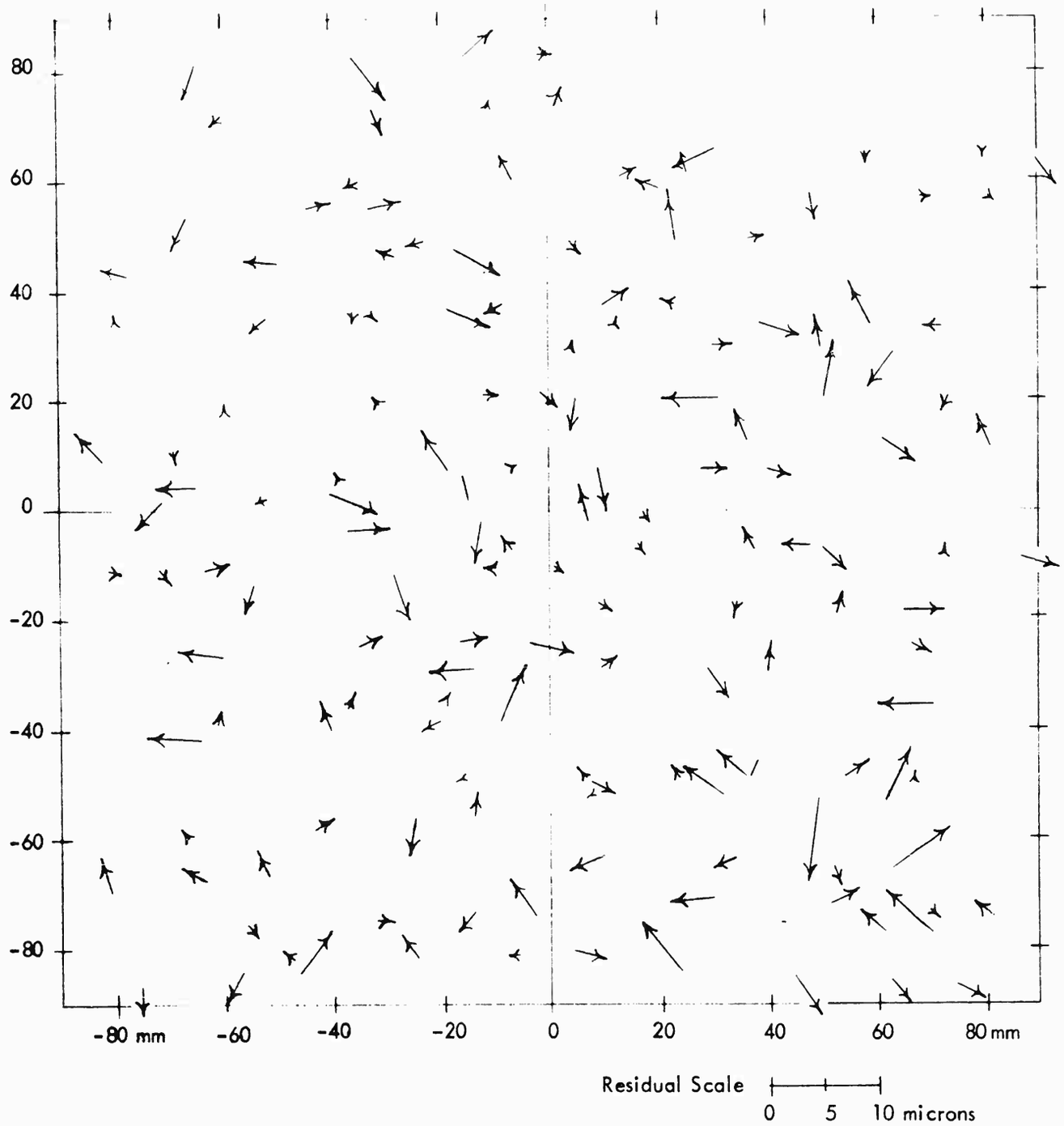

FIGURE 7. Residual vectors from stellar calibration of SSL Camera No. 001 as obtained from Advanced Plate Reduction considering decentering distortion and random error in star catalogue (same original data as in Figure 4); mean error = 2.1μ.

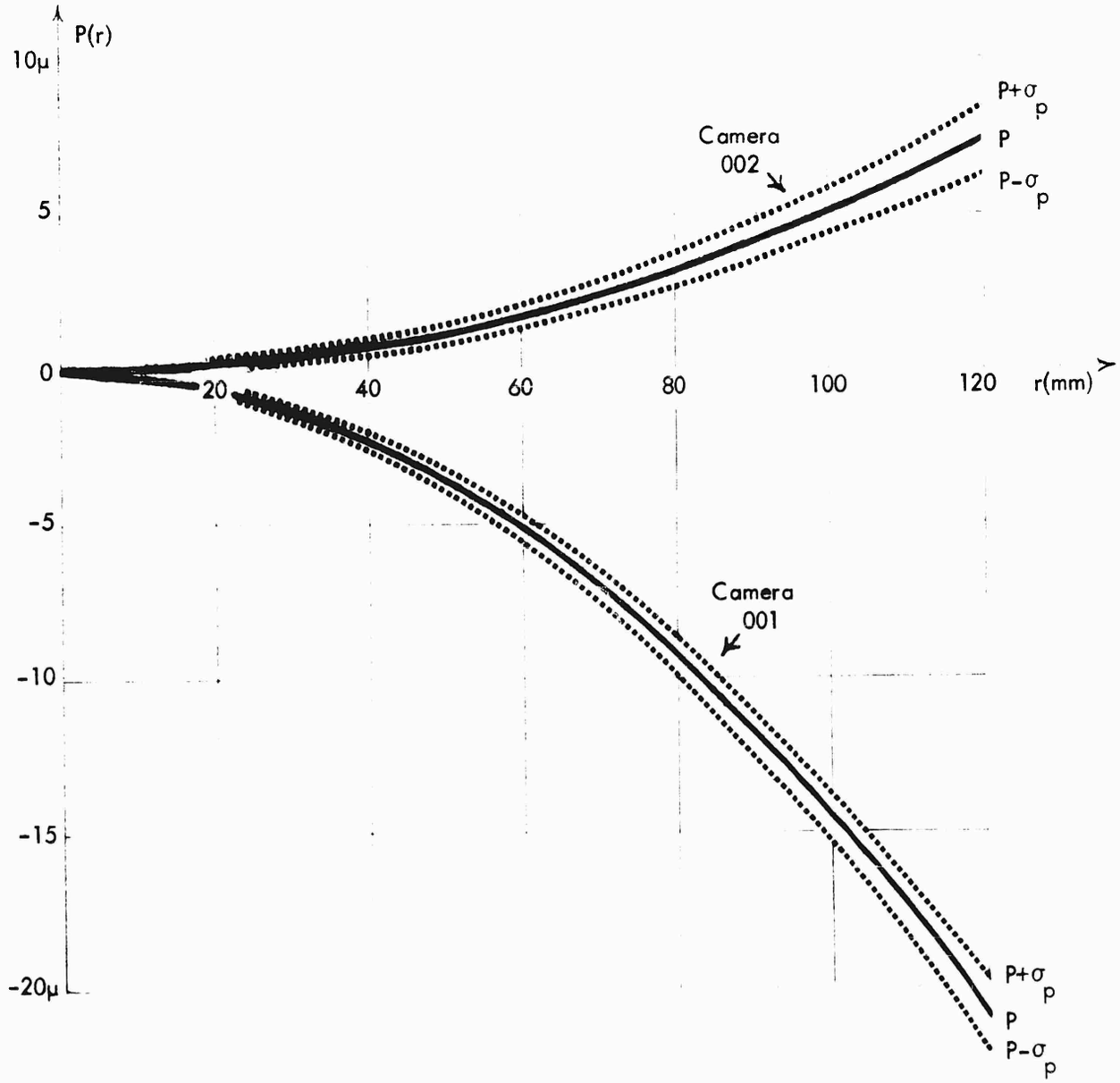

FIGURE 8. Profile functions and associated one sigma confidence limits of decentering distortion resulting from stellar calibrations of SSL Cameras 001 and 002 by means of the Advanced Plate Reduction.

11. GENERAL CONSIDERATIONS

In its fully developed form the mathematical model for the Advanced Plate Reduction contains 18 physical parameters. These may be classified into the following three groups:

(1)	Ideally Invariant:	x_p, y_p, c
		k_1, k_2, k_3
		J_1, J_2, Φ_0
(2)	Generally Variable, but highly constrained:	$\Delta x, \Delta y$
		$\eta_1, \eta_2, \eta_3, \eta_4$
(3)	Generally Variable, weakly constrained:	ψ, ω, κ .

The parameters of the first group are those which depend upon the physical structure of the camera and lens. Under ideal circumstances they could be considered to be constants of the camera. In practice, however, they may be influenced somewhat by thermal environment or by camera orientation. For instance, the principal distance c may vary directly with temperature (unless temperature compensating cells are provided). Similarly, if the camera cone is insufficiently rigid the lens centering (and hence J_1, J_2, Φ_0) may change significantly with the attitude of the camera. An extremely poor practice we have observed with some cameras is the mounting within a few inches of the uninsulated metal of the camera cone of a continuously running motor for driving the shutter. This produces a pronounced thermal gradient across the lens, potentially inducing not only significant decentering but also the deformation of some of the optical surfaces by sizeable fractions of a wave length. The resulting distortion is too complex and unstable to be subject to calibration. Such considerations make it clear that the long term stability and reliability of the so called invariant parameters are largely dependent on sound instrumental design and on sound operational procedures. With sound design and procedures, all of the parameters in the first group except c should require redetermination only at infrequent intervals. We shall define a definitive calibration to be one which produces estimates of the invariant parameters

sufficiently accurate to be rigidly enforced in subsequent routine plate reductions. Ordinarily, a definitive calibration will require a minimum of 150 to 200 well-distributed control points. By drastically reducing the number of parameters requiring determination, a definitive calibration makes routine plate reductions appreciably more efficient and effective.

Many photogrammetric operations do not involve observations at zenith distances greater than 70°. When this is the case, only the following five parameters will normally be required in routine reductions once a definitive calibration has been performed: ψ, ω, κ, c, η_1. Of these η_1 may be heavily constrained, and c moderately constrained. We advocate carrying c in each reduction because it automatically provides compensation for any scale effects not explicitly considered in the reduction. For this reason it is well to deliberately underconstrain c, even though a highly accurate value may be available from a definitive calibration. On the other hand, we do not hesitate to fully constrain the refractive coefficient η_1, for c and ω are capable of compensating for small deficiencies in η_1 (as long as ζ does not exceed 70°). By the same token, a and ω are capable of compensating for small errors in the calibrated coordinates of the principal point x_p, y_p. Therefore as long as the calibrated principal point can be recovered to within a few microns by means of fiducial marks, there is no point in carrying x_p, y_p as unknowns in routine reductions. Again, in routine reductions there is relatively little occasion to exploit the parameters of differential bias Δx, Δy, because one normally experiences little difficulty in finding an adequate number of suitably distributed control points of a common type. The parameters Δx, Δy are chiefly of practical value in definitive calibrations and in reductions of stellar plates taken at great zenith distances (in the latter case, most measurable images of stars close to the horizon would consist of breaks rather than points).

The number of stellar control points to be carried in a plate reduction depends on the circumstances, for the objective of the reduction is to reduce the errors in the computed projective parameters to practical insignificance in the determination of directions to unknown points. From equation (9.17) we can express this criterion analytically as

$$(11.1) \quad \mathrm{tr}\, Q_j \dot{M} Q_j^T < \beta^2 \,\mathrm{tr}\, (\ddot{N}_j + \ddot{W}_j)^{-1}$$

This inequality states that the trace of the matrix defining the contribution of the projective parameters to the error in the direction of a point should be less than a stipulated fraction β^2 of the trace of the matrix defining the contribution of errors in the measured plate coordinates of the unknown point. (The trace of a matrix is the sum of its diagonal elements.) As noted earlier M is the covariance matrix of the adjusted parameters. Its trace and hence that of $Q_j \dot{M} Q_j^T$ tends to vary inversely with the number of control points. On the other hand, the trace of $(\ddot{N}_j + \ddot{W}_j)^{-1}$ is independent of the number of control points. Therefore by carrying a sufficient number of control points one can satisfy the inequality for any specified β^2. If β^2 is taken equal to 1/25, and if only the five basic projective parameters considered above are required, a total of 25 to 30 properly distributed stellar control points. will ordinarily be sufficient to satisfy the inequality. However, if star catalogue errors are comparable in significance to plate measuring errors (as would be the case when the GC is used in conjunction with the PC-1000), a greater number of control points will be required for a given β^2 (about 40 to 50 for $\beta^2 = 1/25$).

The criterion (11.1) is quite sensitive to the number of parameters carried as unknowns. This is why a minimum of 150 to 200 control points is required in a definitive calibration. For the same reason, extraneous parameters should not be carried in the final reduction. For example, three coefficients of radial distortion should not be carried when a single coefficient is actually adequate. In many cases one does not know in advance whether a given subset of parameters is essential or not. In such cases all questionable parameters may be carried provisionally, the adjustment being repeated with each provisional subset of parameters excluded in turn. If the exclusion of a given subset of parameters does not significantly increase the quadratic form of the residuals, the subset may be dropped as unessential. An objective statistical basis for determining whether or not the inclusion of additional parameters significantly reduces the quadratic form of the residual may be based on the F ratio.

$$F_0 = \frac{s_{p+q} - s_p}{s_p} ,$$

in which s_p denotes the quadratic form of the residuals (9.8) when p parameters are carried. This statistic has the F distribution with q degrees of freedom for the numerator and f degrees of freedom (eq. (2.11)) for the denominator. The probability of obtaining a value of F as small or smaller than F_0 may be obtained from standard tables of the F distribution. We prefer to work at the 90% level of confidence in rejecting provisional parameters. Hence, if $Pr\ (F \leqq F_0) \geqq 0.10$ we ordinarily accept the provisional parameters. Through successive application of the F test all unessential parameters can be eliminated from a given plate reduction. However, this eliminative process can be unduly burdensome if carried out blindly. Fortunately, physical considerations may be brought to bear to establish a reasonably logical heirarchy of priority for the process. Thus the first parameters to be tested for potential elimination in a definitive calibration would be the higher order coefficients of refraction, radial distortion and decentering distortion. Moreover, such parameters as ψ, ω, κ, c need not be tested at all because they are inherently essential to the reduction. Also there is little merit in including in the initial model, parameters that are known to be unessential because of circumstances or previous experience. This applies particularly to the higher order coefficients of refraction when zenith distances are not great and to the 5th and 7th order coefficients of radial distortion when previous calibrations of the same or similar cameras have unequivocally indicated such coefficients to be insignificant. The end result of the testing process is a compact model, namely one which contains no unessential parameters. The attainment of a compact model should be the goal of any plate reduction, for this leads to the most effective utilization of the given data.

In our opinion three distinct versions of the Advanced Plate Reduction should be programmed for electronic computation, namely:

(1) the definitive calibration in which the entire eighteen parameter model is carried and full provisions are made for statistical compaction of the model;

(2) a plate reduction suitable for great zenith distance after due corrections for previously calibrated invariant parameters have been applied (here

the unknown parameters of the initial model would be ψ, ω, κ, c, Δx, Δy; η_1, η_2, η_3, η_4);

(3) a plate reduction suitable for small to moderate zenith distances ($\zeta \leqq 70°$) after due corrections for previously determined invariant parameters have been applied (here the unknown parameters would be reduced to the compact set ψ, ω, κ, c, η_1 with η_1 being heavily constrained).

While (2) and (3) may be viewed as special cases of (1), the relatively infrequent requirement for the full capabilities of (1) makes it computationally uneconomical to program it as an all-purpose reduction.

In conclusion we would point out that the version of the Advanced Plate Reduction without parameters for decentering distortion has been employed over the past two years by the Photogrammetric Laboratory of D. Brown Associates, Inc. in the reduction of scores of plates. Its application has resulted in a quantum improvement of results for long focal length ballistic cameras with mean errors of residuals of plate coordinates being consistently reduced from the 4.5 to 6 microns typical of previous plate reductions to values between 2.5 and 3.5 microns. With the more recent incorporation of the calibration of decentering distortion into the Advanced Plate Reduction, mean errors of plate measuring residuals have dropped to still lower levels. We are now at the point where mean errors on the order of 2 microns appear to be routine in massive definitive calibrations. In retrospect, therefore, it appears that a small, but significant degree of decentering has in the past precluded the full realization of the potential accuracies of many cameras. Although the emphasis of this study has been on the calibration and reduction of ballistic cameras, we should take note of the possible application of our results to the definitive calibration of aerial mapping cameras. Truly comprehensive calibration of mapping cameras is now of greater significance then ever because of the growing importance of the extension of mapping control by means of analytical photogrammetry. In the past, many of the metric shortcomings of mapping cameras could be tolerated by virtue of the compensation provided by adequate networks of pre-established ground control. On the other hand, in the analytical extension

of a sparse network of ground control it turns out that systematic errors resulting from uncompensated decentering distortion propagate through the model in a most unfavorable manner. Thus, uncompensated decentering distortion as small as 2 to 3 microns has a rapid cumulative effect on the analytical reconstruction of a photogrammetric strip and assumes prominence (relative to propagated random errors) within a few models. This in turn limits the admissible length of extension between absolute control points (the greater the uncompensated decentering distortion, the shorter the admissible extension). Accordingly, we are convinced that the full potential of analytical techniques for extension of control will approach realization in practice only with mapping cameras which have undergone full-scale definitive stellar calibrations of both symmetric radial distortion and decentering distortion according to the method developed in this paper.

11. REFERENCES

[1] D. Brown, 1962. Notes on the Reduction of Stellar Plates for Determination of Directions to Flashing Light Beacons. Proceedings of the First International Symposium on the Use of Artificial Satellites for Geodesy, Washington, D.C., April 26-28, 1962, pp. 163-186. North Holland Publishing Company, Amsterdam.

[2] H. Schmid, 1952. Spatial Triangulation by Means of Photogrammetry, Ballistic Research Laboratories Report No. 784. Aberdeen Proving Ground, Maryland.

[3] H. Schmid, 1953. An Analytical Treatment of the Orientation of a Photogrammetric Camera, Ballistic Research Laboratories Report No. 880. Aberdeen Proving Ground, Maryland.

[4] D. Brown, 1956. The Simultaneous Determination of the Orientation and Lens Distortion of a Photogrammetric Camera, Air Force Missile Test Center Technical Report No. 56-20. Patrick Air Force Base, Florida.

[5] H. Eichhorn, 1962. A Summary of Star Catalogues and Their Accuracies, RCA Mathematical Services Technical Memorandum No. 62-4. RCA Missile Test Project, Patrick Air Force Base.

[6] F. Scott, 1962. Estimates of the Accuracy of Positions taken from Photographic Star Catalogs, Present and Future, Proceedings of the First International Symposium on the Use of Artificial Satellites for Geodesy, Washington D.C., April 26-28, 1962. North Holland Publishing Company, Amsterdam.

[7] F. Scott, 1963. The System of Fundamental Proper Motions, Chapter III of Basic Astronomical Data, Vol. III: Stars and Stellar Systems. University of Chicago Press.

[8] B. Garfinkel, 1944. An Investigation in the Theory of Astronomical Refraction, Astronomical Journal, Vol. 50, No. 8, pp. 169-179.

[9] D. Brown, 1957. A Treatment of Analytical Photogrammetry with Emphasis on Ballistic Camera Applications, Air Force Missile Test Center Technical Report No. 57-22. Patrick Air Force Base, Florida

[10] K. Strand, 1953. Investigation of Atmospheric Refraction at Low Altitudes, Arctic, Desert, Tropic Information Center Publication No. A-102, Air University, Maxwell Air Force Base, Alabama.

[11] D. Brown, 1955. A Matrix Treatment of the General Problem of Least Squares Considering Correlated Observations, Ballistic Research Laboratories Report No. 960. Aberdeen Proving Ground, Maryland.

[12] D. Brown, 1958. A Solution to the General Problem of Multiple Station Analytical Stereotriangulation, Air Force Missile Test Center Technical Report No. 58-8. Patrick Air Force Base, Florida.

[13] Hardy and Perrin, 1932. The Principles of Optics, p. 551, McGraw-Hill.

[14] J. Strong, 1958. Concepts of Classical Optics, P. 304. W. H. Freeman and Co.

[15] A. Bennett, 1927. The Distortion of Some Photographic Objectives, Journal of the Optical Society of America, Vol. 14, pp. 235-244.

[16] F. Washer, 1941. Locating the Principal Point of Precision Airplane Mapping Cameras, Journal of Research, National Bureau of Standards 27. pp. 405-412.

[17] P. Carman, 1949. Photogrammetric Errors from Camera Lens Decentering, Journal of the Optical Society of America, Vol. 39, No. 11, pp. 951-954.

[18] J. Pennington, 1947. Tangential Distortion and Its Effect on Photogrammetric Extension of Control, Photogrammetric Engineering, Vol. XIII, No. 1, pp. 135-142.

[19] E. Sewell, 1952. Field Calibration of Aerial Mapping Cameras, Manual of Photogrammetry, Second Edition, American Society of Photogrammetry.

[20] J. Sharp, 1949. Increased Accuracy of the Multiplex System, Photogrammetric Engineering, Vol XV, No. 3.

[21] R. Livingston, 1951. Tangential Distortion in the Metrogon Lens, Engineer Research and Development Laboratories Report No. 1219, The Engineer Center and Fort Belvoir, Virginia.

APPENDIX

NOTES ON THE REDUCTION OF STELLAR PLATES FOR DETERMINATION OF DIRECTIONS OF FLASHING LIGHT BEACONS

by
DUANE C. BROWN

Presented to the
SYMPOSIUM ON THE USE OF ARTIFICIAL SATELLITES FOR GEODESY
held at the
U. S. Naval Observatory
Washington, D.C.
April 26-28, 1962

A.1 INTRODUCTION

Photographic determination of stellar positions has been a standard astrometric practice for over a half century. The focal lengths of the cameras used for this purpose have generally been 2 meters and greater and the angular fields of view have invariably been under 10° square and usually well under 5° square. (The standard astrographic cameras have focal lengths of about 3 meters and angular fields 2° square.) During the past two decades photogrammetric cameras of much shorter focal length (100-300 mm) and wider fields (30° to 75° square) have been utilized to determine the directions of missile-borne or airborne flashes relative to photographed stellar control. Here entirely new observational and reductional techniques were evolved and perfected. Since these techniques are familiar only to a relatively small group of specialists, engaged for the most part in missile testing, it is appropriate to outline their salient features and to contrast them with the more familiar practices of positional astronomy. For reasons to be developed presently, it is our belief that for the specific problem of obtaining directions to recorded flashes, fixed cameras of given f ratio and focal length can yield results which are appreciably superior to those obtainable from equatorially mounted cameras of similar f ratio and focal length driven at the sidereal rate.

If we are correct in this belief, it is of considerable importance that the fixed camera approach be better and more widely understood and appreciated, particularly inasmuch as we are at the brink of a period wherein geodetic satellites carrying ground controlled flashing lights will be operational.

In what follows we shall use the term "fixed camera" to denote a camera whose orientation remains stationary relative to the earth throughout the period of photographic recording and the term "sidereal camera" to denote one which is equatorially mounted and which tracks at the sidereal rate (i.e., the sidereal camera is fixed in inertial space while the observations are being made). In the case of the fixed camera, stars trail across the

photographic plate and in the case of the sidereal camera stellar images remain essentially stationary on the plate. The key point to keep in mind in the ensuing discussion is that the data reduction of both fixed and sidereal cameras is based ultimately on the theory of the central projection according to which an object point, its image and the center of projection are collinear and all image points are coplanar. Thus reduced to mathematical essentials, the camera consists of but two elements, the center of projection and the image plane, and the photograph is idealized as the central projection of a three dimensional object space onto a two dimensional image space.

A.2 EARLY DEVELOPMENT OF STELLAR ORIENTED FIXED CAMERA TECHNIQUE

In the United States the development of photogrammetric techniques for the determination of positions of flashing lights was pioneered by the Ballistic Research Laboratories of Aberdeen Proving Ground. At the outset in the early 1940's procedures and reductional techniques were freely adapted from positional astronomy. The primary innovation was one of observational technique, for the camera remained fixed relative to the earth during the exposure instead of being driven at the sidereal rate on an equatorial mount. Breaks in the photographed star trails produced by an accurately timed shutter provided the necessary control points. Data reduction was based on straightforward modifications of Turner's method, which has been standard in positional astronomy for well over one half century. The most important application of the stellar-oriented fixed camera during World War II consisted of the precise determination of the position and velocity of a flashing light aboard a bombing aircraft at the instant of bomb release.

This information was vital to the calculation of accurate bombing tables. Because of their role in ballistics measurements stellar-oriented fixed cameras became known as "ballistic cameras", a designation which persists to this day. Directional accuracies of the order of 10 to 20 seconds of arc were obtained from 300 mm f/8 cameras having useable angular fields of approximately $20^\circ \times 30^\circ$; accuracies of triangulation of roughly one foot for aircraft at altitudes of 10,000 feet were achieved. Names associated with the early development of ballistic cameras at BRL during World War II are H. Russell, T. Sterne and R. Zug. It was

Professor Russell of Princeton and the BRL Advisory Committee who originated the concept of the stellar oriented fixed camera and who argued successfully for its implementation instead of sidereal cameras.

By the end of World War II a number of deficiencies in Turner's method had become apparent. Most of these arose from the fact that Turner's observational equations relating the measured plate coordinates x, y and the so-called standard coordinates, ξ, η (these being functions of hour angle and declination) are actually approximations having strict validity only for cameras of rather narrow angular field. These equations which are of the general form

$$
(1) \qquad \begin{aligned} \xi &= a_0 + a_1 x + a_2 y + a_3 x^2 + a_4 xy + a_5 y^2 + \ldots , \\ \eta &= b_0 + b_1 x + b_2 y + b_3 x^2 + b_4 xy + b_5 y^2 + \ldots , \end{aligned}
$$

actually represent expansions of the following rigorous expressions which are based on an undistorted central projection

$$
(2) \qquad \begin{aligned} \xi &= \frac{a_{11} x + a_{12} y + a_{13}}{a_{31} x + a_{32} y + 1} , \\ \eta & \quad \frac{a_{21} x + a_{22} y + a_{23}}{a_{31} x + a_{32} y + 1} . \end{aligned}
$$

Inasmuch as only six independent parameters are required to define an undistorted central projection, it follows that the eight parameters in equation (2) must be constrained by two additional equations. These turn out to be

$$
(3) \qquad \begin{aligned} & a_{11} a_{12} + a_{21} a_{22} + a_{31} a_{32} = 0 , \\ & a_{11}^2 + a_{21}^2 + a_{31}^2 - a_{21}^2 - a_{22}^2 - a_{32}^2 = 0. \end{aligned}
$$

In order for the expansion (1) to be valid with a reasonable number of terms it is necessary that

$$
(4) \qquad 0 \leq | a_{31} x + a_{32} y | < 1,
$$

a condition which is adequately met in practice only when ξ, η are so chosen that the ξ, η plane is nearly parallel to the x, y plane and when the angular field is fairly narrow.

While equations (2) and (3) together define an undistorted central projection, this is true of equations (1) only if appropriate constraints are placed upon the coefficients so that the standard coordinates are expressed ultimately as functions of six independent parameters. Although such constraints can be formulated, they are ignored in practice, the consequence being that the central projection is not rigorously preserved when equations (1) are used. A straight line in the ξ, η plane therefore does not project into a straight line in the x, y plane. This is true even when all known corrections such as refraction, aberration, lens distortion, etc., are explicitly applied to ξ, η and x, y prior to the solution of equations (1) for the coefficients. The reason is that random measuring errors alone are sufficient to prevent the determination of coefficients which will perfectly reproduce a central projection. It is well to note here that the standard astrometric practice of allowing the coefficients of the expansion to absorb the effects of refraction, distortion, aberration and so forth turns out to be unwarranted with cameras of moderate angular field; better results are obtained from Turner's method when these corrections are applied explicitly.

A.3 DEVELOPMENT OF NEW REDUCTIONAL TECHNIQUES AT BRL

By the late 1940's reductions based on equations (1) were largely abandoned in advanced ballistic-camera work, having been superseded by the more rigorous expressions of equations (2). However, the constraints of equations (3) were not enforced in the adjustment until the early 1950's when Dr. H. Schmid investigated the problem. Schmid was also the first to recognize that the customary least-squares adjustments based on equations (1) and (2) were faulty, for they did not accord proper recognition to the quantities actually subject to significant random error, namely the plate coordinates x, y. Thus, for instance, in determining the coefficients in (1) or (2) by minimizing the quadratic forms

$$(5) \qquad s = \Sigma\{[\xi - (a_0 + a_1x + a_2y + \ldots)]^2 + [\eta - (b_0 + b_1x + b_2y + \ldots)]^2\},$$

$$(6) \qquad s = \Sigma \left[\left(\xi - \frac{a_{11}x + a_{12}y + a_{13}}{a_{31}x + a_{32}y + 1} \right)^2 + \left(\eta - \frac{a_{21}x + a_{22}y + a_{23}}{a_{31}x + a_{32}y + 1} \right)^2 \right],$$

one is implicitly assuming that the standard coordinates ξ, η are subject to random error and that the plate coordinates are error free. Quite the reverse is true with cameras of moderate focal length (say, 300 mm or less).

By 1953 Schmid had perfected a new theory of ballistic-camera plate reduction that dispensed entirely with the astrometric theory. Instead, results of classical photogrammetry initially derived by von Gruber were exploited and extended. The fundamental projective relations were placed in the form

$$(7a) \qquad x = x_p + c\,\frac{A\xi + B\eta + C}{D\xi + E\eta + F}, \quad y = y_p + c\,\frac{A'\xi + B'\eta + C'}{D\xi + E\eta + F},$$

or alternatively

$$(7b) \qquad \xi = \frac{A(x - x_p) + A'(y - y_p) + Dc}{C(x - x_p) + C'(y - y_p) + Fc}, \qquad \eta = \frac{B(x - x_p) + B'(y - y_p) + E'c}{C(x - x_p) + C'(y - y_p) + Fc},$$

wherein

x_p, y_p = plate coordinates of principal point,

c = principal distance,

$$\begin{bmatrix} A & B & C \\ A' & B' & C' \\ D & E & F \end{bmatrix} = \text{matrix of direction cosines defining angular orientation of plate coordinate system relative to standard coordinate system.}$$

Inasmuch as all the nine elements of the orientation matrix can be expressed uniquely in terms of three independent quantities, say the three Eulerian angles, the projective relations (7a) or (7b) may be regarded as involving a total of six independent parameters, namely three

translations x_p, y_p, c that define the coordinates of the center of projection in image space, and three rotations, say α, ω, κ, that are implicit in the matrix of direction cosines and uniquely define the orientation of the plate coordinate system relative to the standard coordinate system. The standard coordinates ξ, η are related to Cartesian Coordinates of object space by

$$\xi = \frac{X - X^c}{Z - Z^c}, \quad \eta = \frac{Y - Y^c}{Z - Z^c}, \tag{8}$$

wherein X^c, Y^c, Z^c denote the coordinates of the center of projection in object space and the X and Y axes are parallel to the ξ and η axes respectively. If the X, Y, Z coordinates of a photographed point are finite (as opposed to coordinates of stars which are essentially infinite), equations (7a) and (7b) may also be regarded as being of the form

$$\begin{aligned} x &= x_p + c\,\frac{A(X - X^c) + B(Y - Y^c) + C(Z - Z^c)}{D(X - X^c) + E(Y - Y^c) + F(Z - Z^c)}, \\ y &= y_p + c\,\frac{A'(X - X^c) + B'(Y - Y^c) + C'(Z - Z^c)}{D(X - X^c) + E(Y - Y^c) + F(Z - Z^c)}, \end{aligned} \tag{9a}$$

$$\begin{aligned} \frac{X - X^c}{Z - Z^c} &= \frac{A(x - x_p) + A'(y - y_p) + Dc}{C(x - x_p) + C'(y - y_p + Fc}, \\ \frac{Y - Y^c}{Z - Z^c} &= \frac{B(x - x_p) + B'(y - y_p) + Ec}{C(x - x_p) + C'(y - y_p) + Fc}. \end{aligned} \tag{9b}$$

In Schmid's theory the so-called elements of orientation α, ω, κ, x_p, y_p, c are determined by minimizing the quadratic form

$$s = \Sigma \left[w_x \left(x - x_p - c \frac{A\xi + B\eta + C}{D\xi + E\eta + F} \right)^2 \right.$$

(10)

$$\left. + w_y (y - y_p - c \frac{A'\xi + B'\eta + C'}{D\xi + E\eta + F})^2 \right],$$

wherein w_x, w_y denote the weights of the measured x, y coordinates, and the standard coordinates ξ, η are computed from the hour angle and declination of the star. While a minimum of three stars are sufficient for a unique solution of the elements of orientation, at least 10 were generally carried in the adjustment in order to minimize the effects of random errors in the measured plate coordinates. Current practice is to utilize from 20 to 30 stellar control points whenever possible, thereby producing elements of orientation that make a relatively insignificant contribution to the errors in the directions to the flashing light.

After the least-squares determination of the element of orientation, the projective equations in the form (9a) or (9b) can be employed for the triangulation of the X, Y,Z coordinates of flash points. The first completely rigorous treatment of ballistic-camera triangulation was provided by the writer in 1955; all previous treatments had failed to adjust the measured plate coordinates properly.

A.4 DEVELOPMENTS AT THE ATLANTIC MISSILE RANGE

In 1956 Schmid's theory for ballistic-camera plate reduction was adapted by the author to the reduction of ballistic-camera plates acquired at the Atlantic Missile Range. Here ballistic cameras were employed routinely on scores of missile tests and on aircraft tests designed to evaluate accuracies of electronic tracking systems; hundreds of plates were (and are) reduced each year. Often five or more well-distributed ballistic cameras were employed in a single triangulation, and as many as 20 cameras participated in certain missions. Thus ample opportunity existed for the evaluation of Schmid's plate reduction. By 1958 mean errors of 3 microns were more or less routine and by mid-1959

a sizable fraction of reduced plates had mean errors of 2.5 microns or better. A mean error of 1.5 microns for both orientation calibration and least-squares triangulation was attained in one reduction involving about 30 stellar control points on each plate and over 50 flash points. Comparable results were obtained by Schmid at BRL. Inasmuch as the standard deviations of plate measurements of well-defined stellar and flashing-light images range typically from 2 to 3 microns, the results demonstrated time and again that systematic errors were being successfully suppressed to a level significantly below the standard deviation of the random errors.

Thus within the course of little over a decade a five to tenfold improvement was attained in the accuracies produced by ballistic cameras. A substantial portion of this improvement was attributable to improved techniques of data reduction, particularly the abandonment of classical astrometric techniques in favor of more rigorous procedures that preserved the geometrical properties of the central projection and that were correct from the standpoint of error theory (this implies that the astrometric procedures are deficient from the standpoint of error theory; this is indeed so and astronomers could well benefit from a more careful study of Gauss). The remainder of the improvement is attributable to refinements in cameras and associated equipment. Particularly noteworthy was the series of BC-4 cameras introduced by Wild Heerbrug, Inc., through the efforts of Dr. Schmid. This represented the first time that lenses originally designed for stringent metric applications (in this case for aerial mapping) were adapted to ballistic cameras. The almost perfect centering of these lenses reduced tangential distortion to relative insignificance, while their low degree of radial distortion was amenable to particularly precise calibration because of the absence of excessively steep gradients. Three different camera cones constitute the BC-4 series: the 115-mm f/5.6 Aviogon having a 76° square field; the 210-mm f/4.2 Aviotar having a 45° square field; and the 305-mm f/2.6 Astrotar having a 33° square field. Also of major importance was the introduction of moderately priced photographic plates flat to from 6 to 12 fringes of sodium light (or flat to within ±1 to ±2 microns

from a best fitting plane). This eliminated unflat photographic surfaces as a significant source of error.

Certain innovations made by the author at the Atlantic Missile Range also merit mention. As indicated earlier, control points were provided by short breaks (50 to 100 microns) in the star trails. In 1956 a study was conducted to determine the feasibility of using short exposures of star trails to produce point-like images for control. By using a geometrical series of exposures such as 2, 1, $\frac{1}{2}$, $\frac{1}{4}$ sec, respectively, with 20 to 30 sec between each exposure, one obtains a well-graduated succession of well-spaced point-like images. With a lens such as the 300-mm f/2.6 Astrotar, for instance, a third to fourth magnitude star will generally produce a nearly optimum punctiform image with a $\frac{1}{4}$-sec exposure, whereas a sixth to seventh magnitude star will produce a similar image with a 2-sec exposure. (Exposures significantly longer than 2 seconds lead to excessively elongated images with a camera of 300-mm focal length; with a focal length of 1000 mm the maximum worthwhile exposure is about one second.) The study demonstrated that somewhat greater plate-measuring accuracy could be obtained from optimal punctiform images than from optimal breaks. However, the major advantage from replacing breaks by punctiform images stemmed from the fact that it obviated the need for measuring the plate in direct and reversed positions to eliminate personal bias from the readings. This is necessary when stellar breaks are used as control, for one has no assurance that personal bias will be the same, on the average, in measurements of breaks as in measurements of flash images; personal bias, if assumed constant, can be eliminated by the principle of reversal. On the other hand, it is clear that if the personal bias for the measured stellar control were the same as for the measured flash images, the relative coordinates of control points and flash images would remain unaltered, no matter what the bias and measurement in both direct and reversed positions would therefore be unnecessary. Thus, abandoning stellar breaks in favor of punctiform images halved the measuring effort without impairing accuracies. Moreover, greater flexibility was achieved, for practically every recorded star yielded one image per cycle of exposure which matched closely the characteristics of the flash images (the flashes in

turn were exposed to produce nearly optimum images of 40- to 60-micron diameter). Because each star could be exposed as many times as desired by repeating the basic calibration cycle, little difficulty was generally experienced, even with rather sparse stellar fields, in selecting a group of 20 to 30 optimal control points ideally distributed about the trace of the flashing light. A print of a typical stellar plate taken by a 1000-mm f/5 camera is reproduced in Figure 1.

Another innovation made in 1956 was an improved solution for the stellar calibration of lens distortion. In this solution coefficients defining the radial distortion of the lens were determined simultaneously with the elements of orientation. All previous solutions were dichotomous in the sense that attempts were made to determine orientation and distortion independently. This had never been completely satisfactory, for small errors in provisional orientations were reflected in the calibrated distortion curve and vice-versa. By calibrating orientation and distortion simultaneously using the plate measurements of 100 to 150 stellar images, we attained unprecedented accuracies and repeatibility; independently determined distortion curves for a given camera rarely disagreed by more than ±1 micron. Distortion coefficients were recalibrated periodically as a quality control measure. From the plots of the x, y residual vectors it was possible to determine whether or not the projection was affected by a significant degree of tangential distortion.

Because the duration of the flashing-light sources is so short, a few milliseconds at best, the effects of atmospheric turbulence must be reckoned with. Atmospheric shimmer, as the phenomenon is sometimes called, is of relatively little consequence with stellar images inasmuch as they are accorded much longer exposures, which effectively average out most of the effects of shimmer. Inasmuch as the magnitude of the effect of shimmer on the position of the centroid of the image is approximately inversely proportional to the aperture of the camera, some improvement in directional accuracies of flashes may be realized through the use of cameras of wide aperture. Even so, the problem remains

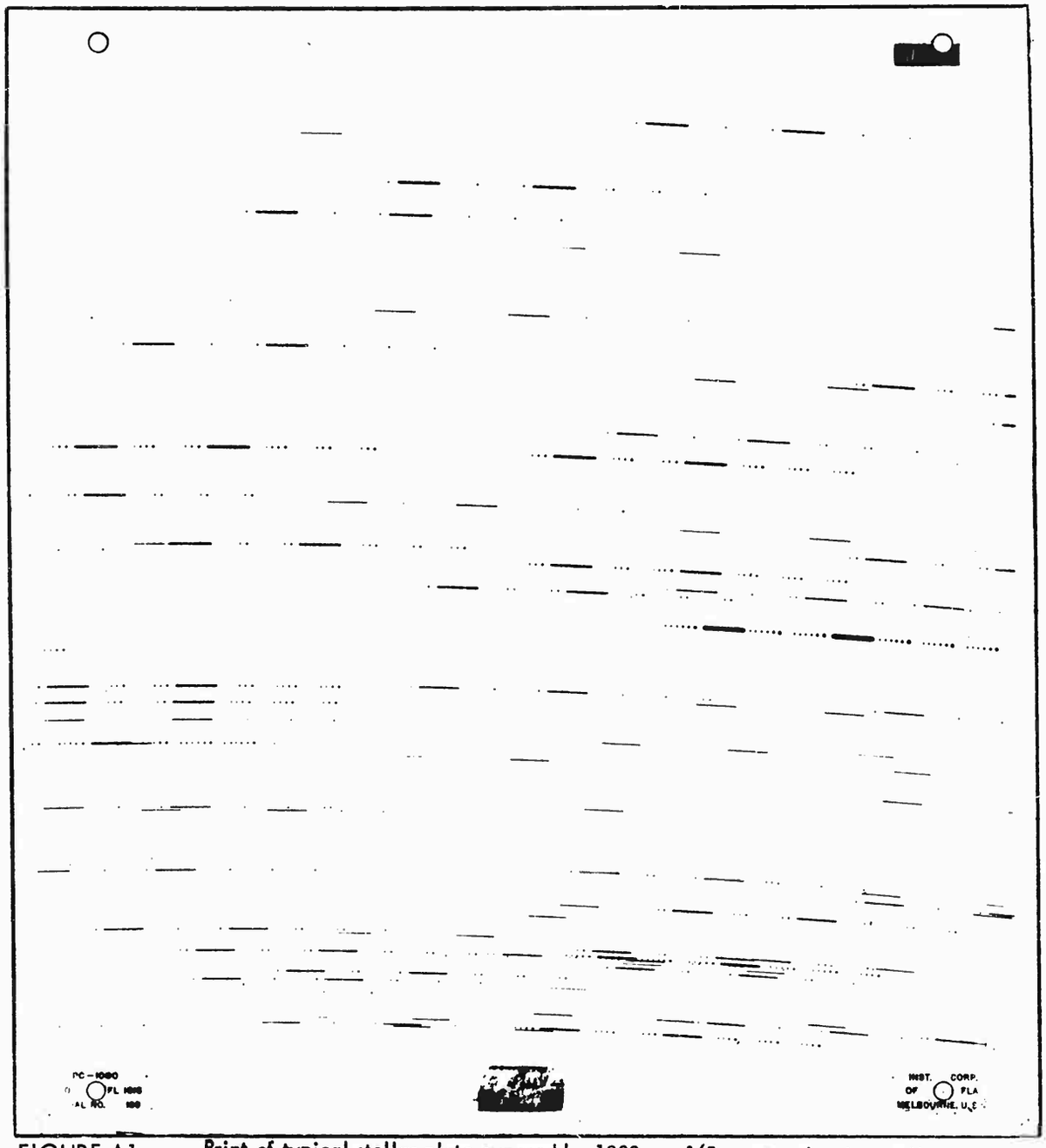

FIGURE A1. Print of typical stellar plate exposed by 1000 mm f/5 camera showing stellar traces of six cycles of five exposures each with two intervening trails.

of estimating the degree to which shimmer affects the coordinates of flash images on a given plate taken by a given camera. Such estimation is most desirable so that the observations from different plates may be properly weighted in the triangulation, for with widely distributed cameras it is entirely possible for shimmer to be insignificant for some cameras, moderate for others and severe for still others. When a long series of successive flashes is recorded, estimates of the standard deviations of the plate coordinates from a given plate may be obtained from a time series analysis of the measurements; such estimates will reflect the combined effect of all sources of random error that influence the relative positions of successive images and will thus include the effects of setting errors, random emulsion instability, atmospheric shimmer, camera vibration (if significant) and so forth. In many operations, however, too few flash images are recorded to permit a sound time series analysis. Here it is possible to employ a sufficiently bright star in the general region of interest to simulate a flashing light by making a series of very short exposures of the stars. This, of course, requires a fast shutter capable of exposures of at least 10 msec to ensure that successive images will be frozen in instantaneous shimmer positions as are the images of flashes. By use of the stellar noise trace technique, as it has been termed, it becomes possible to estimate quite precisely the proper standard deviations to be used in weighting for triangulation. Ordinarily, about 60 or so images are measured on a given noise trace and subjected to a time series analysis. This yields estimates of standard deviations σ, which in turn have standard deviations of about 0.13 σ.

A.5 RECENT DEVELOPMENTS

By 1960 it was clear that significant further improvement in accuracies attainable from stellar-oriented fixed cameras was to be realized only through the development of cameras of longer focal length and wider aperture. Increased apertures were necessary to offset the influence of shimmer, which would otherwise negate the potential gains of longer focal lengths. Accordingly, the Atlantic Missile Range undertook the development of a 600-mm f/2 camera with 17° square field and Air Force Cambridge Research Laboratories undertook the development of a 1000-mm f/5 camera with 10° square field. The

latter camera was based on a telescopic lens designed for aerial reconnaissance by Dr. James Baker during World War II. Surplus lenses produced by Perkin Elmer in 1952 were completely disassembled, rematched and refurbished where desirable, and critically re-aligned. A total of 20 of these cameras, designated the PC-1000, were produced by Instrument Corporation of Florida for the Air Force and the Navy. Most of these will be employed extensively for observations of forthcoming geodetic satellites. The 600-mm f/2 camera was developed by Nortronics. Six were contracted to be produced for AMR. Three have so far been delivered. Since they have yet to be declared operational, further pertinent information is unavailable at this time.

The calibration of the PC-1000 cameras for distortion was originally accomplished by the method developed by the writer while at AMR. However, on plate after plate the mean error resulting from the calibration amounted to between 4 and 5.5 microns instead of the 2 to 3 microns considered to be compatible with plate measuring accuracies. A plot of the x, y residual vectors from a typical plate is presented in Figure 2. Each star was exposed for 1, 1/2, 1/4 and 1/8 sec respectively, this cycle of exposures being repeated four times thereby leading to a total of 16 well-spaced images per star. The most nearly optimum image from each cycle of exposure of a selected star was measured. The straight lines in Figure 2 connect the images corresponding to each star. Perhaps the most striking feature of the plot of residuals is the systematic nature of successive residual vectors for many of the stars. Yet, residual vectors of adjacent stars appear quite uncorrelated. This strongly suggests that the effect is not attributable to either the camera or the emulsion but rather is attributable to random errors in the catalogued right ascensions and declinations of the stars. Accordingly, the star catalogue employed, namely the Boss Catalogue, was investigated and the conclusion was reached that random errors in the proper motions could indeed conceivably account for the observed effect. The estimated standard deviations of updated right ascensions and declinations were found to vary from about 0".4 to as much as 1".5, the value 0".7 being typical. An angle of 0".7 is equivalent to 3.5 microns on a PC-1000 plate, which is somewhat greater than the typical plate measuring accuracy. In

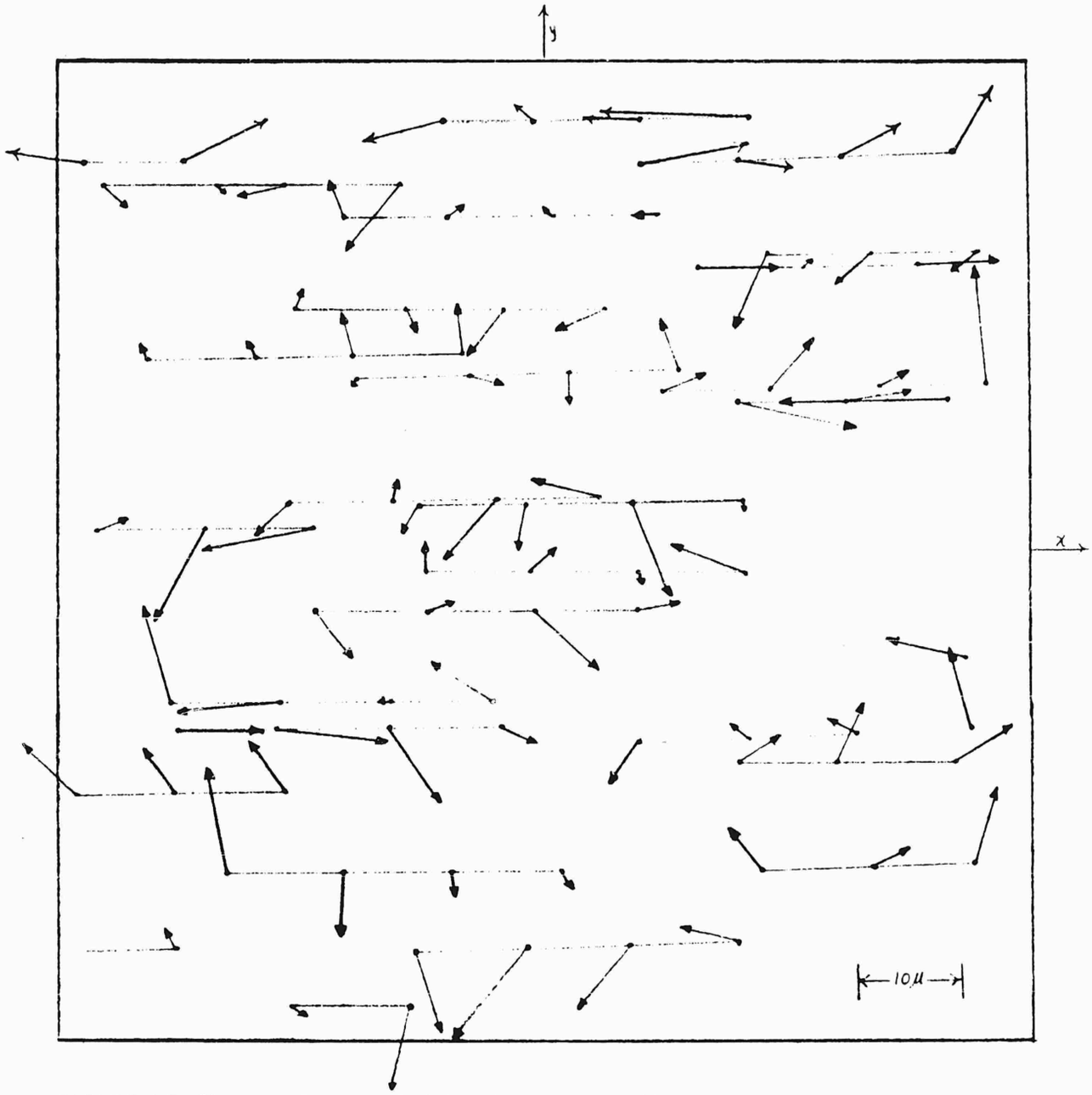

FIGURE A2. Plate coordinate residuals from least squares calibration of orientation of stellar plate taken by 1000 mm f/5 camera; star catalogue errors not taken into account; mean error of residuals 5.2 μ.

spite of this, in the adjustment giving rise to the residual plot of Figure 2 only errors in the measured plate coordinates were considered, the catalogued positions of the stars being regarded as error free. Hence, the errors in the catalogued positions were transferred to the plate coordinates. This effect had not been noted in earlier fixed camera reductions because the focal lengths, being 300 mm and shorter, were not sufficiently great for the catalogue error to be significant relative to the plate measuring error.

In view of the foregoing it was considered advisable to develop a new plate reduction wherein random errors in both plate coordinates and catalogued positions were properly adjusted. A research program to achieve this end was undertaken by Instrument Corporation of Florida under the sponsorship of Air Force Cambridge Research Laboratories. It is not our intention to consider details of the resulting reduction here, inasmuch as the derivation is rather lengthy and is being documented in a separate paper to be published later. Suffice it to say that the adjustment is based on the minimization of the following quadratic form, the residuals of which are interrelated by the fundamental projective relations:

$$(11) \qquad s = \sum_{i=1}^{m} \sum_{j=1}^{n} (W_{x_{ij}} v_{x_{ij}}^2 + W_{y_{ij}} v_{y_{ij}}^2) + \sum_{j=1}^{n} (W_{A_j} v_{A_j}^2 + W_{D_j} v_{D_j}^2),$$

where

$v_{x_{ij}}, v_{y_{ij}}$ = residuals of measured plate coordinates of ith images of jth star;

$W_{x_{ij}}, W_{y_{ij}}$ = weights of measured plate coordinates (inversely proportional to measuring variances);

v_{A_j}, v_{D_j} = residuals of updated right ascension A and declination D of jth star;

W_{A_j}, W_{D_j} = weights of updated A, D (inversely proportional to variances computed from catalogued probable errors).

Thus the reduction yields not only plate coordinate residuals but also residuals of right ascension and declination. It follows that some measure of improvement is to be expected in the catalogued positions as a consequence of the adjustment. It can be shown theoretically that if the standard deviations of the catalogued positions were 0".7 in A and D, if plate measuring standard deviations were 3 microns, if a total of 8 different stars were measured on a given plate, and if 6 different images were measured on each stellar trace, the adjusted values of A and D from the reduction of a PC-1000 plate would have standard deviations of slightly better than 0".35, or about half that of the values input into the computer. More generally, the following approximate formula may be employed to predict the standard deviations to be expected for adjusted right ascensions and declinations:

$$\bar{\sigma} \cong \sqrt{\frac{\hat{\sigma}^2}{n} + \frac{1}{m}\left(\frac{\tilde{\sigma}}{c}\right)^2}$$

In this formula, which ignores the degrees of freedom involved in the adjustment and thus has increasing validity with increasing m and n,

$\bar{\sigma}$ = approximate standard deviation in radians of adjusted right ascension and declination;

$\hat{\sigma}$ = standard deviation of catalogued right ascensions and declinations in radians (assumed same for all stars);

$\tilde{\sigma}$ = standard deviation of measured plate coordinates (assumed same for all points);

c = focal length of camera in same units as σ;

m = number of images measured per stellar trace;

n = number of different stars measured.

In order to gain insight concerning the effectiveness of the new plate reduction, we performed a numerical simulation wherein the adjustment was applied to artificially generated data. A uniform array of 25 "stars" was generated. To the "true" right ascensions and declinations of these "stars" were added random errors drawn from a table of random normal deviates normalized to have a standard deviation of 0".7. This produced

simulated "observed" right ascensions and declinations. The "true" plate coordinates of the "stars" were computed for four different instants of time from a postulated set of elements of orientation. Random errors drawn from a population having a standard deviation of 3 microns were then added to the "true" plate coordinates to produce simulated "observed" plate coordinates. The resulting simulated data were then subjected to Schmid's adjustment which, it will be recalled, considers only errors in the measured plate coordinates. The resulting residual vectors are plotted in Figure 3. The similarity of these results to those of Figure 2 is quite striking. Next, the same simulated data were subjected to the new adjustment which treats both plate coordinates and catalogued positions as subject to random error. The resulting plate coordinate residuals are plotted in Figure 4. Here it is seen that randomness is achieved not only from star to star as in Figure 2, but also for the successive images of each individual stellar trace, which is as it should be. The mean error of the plate coordinates is reduced from the 4.2 microns of Figure 2 to 2.7 microns, a figure statistically consistent with the true value, which in this case is known to be 3 microns. Inasmuch as the solution also produces residuals of right ascension and declination, it is particularly interesting to plot these and to compare them with the actual errors. This is done in Figure 5, the signs of the errors being reversed to facilitate the comparison. An excellent degree of correlation is seen to exist between the residual vectors and the error vectors. The results of the simulation thus demonstrate the validity and effectiveness of the reduction within the framework of the assumptions.

The data giving rise to Figure 2 were also processed through the new reduction. The resulting plate coordinate residuals are plotted in Figure 6. Virtually complete randomness is achieved and the mean error of the plate coordinate residuals is reduced from 5.2 microns to 2.6 microns. In future studies, results obtained from different cameras for a common star field will be used to determine the consistency of the adjusted right ascensions and declinations. Preliminary results with three plates indicate a good measure of consistency for those stars having the larger residuals.

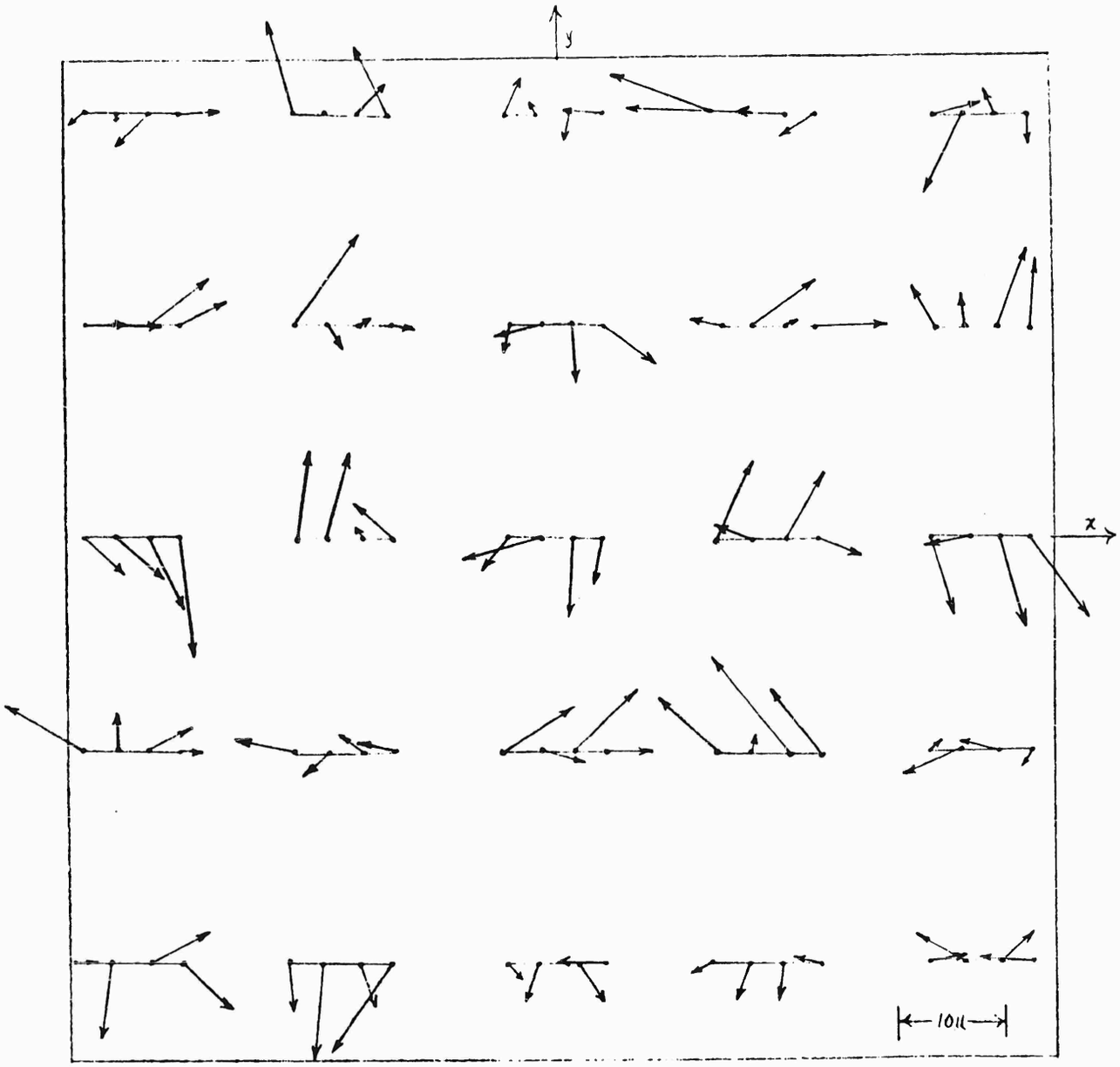

FIGURE A3. Plate coordinate residuals from least squares claibration of simulated stellar plate taken by 1000 mm focal length ballistic camera; rms errors of 0".7 in catalogued right ascensions and declinations are not taken into consideration; mean error 4.2 μ.

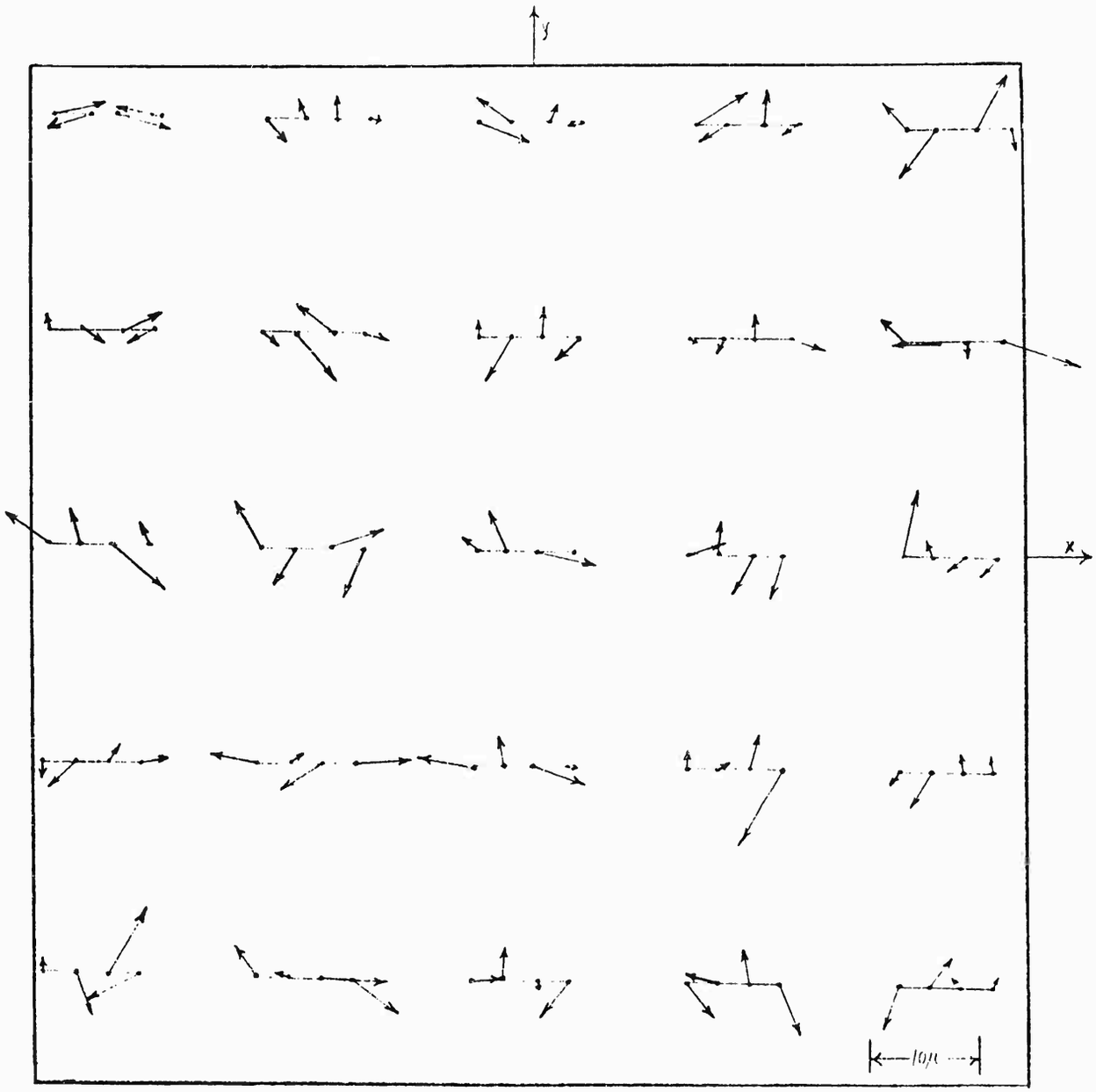

FIGURE A4. Plate coordinate residuals from least squares calibration of simulated stellar plate taken by 1000 mm focal length ballistic camera; rms errors of 0".7 in catalogued right ascensions and declinations are properly taken into consideration; mean error 2.7 μ.

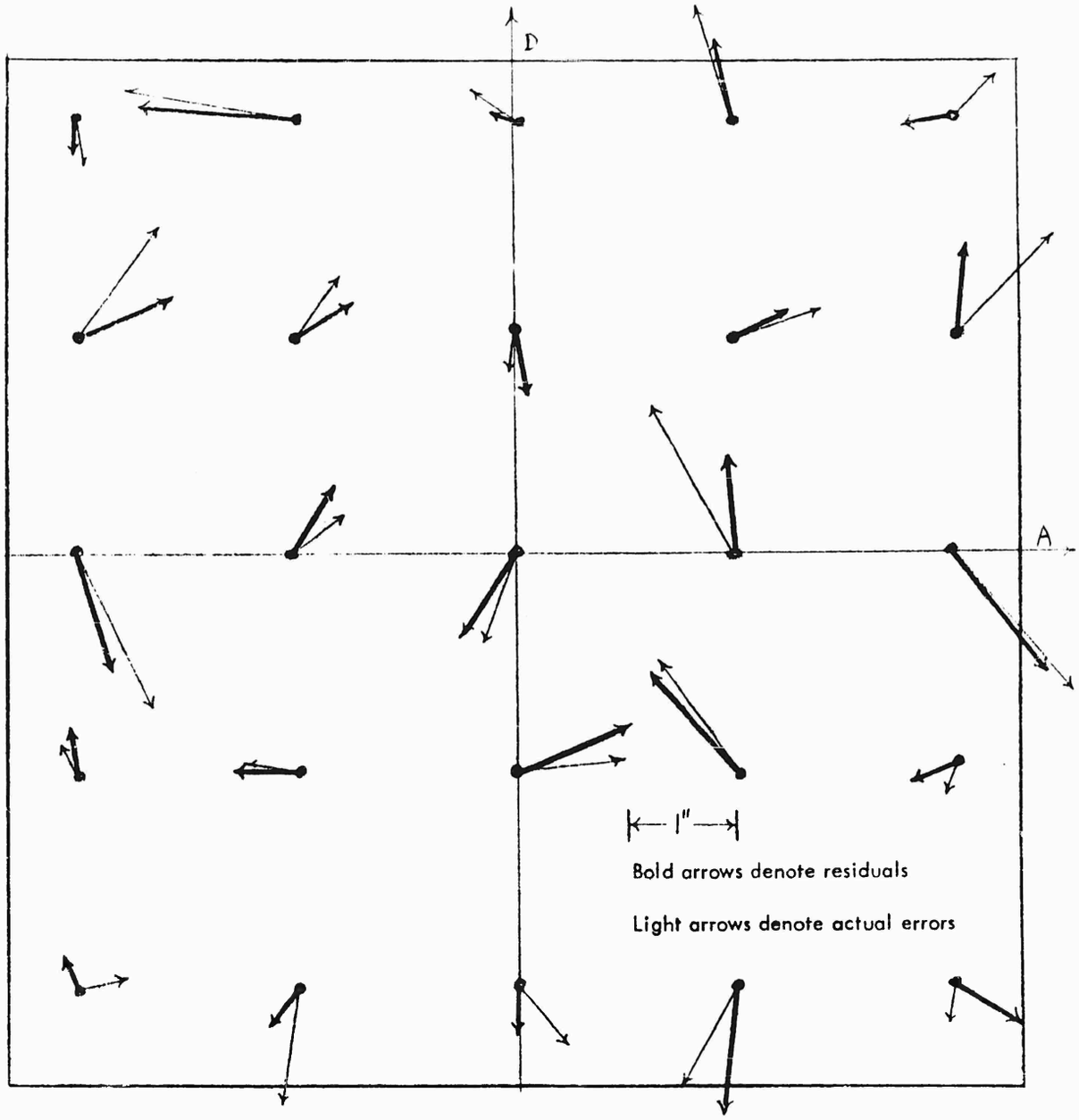

FIGURE A5. Right ascension and declination residuals from least squares calibration of simulated stellar plate taken by 1000 mm focal length ballistic camera; rms errors of 3 microns in plate coordinates and of 0".7 in catalogued right ascensions and declinations are properly taken into account; mean error of catalogue residuals 0".6.

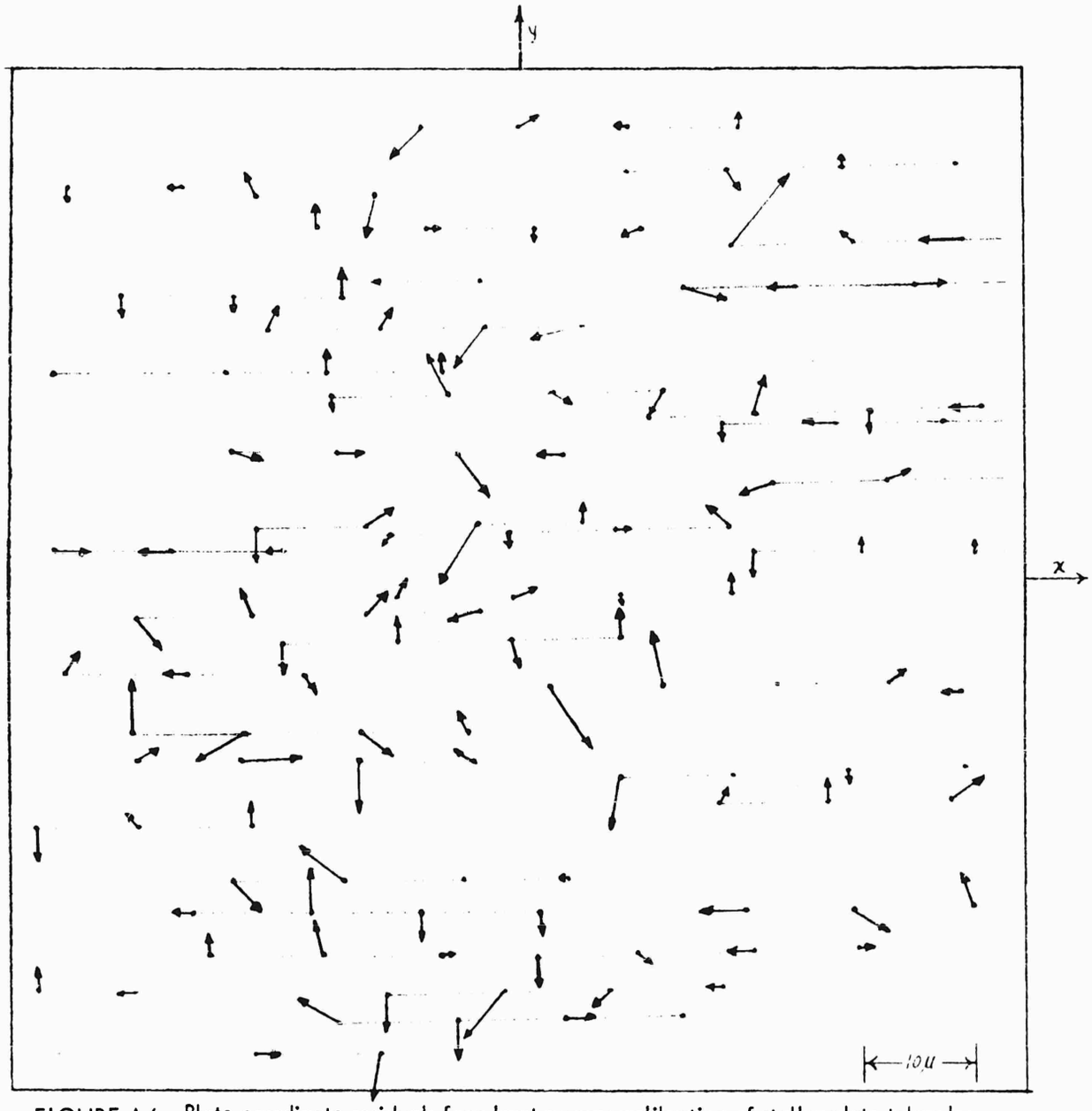

FIGURE A6. Plate coordinate residuals from least squares calibration of stellar plate taken by 1000 mm f/5 camera (same original data as in Figure 1); star catalogue errors properly taken into account in adjustment; mean error of residuals 2.6 μ.

It will be noted that there are more stars in Figure 6 than in Figure 2. The extra stars are those which were originally measured but whose coordinates were not subsequently found in the Boss catalogue. Hence they had to be dropped from the original solution. An interesting and useful property of the new solution is that uncatalogued stars can be utilized; it is merely necessary to assign approximations to the unknown right ascensions and declinations and to set the corresponding weights equal to zero. Because the relative hour angles of uncatalogued stars are known by virtue of the measured differences in the times of exposures, it is possible for uncatalogued stars to make a worthwhile contribution to the calibration of orientation (particularly to the determination of scale).

Other noteworthy features of the new solution are the following:

1) Provisions are made for the measurements of both stellar breaks and punctiform images. To accomplish this without making it necessary to measure the plate in direct and reversed positions in order to eliminate personal bias, two additional parameters Δx, Δy are carried as unknowns. These represent the biases of measured stellar breaks relative to the measured punctiform images. The parameters Δx and Δy are constrained to lie between ±5 microns at the one sigma level. The desirability of measuring breaks in addition to points stems from the fact that two additional stellar magnitudes are thereby gained. With the PC-1000, for instance, the faintest stars giving use to acceptable punctiform images are of seventh to eigth magnitude, whereas stars from eighth to tenth magnitude yield well-defined trails. Often there are sizable regions on the plate wherein only trails are to be found. Often these trails are of uncatalogued stars, but as indicated above, this does not prevent their effective use.

2) Provisions are made for carrying coefficients of distortion as additional unknowns so that the solution can be employed to calibrate distortion whenever desired (the data generating Figures 2 and 6 were processed through the version of the solution providing distortion calibration).

3) Provisions are made for incorporating up to four coefficients of Garfinkel's expansion of astronomical refraction as unknowns. These may be constrained, if desired,

to be statistically consistent with a priori values derived from meteorological data. The parametrization of refraction is particularly desirable when zenith distances exceed 60° to 70°; it is of relatively little value when zenith distances are less than 50°. For observations near the horizon (as in flashing light line crossings for determination of azimuth of Hiran lines) it is mandatory to carry at least three coefficients of refraction as unknowns in the adjustment.

A.6 FIXED CAMERA VS. SIDEREAL CAMERA FOR DETERMINATION OF DIRECTIONS TO FLASHES

Now that sufficient background has been established for an understanding of the more advanced fixed camera observational and reductional techniques, it is pertinent to compare the relative merits of the fixed and sidereal cameras for the basic problem of determining precise directions of recorded flashes. The most fundamental difference, of course, is that the fixed camera is stationary relative to the earth, whereas the sidereal camera is stationary relative to inertial space. The most serious deficiency of sidereal cameras for flashing-light applications arises from the fact that the mechanical imperfections of most equatorial mounts and drives constitute a source of significant error by causing the camera actually to be unstable in inertial space. Indeed, in most cases the error introduced by the mount will considerably exceed that introduced by the plate measurements. It should be appreciated that this consideration applies only to flashing-light applications, for small errors or jitter in the drive do not have a significant effect on the relative positions of stellar images, particularly if guiding is practiced to keep the tracking excursions within reasonable bounds. Thus the sidereal camera is well suited to conventional astrometric applications in spite of the imperfections of mounts and drives. On the other hand, the duration of a flash is so short that its position on the plate of a sidereal camera relative to the mean positions of the stars will depend directly on the instantaneous inertial orientation of the camera relative to the mean inertial orientation. It follows that if a particular mount were to provide an rms accuracy of, say, 2 seconds

of arc with guiding (which would be excellent), directional accuracies to recorded flashes could not be recovered to better than two seconds of arc rms even though relative stellar directions on the same plate could conceivably be recovered to a few tenths of a second of arc. Thus it is our contention that the use of sidereal drives can only deteriorate the accuracies potentially obtainable from a given camera (again, we are referring only to flashing-light applications). Beyond this, however, the fixed camera enjoys a number of significant advantages over the sidereal camera, even in certain purely astrometric applications. Aside from stability, the most important factor contributing to these advantages is the fact that precise measurements of time are fully exploited in fixed-camera applications, whereas time does not constitute a useable measurement in sidereal applications. The following table provides a summary of the relative advantages of fixed and sidereal cameras when used for directional determination of flashing lights. In items 4, 5 and 13 the values quoted apply to cameras similar to the PC-1000. These may be revised appropriately to apply to other cameras.

A.7 RELATIVE ADVANTAGES OF FIXED AND SIDEREAL CAMERAS FOR DETERMINATION OF DIRECTIONS OF FLASHES

Fixed camera	Sidereal camera
1. Essentially perfect stability over short periods (a few minutes) is relatively easily attained with earth-fixed orientation.	1. Inaccuracies and jitter of conventional sidereal drive can introduce errors of several seconds of arc in determination of directions of nearly instantaneous flashes relative to stars.
2. Very small but possibly significant changes or disturbances in earth-fixed orientation can be detected through use of stellar images recorded at different times. Therefore, direct check on validity of data is immediate by-product of reduction. This check is independent of subsequent triangulation checks.	2. Very small but possibly significant changes or disturbances in inertial orientation are internally undetectable; they merely result in a slight increase in image diameters. No check on validity of directions of flash points is available prior to triangulation.

3. A given star may be recorded several times, giving rise to a series of well-spaced control points; multiple usage of stars overcomes problem of sparse stellar fields.	3. A given star produces one and only one control point; nothing can be done to augment sparse stellar fields.
4. Use of a series of different exposures (e.g., 1, 1/2, 1/4, 1/8 sec) produces images of graduated diameter so that each recorded star produces at least one nearly optimum image per exposure cycle; repetition of basic cycles can lead to several nearly otpimum images from each star.	4. All stellar images have some exposure so that image diameter is strictly dependent on stellar magnitude and color; selection of sufficient catalogued stellar control having uniform and optimum image diameters is extremely difficult and, in many cases, is impossible (for results of maximum accuracy, images of stellar control should closely match those of flashing light).
5. Stars down to eighth magnitude yield useable point images; fainter stars to ninth or tenth magnitude generate only weak trails; stars fainter than ninth to tenth yield no images at all. Hence confusing extraneous images (i.e., images of uncatalogued stars) are minimal.	5. A few minutes of total exposure will produce distinct images from stars of eleventh, twelfth or even thirteenth magnitude. These together with images of stars of ninth and tenth magnitudes are extraneous and confusing because they are not catalogued; only a few percent of the stellar images are actually usable and these, being produced by the brighter stars, are likely to be oversized.
6. Discrimination of flash images is easy, because a short trail is associated with each star, whereas flashes have no associated trails.	6. Discrimination of flash images from star images can be extremely difficult, particularly when (as in the case of satellite flashes) only five or so are distributed across the plate.
7. Timing data are required for stellar exposures (but not for flashes) in order to determine directions of flashes.	7. Timing data are required for the flashes (but not for stellar exposures, except very nominally) in order to determine directions of flashes.
8. Except for 3 or 4 key stars, stellar identification may be established automatically by the computer as part of the general reduction; hence the sidereal mount offers no basic advantages insofar as identification is concerned.	8. Automatic star identification is equally feasible when sidereal mounts are used; however, because each star is used only once, from two to four times more distinct stars must be identified than with a fixed mount.

9. Initial set-up of camera orientation depends only on expected direction of flashes and is independent of expected time of flashes.	9. Initial set-up of camera orientation depends on both expected direction and time flashes; reorientation is required whenever expected times change, as with missile holds.
10. A fixed camera mount is relatively inexpensive and is readily compatible with a mobile operation.	10. A sufficiently accurate equatorial mount is quite expensive and is not generally well suited to a mobile operation.
11. Standard deviations of effects of atmospheric shimmer on directions of flashes can be estimated for a given plate by means of the "noise trace technique"; this permits proper weighting of such observations in subsequent reductions.	11. Use of stellar mount precludes use of "noise trace" or any other simple technique to estimate effects of shimmer on directions of flashes (unless drive is stopped and high performance shutter is used to produce noise trace as in fixed camera techniques).
12. Images of uncatalogued stars can be used as supplementary control, because the relative hour angles between such exposures depends only on time differences which constitute independent and easily made measurements.	12. Images of uncatalogued stars cannot be used as supplementary control; they serve only to "clutter" the plate and, for all practical purposes, constitute "noise" insofar as discrimination of flash images is concerned.
13. Random errors in catalogued right ascensions and declinations can be estimated with worthwhile accuracy and separated from plate measuring errors by means of observations made on a single plate.	13. Random errors in catalogued right ascensions and declinations can effectively be separated from plate measuring errors only through reduction of multiple plates of the same field.
14. Shutter and shutter timing is required (to accuracies of 5 to 10 msec). Recently developed VLF timing techniques readily permit accuracies of ±1msec to be achieved anywhere in the world.	14. Shutters are not required; this is only advantage of sidereal mount in flashing light applications.

A.8 CONCLUSIONS

We have outlined some of the key points in the evolution of fixed-camera techniques. We have seen that the original application of fixed cameras was to determine the precise directions of flashing beacons. This is still their chief application and is one in which

they excel. Nonetheless, it seems that every so often someone, having little or no familiarity with the theory and evolution of fixed-camera techniques, will seriously suggest replacement of fixed cameras by sidereal cameras or else would revive astrometric data reduction procedures (or would do both). It is our opinion that the time is at hand when sophisticated fixed-camera techniques can profitably be exploited in purely astrometric applications. Geodetic satellites carrying flashing-light beacons will afford an unprecedented opportunity to accomplish not only geodetic objectives but also to effect a significant improvement of star catalogues largely as a by-product of the reduction of plates from fixed cameras (this in turn, of course, would benefit the geodetic objectives). On Project ANNA alone it is estimated that as many as 2000 reducible plates will be exposed by some 20 PC-1000 cameras during the first year of operation. Since the field of the PC-1000 is $10^\circ \times 10^\circ$, this implies that the entire celestial sphere would be photographed five times over during the course of a single year if the observations were uniformly distributed. Accordingly, it would be reprehensible, in our eyes, if a well-thought-out program were not implemented to exploit to the very fullest the vast quantities of information to be obtained (at very considerable expense) in future geodetic satellite operations.

A.9 SELECTED BIBLIOGRAPHY

R. S. Zug, A Photometeoronic Method for Bomb Ballistics and for Measurements of the Flight Performance of Aircraft, BRL Report No. 279 (1942).

R. S. Zug, High Altitude Range Bombing by the Aberdeen Missing Using Ballistic Cameras Report No. 1, Ordnance Research and Development Center, Aberdeen Proving Ground (1945).

H. Schmid, Spatial Triangulation by Means of Photogrammetry, BRL Report No. 784 (1952).

H. Schmid, An Analytical Treatment of the Orientation of a Photogrammetric Camera, BRL Report No. 880 (1953).

O. von Gruber, Ferienkurs in Photogrammetrie (Stuttgart, Verlag von Konrad Wittwer, (1930).

D. Brown, Adjustment and Triangulation of Fixed Camera Observations, Ballistic Research Laboratories Report No. 960(1955).

D. Brown, The Simultaneous Determination of the Orientation and Lens Distortion of a Photogrammetric Camera, Air Force Missile Test Center Technical Report No. 56-20 (1956).

D. Brown, A Treatment of Analytical Photogrammetry with Emphasis on Ballistic Camera Applications, Air Force Missile Test Center Technical Report No. 57-22 (1957).

D. Brown, Photogrammetric Flare Triangulation, a New Geodetic Tool, Air Force Missile Test Center Technical Report No. 59-3 (1958).

B. Garfinkel, An Investigation in the Theory of Astronomical Refraction, Astronomical Journal, 50 (1944) 169.

AF Cambridge Research Laboratories, Bedford, Massachusetts. Rpt No. AFCRL 64-40. AN ADVANCED REDUCTION AND CALIBRATION FOR PHOTOGRAMMETRIC CAMERAS. Final Report. 10 January 1964, 113 p. incl. illus., tables.

Unclassified Report

In order to fully exploit recent advances in photogrammetric technology it has been necessary to develop a comprehensive plate reduction appreciably more powerful than any hitherto employed. In addition to factors considered in previous plate reductions, an advanced reduction must treat with full physical and statistical rigour such factors as: random errors in catalogued stellar positions; atmospheric refraction (particularly at great zenith distances); higher-order symmetric radial distortion; tangential distortion and asymmetric radial distortion resulting from imperfectly centered optics; differential bias between measurements of different types of images; effective utilization of uncatalogued stars for photogrammetric control; introduction of a priori constraints on any of the parameters of the reduction. Such a reduction is developed in this paper and illustrations of its practical application are provided. Special attention is given to decentering distortion, a topic inadequately treated in the photogrammetric literature. It is suggested that uncompensated decentering distortion has often in the past been the major obstacle to the full practical realization of theoretically attainable accuracies. The Advanced Plate Reduction is designed to be valid for any combination of focal length and angular field. By allowing for the possibility of correlated errors in the plate coordinates, it is also valid for cameras not having flat fields (e.g., the Baker Nunn Satellite Camera). Special note is taken of the application of the Advanced Plate Reduction for the definitive calibration of mapping cameras to be used for the analytical extension of photogrammetric control.

1. Photogrammetry
2. Calibration, Cameras
3. Geodesics
4. Astronomy
5. Satellites (Artificial) Optical Tracking

I. Project No. 5930 Task No. 593003
II. Contract AF19-(604)-8493
III. D. Brown Associates
IV. Brown, D.C.
V. In DDC Collection

AF Cambridge Research Laboratories, Bedford, Massachusetts. Rpt No. AFCRL 64-40. AN ADVANCED REDUCTION AND CALIBRATION FOR PHOTOGRAMMETRIC CAMERAS. Final Report. 10 January 1964, 113 p. incl. illus., tables.

Unclassified Report

In order to fully exploit recent advances in photogrammetric technology it has been necessary to develop a comprehensive plate reduction appreciably more powerful than any hitherto employed. In addition to factors considered in previous plate reductions, an advanced reduction must treat with full physical and statistical rigour such factors as: random errors in catalogued stellar positions; atmospheric refraction (particularly at great zenith distances); higher-order symmetric radial distortion; tangential distortion and asymmetric radial distortion resulting from imperfectly centered optics; differential bias between measurements of different types of images; effective utilization of uncatalogued stars for photogrammetric control; introduction of a priori constraints on any of the parameters of the reduction. Such a reduction is developed in this paper and illustrations of its practical application are provided. Special attention is given to decentering distortion, a topic inadequately treated in the photogrammetric literature. It is suggested that uncompensated decentering distortion has often in the past been the major obstacle to the full practical realization of theoretically attainable accuracies. The Advanced Plate Reduction is designed to be valid for any combination of focal length and angular field. By allowing for the possibility of correlated errors in the plate coordinates, it is also valid for cameras not having flat fields (e.g., the Baker Nunn Satellite Camera). Special note is taken of the application of the Advanced Plate Reduction for the definitive calibration of mapping cameras to be used for the analytical extension of photogrammetric control.

1. Photogrammetry
2. Calibration, Cameras
3. Geodesics
4. Astronomy
5. Satellites (Artificial) Optical Tracking

I. Project No. 5930 Task No. 593003
II. Contract AF19-(604)-8493
III. D. Brown Associates
IV. Brown, D.C.
V. In DDC Collection

AF Cambridge Research Laboratories, Bedford, Massachusetts. Rpt No. AFCRL 64-40. AN ADVANCED REDUCTION AND CALIBRATION FOR PHOTOGRAMMETRIC CAMERAS. Final Report. 10 January 1964, 113 p. incl. illus., tables.

Unclassified Report

In order to fully exploit recent advances in photogrammetric technology it has been necessary to develop a comprehensive plate reduction appreciably more powerful than any hitherto employed. In addition to factors considered in previous plate reductions, an advanced reduction must treat with full physical and statistical rigour such factors as: random errors in catalogued stellar positions; atmospheric refraction (particularly at great zenith distances); higher-order symmetric radial distortion; tangential distortion and asymmetric radial distortion resulting from imperfectly centered optics; differential bias between measurements of different types of images; effective utilization of uncatalogued stars for photogrammetric control; introduction of a priori constraints on any of the parameters of the reduction. Such a reduction is developed in this paper and illustrations of its practical application are provided. Special attention is given to decentering distortion, a topic inadequately treated in the photogrammetric literature. It is suggested that uncompensated decentering distortion has often in the past been the major obstacle to the full practical realization of theoretically attainable accuracies. The Advanced Plate Reduction is designed to be valid for any combination of focal length and angular field. By allowing for the possibility of correlated errors in the plate coordinates, it is also valid for cameras not having flat fields (e.g., the Baker Nunn Satellite Camera). Special note is taken of the application of the Advanced Plate Reduction for the definitive calibration of mapping cameras to be used for the analytical extension of photogrammetric control.

1. Photogrammetry
2. Calibration, Cameras
3. Geodesics
4. Astronomy
5. Satellite(Artificial) Optical Tracking

I. Project No. 5930 Task No. 593003
II. Contract AF19-(604)-8493
III. D. Brown Associates
IV. Brown, D. C.
V. In DDC Collection

AF Cambridge Research Laboratories, Bedford, Massachusetts. Rpt No. AFCRL 64-40. AN ADVANCED REDUCTION AND CALIBRATION FOR PHOTOGRAMMETRIC CAMERAS. Final Report. 10 January 1964, 113 p. incl. illus., tables.

Unclassified Report

In order to fully exploit recent advances in photogrammetric technology it has been necessary to develop a comprehensive plate reduction appreciably more powerful than any hitherto employed. In addition to factors considered in previous plate reductions, an advanced reduction must treat with full physical and statistical rigour such factors as: random errors in catalogued stellar positions; atmospheric refraction (particularly at great zenith distances); higher-order symmetric radial distortion; tangential distortion and asymmetric radial distortion resulting from imperfectly centered optics; differential bias between measurements of different types of images; effective utilization of uncatalogued stars for photogrammetric control; introduction of a priori constraints on any of the parameters of the reduction. Such a reduction is developed in this paper and illustrations of its practical application are provided. Special attention is given to decentering distortion, a topic inadequately treated in the photogrammetric literature. It is suggested that uncompensated decentering distortion has often in the past been the major obstacle to the full practical realization of theoretically attainable accuracies. The Advanced Plate Reduction is designed to be valid for any combination of focal length and angular field. By allowing for the possibility of correlated errors in the plate coordinates, it is also valid for cameras not having flat fields (e.g., the Baker Nunn Satellite Camera). Special note is taken of the application of the Advanced Plate Reduction for the definitive calibration of mapping cameras to be used for the analytical extension of photogrammetric control.

1. Photogrammetry
2. Calibration, Cameras
3. Geodesics
4. Astronomy
5. Satellite(Artificial) Optical Tracking

I. Project No. 5930 Task No. 593003
II. Contract AF19-(604)-8493
III. D. Brown Associates
IV. Brown, D.C.
V. In DDC Collection

AF Cambridge Research Laboratories, Bedford, Massachusetts. Rpt No. AFCRL 64-40. AN ADVANCED REDUCTION AND CALIBRATION FOR PHOTOGRAMMETRIC CAMERAS. Final Report. 10 January 1964, 113 p. incl. illus., tables.

Unclassified Report

In order to fully exploit recent advances in photogrammetric technology it has been necessary to develop a comprehensive plate reduction appreciably more powerful than any hitherto employed. In addition to factors considered in previous plate reductions, an advanced reduction must treat with full physical and statistical rigour such factors as: random errors in catalogued stellar positions; atmospheric refraction (particularly at great zenith distances); higher-order symmetric radial distortion; tangential distortion and asymmetric radial distortion resulting from imperfectly centered optics; differential bias between measurements of different types of images; effective utilization of uncatalogued stars for photogrammetric control; introduction of a priori constraints on any of the parameters of the reduction. Such a reduction is developed in this paper and illustrations of its practical application are provided. Special attention is given to decentering distortion, a topic inadequately treated in the photogrammetric literature. It is suggested that uncompensated decentering distortion has often in the past been the major obstacle to the full practical realization of theoretically attainable accuracies. The Advanced Plate Reduction is designed to be valid for any combination of focal length and angular field. By allowing for the possibility of correlated errors in the plate coordinates, it is also valid for cameras not having flat fields (e.g., the Baker Nunn Satellite Camera). Special note is taken of the application of the Advanced Plate Reduction for the definitive calibration of mapping cameras to be used for the analytical extension of photogrammetric control.

1. Photogrammetry
2. Calibration, Cameras
3. Geodesics
4. Astronomy
5. Satellites (Artificial) Optical Tracking

I. Project No. 5930 Task No. 593003
II. Contract AF19-(604)-8493
III. D. Brown Associates
IV. Brown, D.C.
V. In DDC Collection

AF Cambridge Research Laboratories, Bedford, Massachusetts. Rpt No. AFCRL 64-40. AN ADVANCED REDUCTION AND CALIBRATION FOR PHOTOGRAMMETRIC CAMERAS. Final Report. 10 January 1964, 113 p. incl illus., tables.

Unclassified Report

In order to fully exploit recent advances in photogrammetric technology it has been necessary to develop a comprehensive plate reduction appreciably more powerful than any hitherto employed. In addition to factors considered in previous plate reductions, an advanced reduction must treat with full physical and statistical rigour such factors as: random errors in catalogued stellar positions; atmospheric refraction (particularly at great zenith distances); higher-order symmetric radial distortion; tangential distortion and asymmetric radial distortion resulting from imperfectly centered optics; differential bias between measurements of different types of images; effective utilization of uncatalogued stars for photogrammetric control; introduction of a priori constraints on any of the parameters of the reduction. Such a reduction is developed in this paper and illustrations of its practical application are provided. Special attention is given to decentering distortion, a topic inadequately treated in the photogrammetric literature. It is suggested that uncompensated decentering distortion has often in the past been the major obstacle to the full practical realization of theoretically attainable accuracies. The Advanced Plate Reduction is designed to be valid for any combination of focal length and angular field. By allowing for the possibility of correlated errors in the plate coordinates, it is also valid for cameras not having flat fields (e.g., the Baker Nunn Satellite Camera). Special note is taken of the application of the Advanced Plate Reduction for the definitive calibration of mapping cameras to be used for the analytical extension of photogrammetric control.

1. Photogrammetry
2. Calibration, Cameras
3. Geodesics
4. Astronomy
5. Satellites (Artificial) Optical Trucking

I. Project No. 5930 Task No. 593003
II. Contract AF19-(604)-8493
III. D. Brown Associates
IV. Brown, D.C.
V. In DDC Collection

AF Cambridge Research Laboratories, Bedford, Massachusetts. Rpt No. AFCRL-64-40. AN ADVANCED REDUCTION AND CALIBRATION FOR PHOTOGRAMMETRIC CAMERAS. Final Report. 10 January 1964, 113 p. incl. illus., tables.

Unclassified Report

In order to fully exploit recent advances in photogrammetric technology it has been necessary to develop a comprehensive plate reduction appreciably more powerful than any hitherto employed. In addition to factors considered in previous plate reductions, an advanced reduction must treat with full physical and statistical rigour such factors as: random errors in catalogued stellar positions; atmospheric refraction (particularly at great zenith distances); higher-order symmetric radial distortion; tangential distortion and asymmetric radial distortion resulting from imperfectly centered optics; differential bias between measurements of different types of images; effective utilization of uncatalogued stars for photogrammetric control; introduction of a priori constraints on any of the parameters of the reduction. Such a reduction is developed in this paper and illustrations of its practical application are provided. Special attention is given to decentering distortion, a topic inadequately treated in the photogrammetric literature. It is suggested that uncompensated decentering distortion has often in the past been the major obstacle to the full practical realization of theoretically attainable accuracies. The Advanced Plate Reduction is designed to be valid for any combination of focal length and angular field. By allowing for the possibility of correlated errors in the plate coordinates, it is also valid for cameras not having flat fields (e.g., the Baker Nunn Satellite Camera). Special note is taken of the application of the Advanced Plate Reduction for the definitive calibration of mapping cameras to be used for the analytical extension of photogrammetric control.

1. Photogrammetry
2. Calibration, Cameras
3. Geodesics
4. Astronomy
5. Satellite(Artificial) Optical Tracking

I. Project No. 5930 Task No. 593003
II. Contract AF19-(604)-8493
III. D. Brown Associates
IV. Brown, D. C.
V. In DDC Collection

AF Cambridge Research Laboratories, Bedford, Massachusetts. Rpt No. AFCRL-64-40. AN ADVANCED REDUCTION AND CALIBRATION FOR PHOTOGRAMMETRIC CAMERAS. Final Report. 10 January 1964, 113 p. incl. illus., tables.

Unclassified Report

In order to fully exploit recent advances in photogrammetric technology it has been necessary to develop a comprehensive plate reduction appreciably more powerful than any hitherto employed. In addition to factors considered in previous plate reductions, an advanced reduction must treat with full physical and statistical rigour such factors as: random errors in catalogued stellar positions; atmospheric refraction (particularly at great zenith distances; higher-order symmetric radial distortion; tangential distortion and asymmetric radial distortion resulting from imperfectly centered optics; differential bias between measurements of different types of images; effective utilization of uncatalogued stars for photogrammetric control; introduction of a priori constraints on any of the parameters of the reduction. Such a reduction is developed in this paper and illustrations of its practical application are provided. Special attention is given to decentering distortion, a topic inadequately treated in the photogrammetric literature. It is suggested that uncompensated decentering distortion has often in the past been the major obstacle to the full practical realization of theoretically attainable accuracies. The Advanced Plate Reduction is designed to be valid for any combination of focal length and angular field. By allowing for the possibility of correlated errors in the plate coordinates, it is also valid for cameras not having flat fields (e.g., the Baker Nunn Satellite Camera). Special note is taken of the application of the Advanced Plate Reduction for the definitive calibration of mapping cameras to be used for the analytical extension of photogrammetric control.

1. Photogrammetry
2. Calibration, Cameras
3. Geodesics
4. Astronomy
5. Satellite(Artificial) Optical Tracking

I. Project No. 5930 Task No. 593003
II. Contract AF19-(604)-8493
III. D. Brown Associates
IV. Brown, D.C.
V. In DDC Collection